STUDIES OF GENETIC FACTORS MODULATING POLYGLUTAMINE TOXICITY IN THE YEAST MODEL

A Dissertation
Presented to
The Academic Faculty

by

He Gong

In Partial Fulfillment
of the Requirements for the Degree of
Doctor of Philosophy in the
School of Biology

Georgia Institute of Technology
December, 2011

STUDIES OF GENETIC FACTORS MODULATING

POLYGLUTAMINE TOXICITY IN THE YEAST MODEL

Approved by:

Dr. Yury O. Chernoff, Advisor
School of Biology
Georgia Institute of Technology

Dr. Francesca Storici
School of Biology
Georgia Institute of Technology

Dr. Kirill S. Lobachev
School of Biology
Georgia Institute of Technology

Dr. Donald F. Doyle
School of Chemistry and Biochemistry
Georgia Institute of Technology

Dr. Alfred H. Merill, Jr
School of Biology
Georgia Institute of Technology

Date Approved: August 03, 2011

To mom, dad and Haidong
For all your love, faith and support

ACKNOWLEDGEMENTS

I would like to give my sincere appreciation to Dr. Yury O. Chernoff, my thesis advisor. Without his constant and patient guidance, I would never be able to achieve the success of completing my PhD studies. I thank all my committee members, Drs. Al Merill, Kirill Lobachev, Francesca Storici and Donald Doyle for support and feedback on every stage of my progress in PhD study. I would also like to thank Gary Newnam, manager of the Chernoff lab. Gary has always been so kind and helpful to me for the numerous things I encountered daily in the lab, from as simple as looking for a chemical compound on the shelves to resolving mysterious problems of experiments. All the experience that Gary shared with me has become a fortune of mine. The last but not the least, I thank all members of Chernoff lab that I have worked with for the beautiful memories they gave me.

TABLE OF CONTENTS

LIST OF TABLES

LIST OF FIGURES

LIST OF SYMBOLS AND ABBREVIATIONS

AD	Alzheimer's disease
103Q	polyglutamine stretch of 103 glutamine residues
103QP	polyglutamine stretch of 103 glutamine residues and polyproline region of human Htt
25Q	polyglutamine stretch of 25 glutamine residues
aa	amino acid
Ac	acetate
Amp	ampicilin
AQT	Anti-polyQ Toxicity
bp	base pair
CGH	Comparative Genomic Hybridization
CHEF	Contour-clamped Homogeneous Electric Field
Chr	chromosome
CLAC	Cluster Along Chromosome
CUP1	CuSO4-inducible CUP1 promoter
DNA	deoxyribonucleic acid
EDTA	ethylenediaminetetraacetic acid
FITC	fluorescein isothiocyanate
Gal	galactose in the media as carbon source
GAL	galactose-inducible *Gal1, 10* promoter
GFP	green fluorescent protein
HD	Huntiongton's Disease
hr	hour

kb	kilobase
kD	kilodalton
min	minute
ml	milliliter
MW	molecular weight
NC	nitrocellulose
NEM	N-ethylmaleimide
NPD	non-parental ditype
OD	optical density
ORF	open reading frame
PBS	Phosphate buffered saline
PCR	polymerase chain reaction
PD	parental ditype
PFGE	Pulse Field Gel Electrophoresis
PMSF	phenylmethylsulfonyl fluoride
polyQ	polyglutamine
PrD	prion domain
Raf	raffinose in the media as carbon source
RFP	red fluorescent protein
Rg	region
SDD-AGE	Semi-Denaturing Detergent - Agarose Gel Electrophoresis
SDS	sodium dodecyl sulfate
SDS-PAGE	SDS-polyacrylamide gel electrophoresis
sec	second
T	tetratype

TAE	Tris base, acetic acid and EDTA buffer
TBE	Tris base, boric acid and EDTA buffer
TBS	Tris buffered saline
WT	wild-type
Δ	deletion
µl	microliter

SUMMARY

Polyglutamine-expanded fragments, derived from the human huntingtin protein, are aggregation-prone and toxic in yeast cells, bearing endogenous QN-rich proteins in the aggregated (prion) form. Attachment of the proline-rich region targets polyglutamine aggregates to the large perinuclear deposit (aggresome). Aggresome targeting ameliorates polyglutamine cytotoxicity in the presence of the prion form of Rnq1 protein, however, aggresome-forming construct remains toxic in the presence of the prion form of translation termination (release) factor Sup35 (eRF3).

Disomy by chromosome II partly ameliorates polyglutamine toxicity in the strains containing Sup35 prion. The chromosome II gene, coding for another release factor, and interaction partner of Sup35, named Sup45 (eRF1), is responsible for amelioration of toxicity. Plasmid-mediated overproduction of Sup45, or expression of the Sup35 derivative that lacks the QN-rich domain and is unable to be incorporated into prion aggregates, also ameliorate polyglutamine toxicity. Protein analysis indicates that polyglutamines alter aggregation patterns of the Sup35 prion and promote aggregation of Sup45, while excess Sup45 counteracts these effects.

In the absence of Sup35 prion, disomy by chromosome II is still able to decrease polyglutamine toxicity. However, *SUP45* is no longer the gene responsible for such an effect. Taken together with the finding that the presence of both the Rnq1 prion and the Sup35 prion has an additive effect on polyQ toxicity, one gene or few genes on chromosome II are able to ameliorate polyQ toxicity through a *SUP45*-independent pathway. The identification of such a gene is currently ongoing.

Monosomy by chromosome VIII in diploid heterozygous by *AQT* (Anti-polyQ Toxicity mutants that are disomic by chromosome II) counteracted the effect of *AQT*. Similarly, deletion of the *arg4* gene in chromosome VIII in *AQT* haploid was able to eliminate the *AQT* effect. Moreover, analysis of genes involved in the arginine and polyamine synthesis indicated that loss of genes in later stages of arginine biosynthesis causes increase of polyglutamine toxicity. Deletion of genes *arg1*, *arg4*, *arg8* (arginine pathway) and *spe1* (polyamine pathway) all suppressed the Sup35 prion phenotype expression in the nonsense suppression system. Further analysis regarding the mechanisms behind those effects is needed.

Our data uncover the mechanisms by which genetic and epigenetic factors may influence polyglutamine toxicity, and demonstrate that one and the same type of polyglutamine deposits could be cytoprotective or cytotoxic, depending on the prion composition of a eukaryotic cell.

CHAPTER 1

INTRODUCTION

Huntington Disease is a Polyglutamine Disease

There are nine human genetic disorders that have been confirmed to be associated with expansions of polyglutamine (polyQ) repeats in certain proteins (for a list of these diseases, see Table 1.1) (Shao and Diamond 2007; La Spada and Taylor 2010). One well known example is Huntington's disease (HD), which is caused by an expansion of the polyQ stretch, located within the N-terminal stretch of the essential protein called huntingtin (Htt) (The Huntington's Disease Collaborative Research Group 1993). PolyQ expansion promotes formation of aggregates by the proteolytic Htt fragments, containing an expanded polyQ stretch (DiFiglia et al. 1997; Lunkes et al. 2002). As polyQ-expanded N-terminal region of Htt is shown to aggregate and produce HD-like neurodegeneration in the mouse model, it is clear that this region is sufficient for reproducing the characteristic features of polyQ aggregation and toxicity (Mangiarini et al. 1996; Stack et al. 2005). PolyQ associated pathologies cannot be explained solely by the loss of the cellular function of respective protein, e.g. Htt (for review, see Shao and Diamond 2007). Sequestration of other essential proteins by polyQ aggregates was proposed as a possible mechanism of toxicity (Zoghbi and Orr 1999; Shao and Diamond 2007). However,

different experimental models suggested different candidates for sequestration (Steffan et al. 2000; Hay et al. 2004; Ravikumar et al. 2004; Yamanaka et al. 2010), which decreased enthusiasm towards the sequestration model.

Table 1.1 List of polyglutamine diseases

Disease	**Gene**	**Inheritance**	**Protein**	**Normal length**	**Disease length**
Spinobulbar muscular atrophy	*AR*	X-linked recessive	androgen receptor (AR)	9-36	38-62
Huntington disease	*HD*	autosomal dominant	huntingtin	6-35	36-121
Dentatorubral-pallidoluysian atrophy	*DRPLA*	autosomal dominant	atrophin-1	6-35	49-88
Spinocerebellar ataxia type 1	*SCA1*	autosomal dominant	ataxin-1	6-44	39-82
Spinocerebellar ataxia type 2	*SCA2*	autosomal dominant	ataxin-2	15-31	36-63
Spinocerebellar ataxia type 3	*SCA3*	autosomal dominant	ataxin-3	12-40	55-84
Spinocerebellar ataxia type 6	*SCA6*	autosomal dominant	$a1_A$-voltage-dependent calcium channel subunit	4-18	21-33
Spinocerebellar ataxia type 7	*SCA7*	autosomal dominant	ataxin-7	4-35	37-306
Spinocerebellar ataxia type 17	*SCA17*	autosomal dominant	TATA binding protein	25-42	45-63

To complicate the matters further, polyQ expanded proteins form various types of aggregates in mammalian cells (Ross and Poirier 2004; Hands and Wyttenbach 2010). In case of Htt, both nuclear and cytoplasmic aggregates were found (Davies et al. 1997; DiFiglia et al. 1997; Scherzinger et al. 1997). Their contributions to polyQ pathogeneceity remain a topic of intense discussions (Ross et al. 1999; Ross and Tabrizi 2011). At least, most researchers agree that one type of cytoplasmic aggregated structures, so-called aggresome, plays a cytoprotective role via assembling polyQ expanded Htt at one site and possibly promoting its autophagy-dependent clearance (Johnston et al. 1998; Waelter et al. 2001; Taylor et al. 2003; Olzmann et al. 2008). Aggresome is located perinuclearly, associated with the centrosome and assembled with the participation of microtubular cytoskeleton. Other misfolded proteins can also be sequestered into an aggresome, indicating that this structure serves as a universal quality control deposit of aggregating proteins (Johnston et al. 1998; Kopito 2000; Garcia-Mata et al. 2002; Olzmann et al. 2007; Chin et al. 2010; Bondzi et al. 2011).

Yeast Model of Huntington's Disease and Role of Prions in Polyglutamine Toxicity

Experimental assays for studying the molecular mechanism of polyQ aggregation and toxicity have been developed in yeast *Saccharomyces cerevisiae* (Krobitsch and Lindquist 2000; Muchowski et al. 2000; Meriin et al. 2002; Duennwald et al. 2006). It

has been shown that cytoplasmic aggregation and toxicity of the chimeric protein, generated by a fusion of the expanded polyQ stretch of Htt to the green fluorescent protein (GFP), is facilitated by the presence of the endogenous yeast prions, [*PIN*$^+$] and/or [*PSI*$^+$] (Meriin et al. 2002; Gokhale et al. 2005). In the absence of a prion, aggregates of polyglutamine construct were rare and no significant cytotoxicity was detected while in the presence of a prion, multiple peripherally located aggregates were formed and cytotoxicity was observed (Meriin et al. 2002).

Prions are self-perpetuating protein isoforms that are able to convert the normal soluble protein of the same amino acid sequence into the prion form (Figure 1.1A). Prions form fiber like aggregates, called amyloids. Yeast prions [*PSI*$^+$] and [*PIN*$^+$] are prion isoforms of Sup35 and Rnq1, respectively (for review, see Wickner et al. 2007). Sup35 is the yeast translation termination factor (or release factor), eRF3. Molecular function of Rnq1 and biological process it's involved in remain unknown. Both [*PSI*$^+$] and [*PIN*$^+$] are proteins containing glutamine/asparagine-rich (QN rich) regions within the prion domains (PrD) that are responsible for aggregation properties (for review, see Tuite and Cox 2003; Inge-Vechtomov et al. 2007) (Figure 1.1B). [*PIN*$^+$] is required for *de novo* [*PSI*$^+$] induction by overexpressing Sup35 (Tuite and Cox 2003). Normally, yeast cells are still viable when there are prion aggregates inside the cells. However, they are disadvantageous to natural populations (Chernoff et al. 2000) and overproduction of prion proteins is toxic to the cells (Chernoff et al. 1992).

A

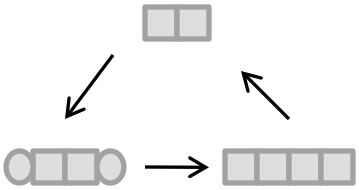

B

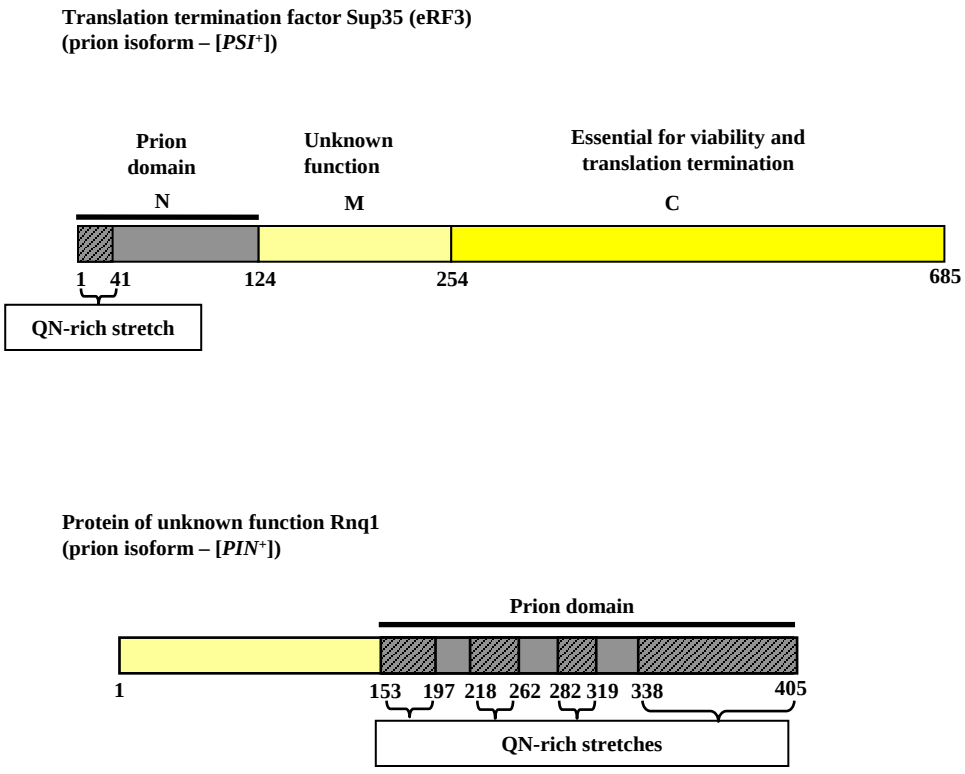

Figure 1.1 Yeast prions [*PSI*$^+$] and [*PIN*$^+$] are proteins with QN rich regions.
A – Cycle of prion propagation. Prion proteins (square) serve as nuclei, converting soluble proteins (eclipse) into prion form. Elongated amyloid fibers generate prion "seeds", which participate in non-prion protein conformational change and polymerization.
B – QN rich regions in [*PSI*$^+$] and [*PIN*$^+$] prions. [*PSI*$^+$] is the prion form of translation termination factor Sup35, which has a QN-rich stretch in the N-terminal end of the prion domain. [*PIN*$^+$] is the prion form of a protein of unknown function, Rnq1, which has multiple QN-rich stretches in the C-terminal prion domain.

It is likely that pre-existing prion aggregates nucleate aggregation of polyQ expanded huntingtin. In case of Rnq1 prion, it was shown that polyQ aggregates sequester some cytoskeletal components and inhibit endocytosis, which apparently contributes to cytotoxicity (Meriin et al. 2003). Inhibition of endocytosis was also detected in the mammalian cells, expressing polyQ (Meriin et al. 2007). As mammalian Htt has been proposed to play a role in vesicle trafficking (Caviston and Holzbaur 2009), these results are likely relevant to human HD.

In the yeast strains containing Rnq1 prion, cytotoxicity was eliminated by using a longer Htt fragment, which includes a proline (P)-rich stretch in addition to polyQ (Wang et al. 2009). This P-rich stretch was shown to target aggregated polyQ protein into a single perinuclear microtubule-dependent deposit, co-localized with the spindle body (yeast counterpart of a centrosome) and therefore resembling mammalian aggresome (Wang et al. 2009). Cytoprotective role of aggresome as opposed to cytotoxicity of some other types of aggregates recapitulates the situation previously observed in mammalian cells (Kopito 2000; Waelter et al. 2001; Taylor et al. 2003).

Translation Termination Factors in Yeast

Translation termination is a crucial process in the cells. It ensures the proper information transfer from mRNA to proteins, which eventually function in all aspects of the life cycle of the cells. In *E. coli*, RFs are discovered first in the 1960s. RF1 recognizes

stop codons UAA and UGA, whereas RF2 recognizes UAG stop codon (Scolnick et al. 1968). A third release factor was discovered to stimulate RF1 and RF2 acitivity. In yeast *Saccharomyces cerevisiae*, two independent genes were identified genetically and biochemically as eRF1 and eRF3. Sup45 (eRF1), which is a class I release factor, plays the role of recognizing all three stop codons at the ribosomal A site (Figure 1.2A). Sup35 (eRF2) is a GTPase, which carries out GTP hydrolysis in translation termination. As previously introduced, [*PSI*$^+$] is the prion form of Sup35. The presence of [*PSI*$^+$] affects the translational fidelity, and causes nonsense suppression.

A nonsense suppression system was developed to monitor [*PSI*$^+$] phenotypically (Inge-Vechtomov et al. 1988) (Figure 1.2B). The *ade1-14* allele that has a premature UGA stop codon was generated. *ADE1* codes for N-succinyl-5-aminoimidazole-4-carboxamide ribotide (SAICAR) synthetase, which is involved in Adenine biosynthesis. In the presence of [*PSI*$^+$], full length Ade1 protein is synthesized due to the nonsense suppression. Therefore, strains bearing [*PSI*$^+$] prion are able to grow on -Ade medium. On the contrary, [*psi*$^-$] strains are not able to grow on -Ade medium since functional Ade1 protein cannot be produced. Additionally, red intermediate compounds of Adenine synthesis accumulate in [*psi*$^-$] cells, and result in a red color on YPD medium.

A

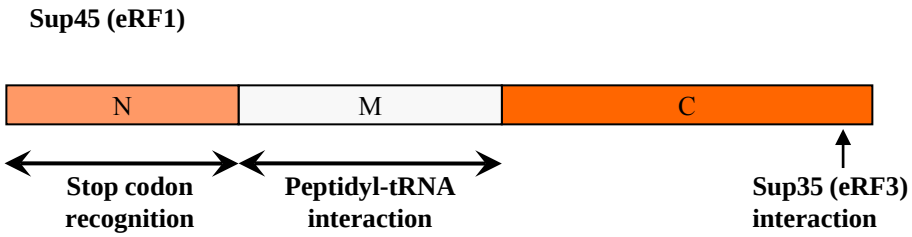

B

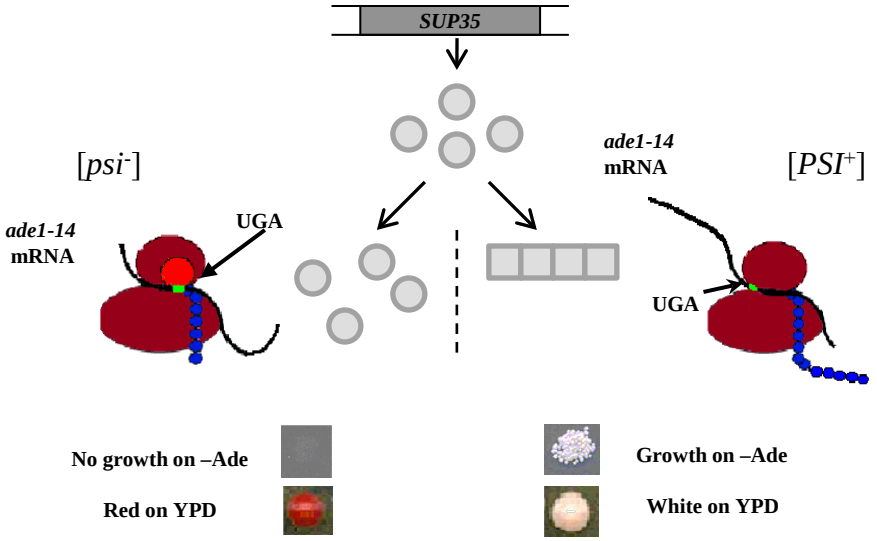

Figure 1.2 Translation termination in yeast.
A – Schematic structure of translation termination factor Sup45 (eRF1). N-domain of Sup45 is responsible for stop codon recognition; M-domain interacts with peptidyl-tRNA; C-terminal end is crucial for interaction with another translation termination factor Sup35.
B – Nonsense suppression system is used to detect [*PSI*$^+$]. In the presence of [*PSI*$^+$], most soluble Sup35 is converted to prion form, resulting in nonsense suppression at the premature UGA stop codon in *ade1-14* allele. Complete Ade1 protein is made, and Adenine biosynthesis is able to be accomplished. Cells are able to grow on –Ade medium, and exhibit white color on YPD. When there is no [*PSI*$^+$], sufficient level of Sup35 soluble protein ensures the translation fidelity. No complete Ade1 protein is synthesized. Therefore, cells are not able to grow on –Ade medium, and the color of the colony is red on YPD due to the accumulation of intermediates in Adenine synthesis pathway.

Spontaneous Mutants with Decreased Polyglutamine Toxicity was Isolated from Strain with *Ubc4* Deletion

To distinguish between the different patterns of polyQ aggregation in yeast, we have employed the previously described constructs (Figure 1.3A) that produce the N-proximal region of Htt, fused to the FLAG epitope at the N-terminus and the green fluorescent protein (GFP) at the C-terminus. The N-terminal Htt region included the polyQ stretch, which is either followed (polyQP) or not followed (polyQ) by the P-rich region. The polyQ expanded versions (103Q and 103QP) contained a stretch of 103 glutamine residues, which corresponds to a severe form of Huntington's Disease, while control non-aggregating versions (25Q and 25QP) contained 25 glutamine residues. As there was no difference in the effects of 25Q and 25QP, some of the figures show only 25Q control. As described previously, 103Q construct was toxic to both [*PIN*$^+$] yeast strains (containing Rnq1 protein in a prion form) and [*PSI*$^+$] yeast strains (containing Sup35 protein in a prion form), with a combination of both prions showing an additive effect (Figure 1.3B). Also in an agreement with the previous observations, 103QP construct was not toxic to the strains containing only [*PIN*$^+$] prion. Surprisingly, the 103QP construct was toxic to the strains containing [*PSI*$^+$] prion, independently of the presence and absence of [*PIN*$^+$] prion (Figure 1.3B). Fluorescence microscopy confirmed that 103QP preferentially formed a single perinuclear aggregate deposit (aggresome) in the cells containing [*PIN*$^+$] and/or [*PSI*$^+$] prions, while 103Q produced multiple

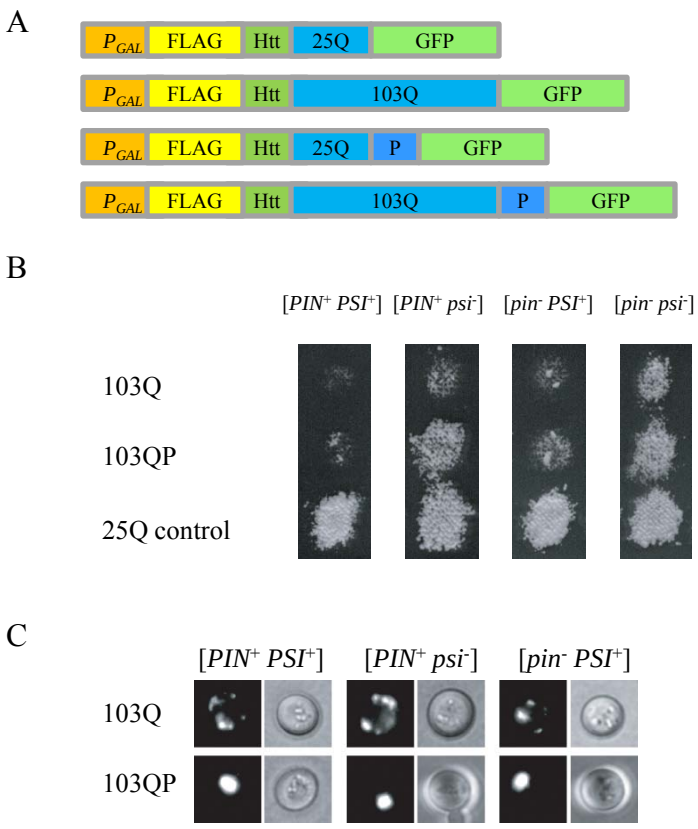

Figure 1.3 Polyglutamine toxicity and aggregation in the yeast strains with various prion compositions.
A – Polyglutamine constructs used in this work. All constructs were under the control of the galactose-inducible promoter (P_{GAL}), and contained the FLAG epitope, N-terminal 17 amino acid residues and poly-Q stretch of human Htt, and were fused to the gene coding for green fluorescent protein (GFP) at C-terminus. Numbers indicate length of poly-Q stretch. Poly-QP constructs also contained the proline-rich region of Htt (designated as P), immediately following the poly-Q stretch.
B – Expanded poly-Q without a P-rich region (103Q) is toxic in the presence of either [*PIN*$^+$] or [*PSI*$^+$] (or both), with two prions showing an additive effect, while expanded poly-Q with a P-rich region is toxic only in the presence of [*PIN*$^+$] and [*PSI*$^+$]. The 25Q construct, not exhibiting toxicity under these conditions, is shown as a control. The 25QP construct (not shown) behaved in the same way as 25Q.
C – 103Q and 103QP form multiple peripheral aggregates and single aggregate (aggresome), respectively, in cells containing either or both prions ([*PIN*$^+$] and/or [*PSI*$^+$]), as visualized by fluorescence microscopy. Perinuclear location of aggresome (not shown) was confimed by DAPI staining as described previously (Wang *et al.* 2009).

peripheral aggregates (Figure 1.3C). Therefore, ability of polyQP to form an aggresome was not affected by the [*PSI*$^+$] prion. However, the ability of aggresome to ameliorate toxicity was impaired. These data show that the mechanisms of polyglutamine toxicity, promoted by the [*PSI*$^+$] prion, are different from the mechanism of polyglutamine toxicity promoted by the [*PIN*$^+$] prion.

As ubiquitin-proteasome system (UPS) is known to influence polyQ effects in mammalian cells, we have studied polyQ toxicity in the yeast strain with a deletion of the *UBC4* gene, coding for one of the major yeast ubiquitin-conjugating enzymes (Seufert and Jentsch 1990). In both WT and *ubc4*Δ strains, 103Q and 103QP cause severe toxicity, respectively (Figure 1.4A). However, spontaneous papillation occurred frequently to *ubc4*Δ strain instead of WT. Three independent papillae were colony purified and confirmed to retain [*PSI*$^+$] and [*PIN*$^+$] prions (Figure 1.4B). Each isolate was confirmed to stably reproduce the anti-toxic phenotype (Figure 1.4C), and also to ameliorate toxicity of 103QP (Figure 1.4D). These derivatives were named *AQT* for *A*nti-poly*Q T*oxicity, with respective phenotype designated as Aqt$^+$. The Aqt$^+$ phenotype was dominant in the *ubc4*Δ background (Figure 1.4E), and was partly, although not completely suppressed by reintroduction of the wild-type *UBC4* gene (Figure 1.4F). In each derivative, the Aqt$^+$ trait segregated in a Mendelian fashion in meiosis (Table 1.2).

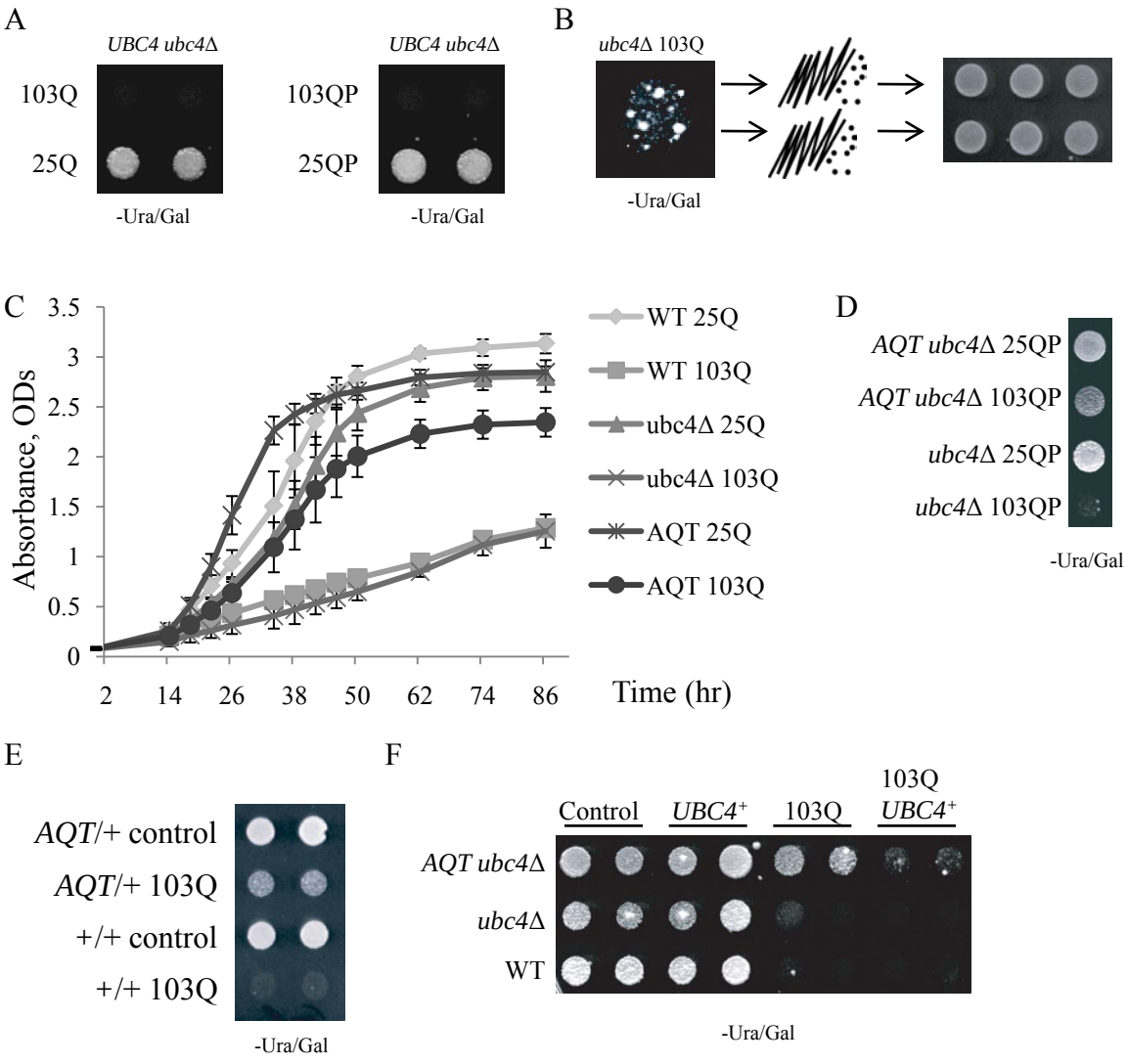

Figure 1.4 Isolation and characterization of Anti-polyQ toxicity (*AQT*) derivatives.
A – *Ubc4*Δ has no effect on toxicity of 103Q but slightly ameliorates toxicity of 103QP in the [*PIN*$^+$ *PSI*$^+$] background.
B – Papillae arise spontaneously in the *ubc4Δ* [*PIN*$^+$ *PSI*$^+$] strain expressing 103Q, and are able to stably maintain the anti-polyQ-toxic phenotype after colony purification.
C – Comparison of the growth curves of *ubc4Δ* [*PIN*$^+$ *PSI*$^+$] strains that differ by polyglutamine constructs and by the presence or absence of AQT. Growth was measured by optical density at 600 nm in the liquid –Ura medium with galactose and raffinose instead of glucose. At least 3 independent cultures were characterized per each combination. Error bars represent standard deviations.
D – *AQT* is able to ameliorate 103QP toxicity.
E – *AQT* is dominant (all strains are [*PIN*$^+$ *PSI*$^+$] and *ubc4Δ* homozygotes.
F – Reintroduction of the *UBC4* gene under galactose-inducible promoter on a multicopy plasmid partly suppresses but does not completely eliminate anti-toxic effect of *AQT*. Plates were scanned after 10 (B and F) days of incubation.

Table 1.2 Mendelian inheritance of *AQT*.

	Numbers of tetrads with *AQT*:WT ratios					Total number
AQT isolate	4:0	3:1	2:2	1:3	0:4	of tetrads
AQT2	0	0	5	0	2	7
AQT7	0	0	10	0	3	13
AQT9	0	0	8	0	0	8

Each *AQT* strain was mated to the isogenic wild type (WT) *ubc4*Δ strain of the opposite mating type.

All pairwise genetic crosses between three independent *AQT* derivatives produced 4 *AQT*: 0 wild-type pattern of segregation in the vast majority of tetrads (Table 1.3), indicating that all *AQT* derivatives are formally confined to a single genetic locus.

Table 1.3 Recombination test for allelism of *AQT* derivatives.

Crosses	*AQT*: WT ratios[*]	Total number of tetrads analyzed
AQT2 X *AQT7*	4:0 (6)[**]	7
AQT2 X *AQT9*	4:0 (8)	8
AQT7 X *AQT9*	4:0 (9)	9

All crosses were performed in the *ubc4*Δ [PIN^+ PSI^+] background.

[*] In parentheses, number of tetrads showing a respective ratio.

[**] One exceptional tetrad with 3:1 ratio was recovered.

Characterization of *AQT* Mutants

Despite their anti-toxic effect, *AQT* derivatives retained the typical mode of cytologically detectable aggregation for both 103Q (multiple peripheral aggregates, Figure 1.5A) and 103QP (single perinuclear aggregate, Figure 1.5B), indicating that amelioration of toxicity is not due to lack of aggregation.

Overproduction of Sup35 protein or its prion domain, Sup35N, is known to inhibit growth of the [*PSI*$^+$] strains. This effect was ameliorated in *AQT* derivatives (Figure 1.5C). Interestingly, *ubc4*Δ increased temperature sensitivity of our strains to near-permissive conditions, and this phenotype was also ameliorated in *AQT* derivatives (Figure 1.5D).

Objectives

The main goal of this study is to identify genetic factors that are able to modulate polyglutamine toxicity in the yeast model, and to understand the mechanism by characterizing the interaction among those factor, yeast prions, and ubiquitin-proteasome system. Utilizing the well established yeast model of Huntington Disease, we hope our findings would shed some light on pathology of polyglutamine diseases in humans and treatment strategies.

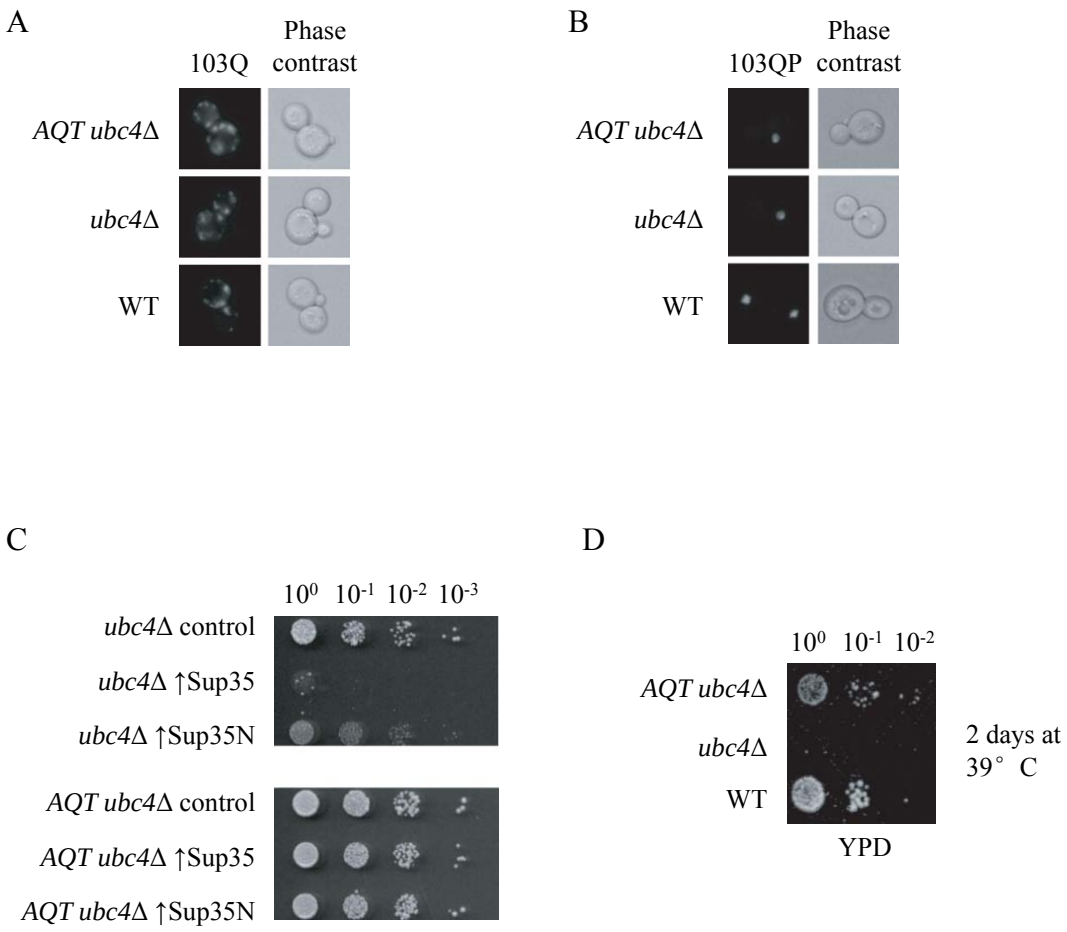

Figure 1.5 Phenotypes associated with *AQT*.
A and B – Typical aggregation patterns of 103Q (multiple dots, A) and 103QP (single clump, B) are not affected by *AQT*, as confirmed by fluorescence microscopy.
C – *AQT* mutant ameliorates toxicity of excess Sup35 or Sup35N in the [*PSI*$^{+}$] strain. Sup35 and sup35N proteins were expressed from centromeric plasmid under control of the galactose-inducible promoter. Cultures were grown in the -Ura glucose medium selective for the plasmid for 1 day. Serial decimal dilutions were plated onto -Ura glucose/raffinose medium.
D – *AQT* ameliorates temperature sensitivity of the *ubc4*Δ strain. Growth of *ubc4*Δ at 39^{o}C is completely inhibited, while isogenic WT strain and *AQT ubc4*Δ strain are slightly growing. Deletion of *ubc4* causes temperature sensitivity at 39° C. *AQT* mutant compensates for the effect of *ubc4*Δ and display temperature resistance at 39° C. Cultures were grown in the YPD liquid medium for 1 day and serial decimal dilutions were plated onto YPD medium.

CHAPTER 2

MATERIALS AND METHODS

Materials

Strains

All yeast strains used in this study are listed in APPENDIX A Table A.1. Detailed description and additional information are stated in the corresponding chapters. Strains used in this study are [*PSI*$^+$][*PIN*$^+$], [*psi*$^-$][*PIN*$^+$], [*psi*$^-$][*pin*$^-$], and [*PSI*$^+$][*pin*$^-$] derivatives of strain GT81-1C(Chernoff et al. 1999; Chernoff et al. 2000). GT81-1C is considered the wild type strain in this study, and GT349 is the isogenic strain of GT81-1C with deletion of gene *ubc4*. GT573, GT574 and GT575 are the spontaneous mutants obtained from polyglutamine cytotoxicity plate assay. Among the three mutants, GT574, which is the No. 7 *AQT* mutant, is most commonly used throughout this study.

Plasmids

Plasmids used in this study are listed in APPENDIX B Table B.1, in which the yeast selection markers and plasmid types are included. PolyQ/QP producing constructs were described previously (Meriin et al. 2002; Wang et al. 2009). Centromeric plasmids bearing wild type or mutant (*sup45-103*) alleles of *SUP45* gene under its endogenous

promoter (Le Goff et al. 2002; Moskalenko et al. 2004) were a gift of G. Zhouravleva (St. Petersburg State University). Plasmid CEN-SUP45ΔC19, bearing the deletion of 19 C-terminal codons in *SUP45*, that impairs protein function and its interaction with Sup35 (Kallmeyer et al. 2006), was a gift of D. Bedwell (University of Alabama at Birmingham). Centromeric plasmid bearing the *SUP45ΔC5* allele that lacks 5 C-terminal codons and causes only slight impairment of Sup45 function, was constructed inserting the 5.1kb *Bam*HI-*Hin*dIII fragment, containing *SUP45* gene, from plasmid Yep13-SUP1 (Chernoff et al. 1992), into the *Bam*HI-*Hin*dIII digested vector pRS315 (Sikorski and Hieter 1989). The galactose-inducible *SUP45* plasmid, containing the *SUP45* cDNA under the control of *GAL1* promoter, was previously isolated in Chernoff laboratory in a library screen aimed at amelioration of excess Sup35 toxicity. The CEN-SUP35C plasmid was constructed by inserting the *Pst*I-*Xba*I fragment, bearing the *SUP35C* region under the endogenous *SUP35* promoter, from plasmid pEMBL-yex-SUP35 del3ATG (Ter-Avanesyan et al. 1993), into pRS315. The *Eco*RI-*Sac*II fragment containing copper promoter and NM domains of Sup35 from plasmid pmCUPNMsGFP (Serio et al. 1999) was inserted into the corresponding sites in vector pRS315, and DsRed2 from pDsRed2-N1 (Clontech) was fused in frame with the Sup35NM to yield the plasmid pCUP-Sup35NM-DsRed. The plasmid overexpressing *UBC4* was constructed by subcloning the *UBC4* ORF between the *GAL1* promoter and *CYC1* terminator in pTRP (Laney and Hochstrasser 2003). Plasmids carrying the promoter and N-terminal domains

of the yeast *PGK* gene, fused to the bacterial β-galactosidase (*lacZ*) gene either in frame or via a UGA stop codon (Firoozan et al. 1991) were a gift of M. Tuite (University of Kent).

Primers

Primers used in this study were synthesized DNA oligonucleotides without modifications from Invitrogen and IDT. Refer to Appendix C for a full list of primers.

Antibodies

Rabbit polyclonal antibodies to Sup35C and Sup45 were generous gifts from Dr. D. Bedwell. Anti-GFP, N-terminal antibody produced in rabbit was purchased from Sigma-Aldrich. Purified Ade2p, kindly provided by Dr. V. Alenin, was used to raise rabbit polyclonal antibody to Ade2 by Cocalico, Inc.

Secondary antibody, Anti-Rabbit HRP, for regular Western Blot experiments was purchased from Sigma-Aldrich. DyLight 549 Goat Anti-Rabbit secondary antibody, from Jackson ImmunoResearch Laboratories, Inc., was used for immunofluorescence microscopy.

Methods

Standard Yeast Media and Growth Conditions

Standard yeast media, procedures (including transformation, phenotype scoring, velveteen replica plating, mating and sporulations) were used (Sherman 2002).

Synthetic complete media lacking adenine, leucine, uracil, tryptophan, and histidine were designated as -Ade, -Leu, -Ura, -Trp and -His, respectively. Induction media for *GAL*-inducible plasmid constructs contained 2% galactose instead of dextrose for plate assays and additional 2% raffinose was added for the induction in liquid cultures. 200 μM $CuSO_4$ was used to induce genes under the *CUP* promoter. Yeast cultures were grown at 30°C except for the temperature-sensitivity assays (employing 39°C). Liquid cultures took up at least 1/5 volumeric ratio of liquid/flask and grew in the 30°C shaking incubator at the speed of 200-250 rpm.

To prepare diploid cell for tetrad dissection experiments, cells were patched onto presporulation medium (0.8% yeast extract; 0.3% peptone; 10% dextrose; 1.5% agar and 10X adenine) overnight prior to being patched onto sporulation medium (10 mM CH_3COOK; 0.05% dextrose; 0.1% yeast extract; 1.5% agar; amino acids of corresponding auxotrophic markers).

E. coli Transformation

Competent *E. coli* Dh5 α cells were thawed on ice. Aliquot 50 μl cell suspensions for each transformation reaction. Add 1 μl plasmid and mix well with competent cells. Let tube stand on ice for 30min before a heatshock at 42°C for 30 sec.

Insert tube into ice immediately after heatshock to cool for 1-2 min. Add prewarmed SOC 500 µl and incubate with rotation at 37°C for 1 hour. Collect cells at 6000 rpm for 2 min. Discard the supernatant and plate all cells onto LB agar medium with proper selectable antibiotic marker carried by the plasmid.

Yeast Transformation

Yeast transformation was done according to the standard protocol using the lithium treatment approach with minor modifications. Tranformation mixture was heatshocked at 42°C for 5-7 min, and plated onto synthetic dropout media selecting the appropriate auxotrophic markers beared by the plasmids or plated onto YPD for 1 day before being replica plated onto antibiotic containing YPD if the selectable marker is an antibiotic resistant gene.

Micromanipulation

Cells were incubated on sporulation medium for 3-5 days. Sporulation was confirmed first by resuspending a small aliquot of sporulating culture into 5 µl water and checking under the microscopy. Resuspend sporulating culture in 40 µl ddH_2O with 2 µl of 4 mg/ml lyticase. Incubate at 37°C for 10 min. Spin cells down at 3000 rpm for 1min. Discard the supernatant and gently resuspend cell pellet in 300 µl ddH_2O. Transfer 10-20 µl the lyticase treated diploid cells onto the dissecting plate and let it dry. Tetrad

dissection was performed by using MSM System 300 micromanipulator from Singer Instrument Co. Ltd.

Thermotolerance Assay

Thermotolerance assay was used to test the thermoresistance of *AQT* strain and its derivatives on the growth at 39°C. Cultures were grown in liquid media for 1 day and counted using the hemocytometer. Adjust the cell concentrations of each culture according to the cell counts, and make serial dilution spotting onto appropriate media. Pictures were scanned after 2 days of incubation in 30°C (control) and 39°C.

Plate Assay for Polyglutamine Cytotoxicity

Polyglutamine cytotoxicity was detected as growth inhibition on the synthetic dropout medium with galactose instead of glucose where polyglutamine constructs were selectively maintained and induced. Unless specified otherwise, velveteening plates were scanned after 5-6 days of incubation after a second passage from galactose medium, and spotting plates were scanned after 3-5 days of incubation.

Bacterial Plasmid DNA Isolation

Alkaline lysis method(Sambrook and Russell 2001) with modifications is used for both mini-prep and maxi-prep of plasmid DNA from *E. coli*. A single colony is inoculated into LB liquid medium (10g/L tryptone, 5g/L yeast extract, 10g/L NaCl, pH

7.0) with proper antibiotic (ie, 50 μg/ml Ampicilin) to grow overnight. Cells are pelleted at 10,000 rpm for 10min and resuspended with 1X TE buffer (100mM Tris-HCl, 10mM EDTA, pH 8.0). Solution II (0.2M NaOH, 1% SDS) is added to the cell suspension. Mix by inverting tubes for 5 times, then add solution III (3M KAc, pH 5.0). Invert tubes for 5 times and place on ice for 5min. Volumes of solution I, II and III added should follow the ratio 1:2:1.5. Spin lysed cell suspension at 10,000 rpm for 20min to pellet cell debris. Transfer the supernatant into a new tube, mix with 0.6 volume of isopropanol, and incubate on ice for 15min. Centrifuge at 10,000 rpm for 10min. Add 0.5ml of ddH_2O to resolve the pellet and transfer to an eppendorf tube. Add 0.3ml 9M $(NH_4)Ac$, incubate at -20°C for 20min, then spin at 13,000 rpm for 5 min. Transfer the supernatant into a new tube and mix well with 0.6 volume of isopropanol, then incubate on ice for 15min. Pellet DNA by spinning at 13,000 rpm for 5min. Wash the pellet with 1ml 70% ethanol, centrifuge again, and discard the supernatant as much as possible. Briefly dry the pellet, then dissolve it in ddH_2O with 0.1mg/ml RNase.

Yeast Plasmid DNA Isolation

Grow yeast in 50ml of selective medium to OD ~ 1.5 at 600nm. Collect cells, resuspend the cells in 0.5ml of (1M Sorbitol, 0.1M EDTA, pH 8.0). Add 20μl of 4mg/ml Lyticase solution and incubate at 37°C for 2 hours. Centrifuge at 3000 rpm for 1min, and remove the supernatant as much as possible, then resuspend the cells in 200μl of TE by

pipetting gently. Mix with 400µl of (0.2M NaOH, 1% SDS) by inverting the tube several times. Incubate at room temperature for 30min. Add 300µl of 5M KAc, pH 4.8. Place on ice for at least 30min. Centrifuge for 10min at 4°C. Transfer the supernatant to a new tube and add 600µl of isopropanol. Mix by inversion. Incubate for 20min at room temperature, then centrifuge for 5min at 13,000 rpmn. Wash with 70% ethanol. Spin at 13,000 rpm for 5min, then dry the pellet briefly. Resuspend the pellet in 50µl of ddH_2O. Take 10-15µl to transform a 50µl culture of *E. coli* competent cells.

Yeast Genomic DNA Isolation

Yeast DNA mini-prep procedure from Methods in Yeast Genetics: A Laboratory Course Manual (Sherman et al. 1987) with modifications is used to isolate yeast genomic DNA.

Grow cells overnight to reach stationary phase in YPD liquid medium at 30°C. Pellet cells at 3000 rpm for 5min, and then discard the supernatant. Resuspend the cells in 0.5ml of (1M Sorbitol, 0.1M EDTA, pH 7.5); transfer to an eppendorf tube. Add 20µl of 4mg/ml lyticase solution and incubate at 37°C for 60-90min. Centrifuge at 4000 rpm for 1min. Discard the supernatant and resuspend the cells in 0.5ml of (50mM Tris-HCl, 20mM EDTA, pH 7.4) by pipetting. Add 55µl of 10% SDS, and mix well by inversion. Incubate at 65°C for 30min, then add 0.2ml of 5M KAc and incubate on ice for 60min. Centrifuge at 13,000 rpm for 5min. Transfer the supernatant to a new eppendorf tube and

add 0.75ml of isopropanol. Mix by inversion and centrifuge at 13,000 rpm for 5min. Wash the pellet with 70% ethanol, spin for 3 min at 13,000 rpm, and briefly dry the pellet. Resuspend the pellet in 50-100µl ddH_2O with 100µg/ml RNase. Warm pellet to 55°C to help dissolve if needed.

Yeast genomic DNA prepared this way is good for regular PCR reactions. If used for sequencing, additional purification steps are required.

DNA Electrophoresis

1% argarose in 1X TAE buffer is used to make the DNA electrophoresis gel. DNA electrophoresis is run under a constant voltage no more than 10V/cm of the gel. DNA bands were visualized

Restriction Digestion and Ligation

Digestion and ligation procedures follow the standard protocols(Sambrook and Russell 2001). Restriction enzymes are purchased from New England BioLabs, Inc.

PCR

PCR reactions were performed according to the standard protocol. Taq DNA polymerase with ThermoPol buffer was purchased from New England BioLabs, Inc. Phusion High Fidelity PCR Master Mix (manufactured by New England BioLabs) was used to amplify DNA fragments longer than 5kb.

PCR-Based Gene Deletion

The individual gene deletions were made by using PCR-mediated transplacement with the cassette bearing either *Schizosaccharomyces pombe HIS5* gene, an ortholog of *S. cerevisiae HIS3* gene (thus designated in this work as *HIS3*), or bacterial *kan*^{r} gene, which is resistant to G418 (Longtine et al. 1998). PCR was performed using primers containing 40-50 bp homologous sequences flanking the region to be deleted and 20 bp complimentary to the plasmid vector bearing the selectable marker. PCR amplified DNA fragment was used to transform yeast cells. Transformants were selected either on the synthetic dropout medium (auxotrophic gene marker) or plated on YPD for one day before being replica plated onto antibiotic containing YPD (antibiotic resistant gene marker). Resulting transformants were subject to be confirmed by PCR and sequencing analysis.

Constructions of Chromosomal Deletions

Chromosomal deletions in the extra copy of chromosome II were made in two consecutive steps of PCR-mediated genome alteration. The first step involved the insertion of a cassette containing *KlURA3* and *hyg* genes into the targeted regions as counterselectable markers (Storici and Resnick 2006); the second step employed the replacement of targeted regions with *LEU2* gene amplified from vector pRS315 (Sikorski

and Hieter 1989). Resulting $Ura^{-}Leu^{+}$ hygromycin sensitive transformants were subject to PCR and sequencing analysis to verify the deletions.

Transposon Mutagenesis and Identification of Insertion Locations

A transposon insertion library was used in the initial screening of *AQT* gene(Kumar and Snyder 2001). Each plasmid from the insertion library carries a picec of yeast genomic DNA with a single random insertion of a bacterial transposon and a selectable marker *LEU2*. The transposon mutagenized library was introduced into yeast by regular transformation of the plasmid DNA from each pool (total 15 pools) of the library. Library DNA was transformed into *E. coli* ensuring approximately 100,000 transformants per pool. Transformants were collected by adding 6 ml of LB medium onto the plate and scrape cells off to an eppendorf tube. Resuspended *E. coli* transformants into LB with 3 μg/ml tetracycline and 40 μg/ml kanamycin and grew at 37°C. Saturated cell culture was subject to standard plasmid DNA isolation.

*Not*I digested insertion library DNA of 2.1 kb length was used to transform yeast cells. Total 30,000-50,000 colonies were screened to ensure 95% coverage of the genome. Vectorette PCR was used to identify the insertion sites as follows. Yeast genomic DNA was digested with *Alu*I, which was intactivated by heating 20 min at 65°C after a overnight digestion. Adaptor were made by annealing primer ABP1 and ABP2 (ABP1: GGAGGAGAGGACGCTGTCTGTCGAAGGTAAGGAACGGACGAGAGAAGGGAG

AG; ABP2:

GACTCTCCCTTCTCGAATCGTAACCGTTCGTACGAGAATCGCTGTCCTCTCCT

TC) in 200 µl of annealing buffer (10 mM Tris, 10 mM $MgCl_2$, 50 mM NaCl) at 70°C for 5 min then slowly cooled to room temperature. The adaptors were ligated with the digested genomic DNA fragments. Standard PCR using primers UV and M13-47 (UV: CGAATCGTAACCGTTCGTACGAGAATCGCT; M13-47: CGCCAGGGTTTTCCCAGTCACGAC) was performed and purified PCR product containing piece of yeast genomic DNA that was adjacent to the insertion was sequenced with primer PRSQZ (CGACGGGATCCCCCTTAACG).

Pulse Field Gel Electrophoresis

Yeast cells were cultured in YPD for 1 day and 2 $x10^8$ cells were collected from each sample. Treat cells in buffer of (270µl 0.5M EDTA pH 7.5, 3µl 1M Tris, and 30 µl 5mg/ml lyticase). Add 210 µl 2% low melting temperature agarose (IBI Scientific) gel in 0.1 EDTA at 42°C. Load agarose cell suspension into the plug mold (Bio-Rad). Plugs were incubated in 800µl 0.5M EDTA, 8µl 1M Tris at 37°C for 2-4 hours, then incubated at 30°C overnight with addition of 200µl proteinase K (5% sarcosyl, 5mg/ml proteinase K in 0.5M EDTA, pH 7.5). Plugs were sliced and equilibrated for 30min in 4 ml of 0.5 X TBE prior to loading onto the gel, and then covered with 0.5% agarose gel to immobilized the plugs in the gel well. 1.5% agarose gel was used and run in 0.5X TBE

for 40 hours in Bio-Rad CHEF (Contour-clamped Homogeneous Electric Field) Mapper XA following the protocol described previously (Narayanan et al. 2006).

Southern Blot

Soak the DNA agarose gel in depurination solution (0.25M HCl) for 10 min, then rinse once by dH_2O. Denature the DNA for 25min in denaturation solution (1.5M NaCl, 0.5M NaOH), then rinse once by dH_2O. Neutralize for 30 min in neutralization solution (1.5M NaCl, 0.5M Tris, 1mM EDTA, pH 7.2), then rinse once by dH_2O. DNA was transferred to Hybond-N^+ membrane (GE Healthcare) by capillary blotting. Specific chromosomes were identified by either using Random-Prime kit (GE Healthcare) or P^{32} labeled probes.

Protein Isolation and Differential Centrifugation Assay

For protein isolation, cells were destroyed by vortexing with glass beads in the lysis buffer (25 mM Tris-HCl, pH 7.5; 0.1 M NaCl; 10 mM EDTA; 4 mM PMSF; 200 µg/ml Cycloheximide; 2 mM Benzamidine; 20 µg/ml Leupeptin; 4 µg/ml Pepstatin A; 1 mM NEM; Roche cOmplete protein inhibitor cocktails of suggested dose), and cleared of cell debris at 735 g. Protein concentrations were measured by Bradford reagent (BioRad) and if necessary, verified by coomassie staining of the SDS-PAGE gels. Differential centrifugation experiments employed 8,000 g for 10 min at 4°C unless specified otherwise. Pellets were resuspended in the volume of lysis buffer that was equivalent to

the volume of supernatant. Protein samples were always boiled prior to loading onto SDS-PAGE.

SDS-Polyacrylamide Gel Electrophoresis (SDS-PAGE)

Prepare the SDS-polyacrylamide gel as follows: 10% separating gel for two (H_2O 2.64 ml; 30% acrylamide 3.33ml; 2% bis-acrylamide 1.33ml; 1.5M Tris pH 8.8 2.5ml; 10% SDS 100 µl; 10% APS 100 µl; TEMED 4µl), and 4% stacking gel for two (H_2O 3.1ml; 30% acrylamide 0.833ml; 2% bis-acrylamide 0.332 ml; 1M Tris pH 6.8 0.63ml; 10% SDS 50µl; 10% APS 50µl; TEMED 7µl)

Electrophoresis was run with electrode buffer (25mM Tris, 192 mM glycine, 0.1% SDS, pH 8.3) under 100V for 2-3 hours.

Semi-Denaturing Detergent – Agarose Gel Electrophoresis

Semi-Denaturing Detergent-Agarose Gel Electrophoresis (SDD-AGE), used to fractionate the SDS-resistant protein polymers according to their sizes, was performed according to the standard protocol (Halfmann and Lindquist 2008). Proteins were isolated in the same lysis buffer described previously with the exception that the dose of Roch cOmplete protein inhibitor cocktails was doubled. Cell debris was cleared by centrifuging the lysate at 7000 rpm (4000g) for 2 min. Proteins were diluted in 2% SDS sample buffer, incubated for 5 min at room temperature before loading, and run in the 1.5 % agarose gel

with 0.1% SDS in 1X TAE buffer containing 0.1% SDS at 4°C at 86V for 45 min and then 36Vuntil the dye reached 1cm from the end of the gel.

Western Blotting and Immunodetection

After SDS-PAGE, proteins were transferred onto Hybond ECL nitrocellulose membrane (GE Healthcare) in Wet Blotting System from Bio-Rad at 285 mA for 45 min. After SDD-AGE, protein was transferred from agarose gel to nitrocellulose membrane (Whatman) by capillary blotting overnight in 1X PBS buffer containing 0.1% SDS.

Membranes were blocked in 5% non-fat milk for at least 1 hour before reacted to proper primary antibodies, and secondary antibodies. Reaction was detected by using the chemiluminescent detection reagents as described in the GE Healthcare protocols. Densitometry was performed to determine relative protein levels using the VisionWorks LS program from UVP (UVP, LLC, Upland, CA).

Fluorescence Microscopy

GFP and/or DsRed visualization in live cells was typically performed after 6 hours of induction in liquid media containing 2% galactose and 2% raffinose, and/or 200 μM $CuSO_4$, depending on the promoter(s) used. A 5 μl aliquot of culture was place on the center of a glass slide and covered with a cover slip. The cover slip was then sealed with clear nail polish. Fluorescnece was detected under a BX41 microscope (Olympus) with

the endow GFP bandpass emission (green) or tetramethyl rhodamine isocyanate (rhodamine/Dil; red) filters.

Immunofluorescence Microscopy

Immunofluorescence experiments was done following the protocol described previously (Wegrzyn et al. 2001). Cultures were in -Ura gal/raf medium for 12 hours induction before a final concentration of 4% formaldehyde was added to fix the cells for 30 min shaking at 25°C. Cells were then spun down at 3000 rpm for 5 min, washed twice in solution B (100 mM potassium phosphate buffer pH 7.5, 1.2M sorbitol). Cell pellets were resuspended in 0.5 ml solution B with 1 µl of β-mercaptoethanol and 5 µl of 4 mg/ml lyticase and incubated at 37°C for 30 min. Cells were precipitated again and washed twice with solution B. Fixed cells with destroyed cell walls were then resuspended in 100 µl of solution F (100 mM potassium phosphate buffer pH 7.4, 1mg/ml BSA, 15 mM NaN_3, 15 mM NaCl) with a 1:500 dilution of appropriate primary antibody, incubated for 1 hour, washed 10 times with solution F, and resuspended in solution F containing the secondary antibody (see **Antibodies**), incubated in the dark for 1 hour, washed 10 time with solution F and resuspended in antibleaching mounting solution (1 mg/ml *p*-phenylenediamine in 1X PBS and 90% glycerol). A 5 µl aliquot was place on a glass slide, covered by a cover slip, and sealed in clear nail polish. The slides can be stored in the dark at 4°C for a week.

Confocal Microscopy

The colocalization experiments were performed by using LSM510 Laser Scanning Microscope (Karl Zeiss MicroImaging GmbH, Germany), with argon laser Ex 488-543 (FITC/CY3), 488 nm for GFP detection, and helium-neon laser Ex 488-543 (FITC/CY3), 543 nm for red fluorescence detection. The pinhole size was 106 μm. Software packages ZEN 2009 and ZEN 2009 Light Edition were used for picture taking and analysis.

Microarray Analysis

Genomic DNA of *AQT* derivatives as well as controls was hybridized to the complete DNA microarray of the *Saccharomyces cerevisiae* genome, as described previously (Lemoine et al. 2005). Comparative Genomic Hybridization (CGH) analysis was performed to determine the copy number of genes in *AQT* derivatives. The Cluster Along Chromosome (CLAC) consensus plot was generated using CGH-Miner (Wang et al. 2005).

Assay for Beta-Galactosidase Activity

Assay for β-galactosidase activity was performed according to standard protocol (Russell et al. 1986). Cultures were first inoculated in -Ura -Trp glucose medium to select for both *lacZ* and polyglutamine plasmids. Cells were collected and washed in ddH_2O for 3 times before introduced into -Ura -Trp galactose/raffinose medium for 24 hours

induction of overexpression of polyglutamine. Cultures were grown to reach OD_{600} less than 1.0. The OD at 600 nm was measured three times for each sample.Place 1 ml of culture into an eppendorf tube (each sample was tested in triplicates), and spun at maximal speed for 2 min. Pellet was washed by Z buffer once, and spun at maximal speed for 5min. Cell pellet was resuspended in 150 µl of Z buffer with β-mercaptoethanol. 50 µl of chloroform and 20 µl of 0.1% SDS were added to each tube. Mix by vortexing at high speed for 15 sec. 700 µl of pre-warmed (30°C) 1 mg/ml ONPG solution in Z buffer with β - mercaptoethanol was added, and time was recorded at this point. Reaction was carried out in a 30°C waterbath till a pale yellow color was observed. Reactions were stopped by adding 500 µl of 1M Na_2CO_3 and vortexing for 10 sec. Cell debris was pelleted at maximal speed for 2 min. Supernatant was taken for OD measurement at 420 nm.

Miller Units was calculated using the following formula (OD_{420} was the absorbance reading at 420 nm, OD_{600} was the absorbance reading at 600nm, min was the reaction time in minutes, ml was the reaction volume in ml):

Miller Units = $(OD_{420}*1000)/(OD_{600}*min*ml)$

CHAPTER 3

GENETIC BASIS OF *AQT*

Materials and Methods

Strains and Plasmids

Yeast strains GT532-9A and GT532-9C are Aqt$^-$ segregants of GT532, which is the diploid homozygous by *ubc4*Δ and heterozygous by *AQT*, made by crossing *AQT* derivative No. 2 with [*pin*$^-$ *psi*$^-$] *ubc4*Δ strain. The resulting diploid served as non-*AQT* control strains in plate toxicity assay for attempt of identification of *AQT* using transposon mutagenesis library. GT532 was used to screen library pools #22, #24, #28, #36, and #37. And GT534, made by crossing *AQT* derivative No. 7 with [*pin*$^-$ *psi*$^-$] *ubc4*Δ strain was used to screen library pools #21, #23, #25, #26, #27, #29, #31, #34, #35, and #38. The strain used for centromere-linked gene deletion was GT532-9A.

Plasmids bearing 103Q and 25Q with *URA3* marker were used in polyglutamine toxicity assay on -Ura/Gal medium. Plasmid construct used for centromere-linked gene disruption contained *Kan*^{r}gene, which conferred the resistance to G418, and was described in (Longtine et al. 1998) previously. YPD agar plates containing 0.3% G418 were used to select deletion potentials after yeast plasmid transformation and 1 day growth on plain YPD agar plates.

Methods

See Chapter 2 Methods for detailed description of pulse field gel electrophoresis, and microarray analysis.

In tetrad analysis, for each experiment at least 20 full tetrads containing 103Q plasmid were tested through plate toxicity assay on -Ura/Gal. Genetic locus information and gene sequences were obtained from *Saccharomyces* Genome Database (http://www.yeastgenome.org/).

Results

Attempt of Identification of *AQT* gene by Transposon-Mutagenesis

As previously characterized (see description of characteristics of *AQT* mutants in Chapter 1), *AQT* was determined to be in a single and the same genetic locus for all three isolates and exhibit dominance according to classic tetrad analysis, in which different isolates were mated to each other or isogenic WT strain of the opposite mating type.

In order to identify the gene altered by the *AQT* mutation, we have attempted the transposon mutagenesis approach, aimed at inactivation of the dominant *AQT* allele in the [*PSI*$^{+}$] diploid, homozygous by *ubc4*Δ and heterozygous by *AQT*. A yeast genomic library with transposon insertions was employed (Kumar and Snyder 2001). Each plasmid from the transposon mutagenesis library carry a piece of yeast genomic DNA flanked by *Not*I restriction sites (Figure 3.1A), in which a DNA cassette containing

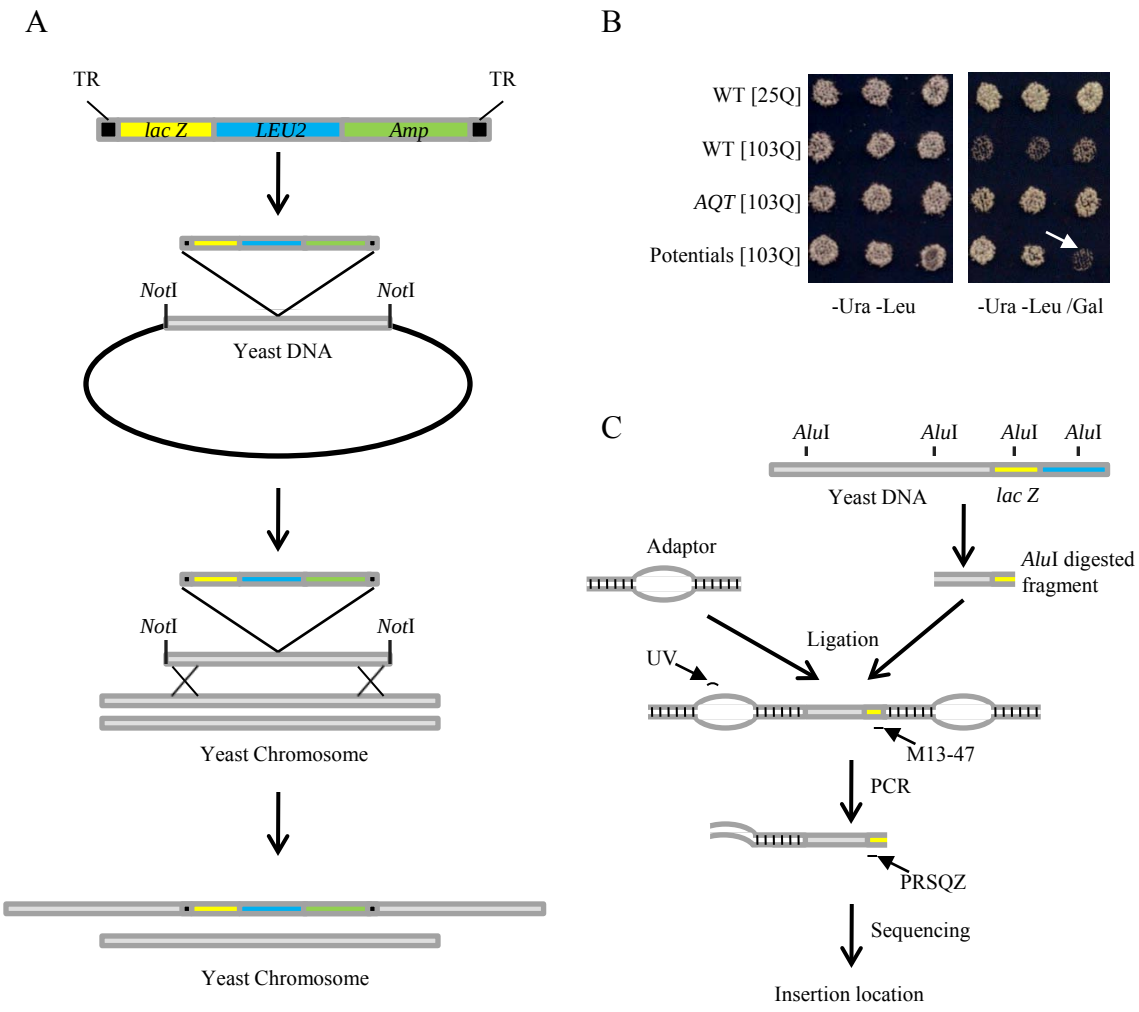

Figure 3.1 Experimental design of the transposon insertion library screening.
A – Transposon mutagenesis library. The transposon cassette contains *lacZ*, *LEU2*, and *Amp* genes, flanked by Tn3 terminal inverted repeats (TR). The insertion cassette was inserted into yeast genome. Each plasmid of the library bears a piece of transposon cassette containing yeast DNA with *Not*I restriction enzyme on the ends. The *Not*I-*Not*I fragment is used to transform yeast cells, resulting in transformants with transposon cassette intergrated into the genome.
B –Plate toxicity assay was performed to identify the preliminary potentials for additional confirmation. A positive potential out of three potentials shown is indicated by the arrow.
C – Identification of the insertion location using vectorette PCR. *Alu*I digested yeast genomic DNA was ligated with adaptors. Primers from inside the bubble of the adaptor and gene in the insertion cassette are used to amplify a fragment containing the respective pieces of genomic DNA where the insertion happen. Subsequent sequencing analysis gives the insertion location information.

flanking Tn3 terminal inverted repeat, a 5' truncated *lacZ* gene for β-glactosidase activity assay, a *LEU2* gene for plasmid selection in yeast, and an amp^r gene for plasmid selection in bacteria.

The *Not*I digested fragment from each library pool was used to transform the [PSI^+] diploid, homozygous by *ubc4*Δ and heterozygous by *AQT*. The transposon-containing cassettes were integrated into the genome via homologous recombination. As previously demonstrated, diploid heterozygous by *AQT* exhibited *AQT* effect in the presence of 103Q due to the dominance of *AQT* allele, whereas WT homozygous by *aqt-wt* suffered polyglutamine toxicity as shown in Figure 3.1B. Transformants were selected on -Ura -Leu medium after transformation to ensure both successful insertion of transposon cassettes and the presence of 103Q plasmid. Ura^+ Leu^+ transformants were patched as deletion potentials together with proper controls to be checked on -Ura -Leu/ Gal medium for polyglutamine toxicity assay. Potentials which became Aqt^- (pointed by an arrow in Figure 3.1B) were collected for further identification.

To obtain at least 30,000 transformants in total from all 15 pools of library plasmids, which ensures the 95% coverage of the yeast genome, no fewer than 50 master plates with 55 potentials on each plate were screened for each library pool. 15 potentials that have lost Aqt^+ were performed the vectorette PCR (Figure 3.1C). Genomic DNA of potentials was isolated and digested with *Alu*I restriction enzyme. Adaptors made by

annealing primers ABP1 and ABP2 at 70°C for 5 min then slowly cooling to room temperature in 2 hours. *Alu*I digested genomic fragments were ligated with adaptors. Then PCR with primers UV and M13-47 was conducted using the ligation mixture as the template. Purified PCR products of 7 out of the 15 potentials were sent out for sequencing. Four potentials were identified to have the insertion within an ORF. These ORFs are *GRS2*, *MGE1*, *TID3*, and *MSS1*. However, none of these insertions was linked to *AQT* as demonstrated by sporulation and tetrad analysis (data obtained by Nina Romanova), suggesting that in each case, loss of Aqt^+ phenotype occurred by a mechanism distinct from alteration of the mutant *AQT* allele.

Out of 14,000 transformants obtained from 7 pools in screening, 88 potentials were isolated. Based on the high possibility that majority of the potentials were false positive potentials, an experimental strategy involving extensive genetic crossing, sporulation and tetrad dissection were utilized. Potentials were first placed on sporulation medium to reach a sporulation rate of at least 10-20%, which was determined by counting the tetrads under a microscope. Haploid *AQT* strain previously transformed with a plasmid vector carrying *TRP1* gene was plated on YPD to grow to a cell lawn. Potentials with sufficient sporulation rate were then velveteened onto the *AQT* cell lawn on YPD and incubated for 1 day. The YPD plate was then velveteened onto -Ura -Leu -Trp medium to select diploids that resulted from the crossing of *AQT* haploid (Trp^+) and the Aqt^- Leu^+ (Ura^+ Leu^+) spore from the Aqt^- potential. Each resulting diploid was

numbered after the same number of the original potential, and colony-purified on -Ura -Leu -Trp medium. After such preparation, the potentials were patched on masterplates and velveteened onto sporulation medium. After 4-7 days, tetrads were dissected on YPD plates and tetrad analysis was conducted. By doing this, we expected the tetrad analysis data to fall into 3 categories explained in Figure 3.2. When insertion cassette restored the WT *aqt* by the recombination with flanking homologous sequences, the first sporulation would yield all 4 Aqt^- spores with a 2:2 ratio of Leu^+ : Leu^-. By mating the sporulated culture with *AQT* haploid and selecting for the diploids containing both insertion cassette and *AQT*, the second sporulation was expected to yield tetrads of 2 Aqt^+ Leu^- and 2 Aqt^- Leu^+ spores only (Figure 3.2A). Potential artifacts that were resulted from loss of *AQT* by spontaneous crossingovers and unrelated insertion of *LEU2* were ruled out in the tetrad analysis since *AQT* and *LEU2* would follow the random assortment pattern instead of a 2:2 segregation. The second scenario was that the loss of *AQT* was due to the deletion of *AQT* allele by the insertion cassette leaving only one copy of WT *aqt* gene in the potential (Figure 3.2B). Similar to the first category, the second sporulation should yield all tetrads of 2 Aqt^+ Leu^- : 2 Aqt^- Leu^+ with the exception that *aqt* was an essential gene, and deletion of it would cause inviability of the spores. If this was the case, the only two viable spores in the tetrads would be 2 Aqt^+ Leu^- spores. The inviability would not be seen in the first sporulation step because the sporulating culture was directly mated with haploid *AQT* strain without entering mitosis. Lastly, the possibility of the *AQT* allele

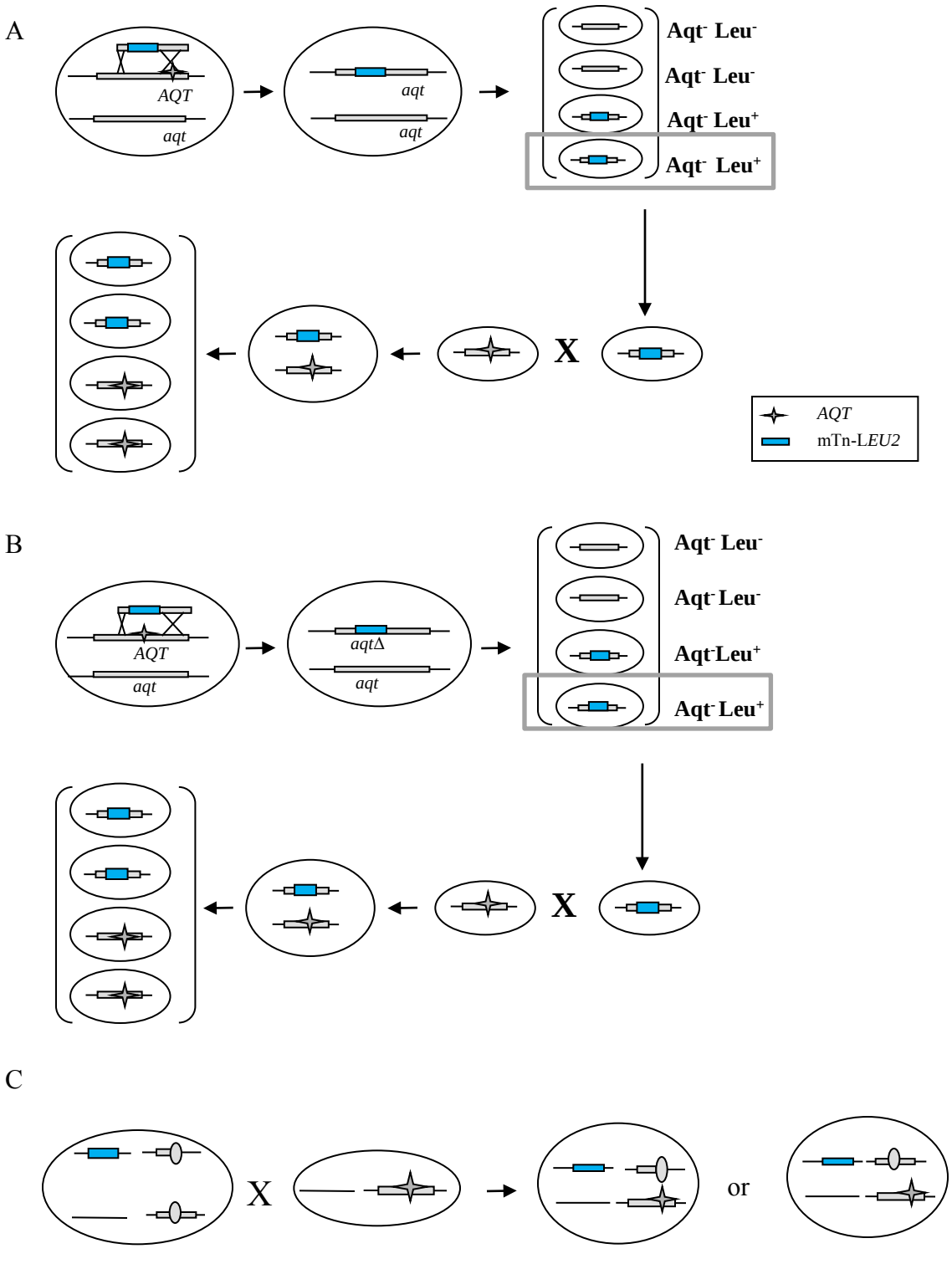

Figure 3.2 Possible scenarios that positive potentials may exhibit in tetrad analysis.
A – Insertion restores the WT copy of *AQT*.
B – Insertion deletes the mutant *AQT*.
C – Loss of *AQT* containing chromosome fragment unrelated to insertion.

containing chromosome spontaneous arm loss cannot be excluded (Figure 3.2C). The insertion cassette was not linked with *AQT* in such a situation. The tetrad analysis would show either all tetrads of 2 viable Aqt^+ spores or tetrads of 2 Leu^+: 2 Leu^- spores, however, Aqt^+ and Leu^+ were not linked to each other. Table 3.1 shows the summary of all potentials that have been tested according to this experimental strategy. 20 tetrads in total were dissected for each potential except for potential #25 (40 tetrads dissected). Only the full tetrads containing polyQ plasmid were analyzed through toxicity assay and tetrad analysis. In general, almost all insertion cassette follows the 2:2 segregation pattern, in which 2 His^+ : 2 His^- spores in each tetrad. However, Aqt^+ frequently failed to give a 2:2 segregation pattern which indicated the complication that many factors might be involved in polyglutamine cytotoxicity.

Table 3.1 Tetrad analysis of Aqt^- potentials after insertion of transposon mutagenesis library screening

Potential	**Number of full tetrads containing PolyQ plasmid**		**Phenotype**
#23	10	PD	2x(2Leu^+Aqt^- : 2Leu^-Aqt^+)
		NPD	1x(2Leu^+Aqt^+ : 2Leu^-Aqt^-)
		T	6x(1Leu^+Aqt^+ : 1Leu^-Aqt^+ : 1Leu^+Aqt^-: 1Leu^-Aqt^-)
			1x(2Leu^+Aqt^- : 1Leu^-Aqt^+ : 1Leu^-Aqt^-)
			41

#25	17	PD	1x($2Leu^{+}Aqt^{-}$: $2Leu^{-}Aqt^{+}$)
		NPD	1x($2Leu^{+}Aqt^{+}$: $2Leu^{-}Aqt^{-}$)
		T	2x($1Leu^{+}Aqt^{+}$: $1Leu^{-}Aqt^{+}$: $1Leu^{+}Aqt^{-}$: $1Leu^{-}Aqt^{-}$)
			8x($2Leu^{-}Aqt^{+}$: $2Leu^{+}Aqt^{+}$)
			3x($2Leu^{-}Aqt^{+}$: $1Leu^{+}Aqt^{+}$: $1Leu^{+}Aqt^{-}$)
			1x($2Leu^{+}Aqt^{-}$: $1Leu^{-}Aqt^{+}$: $1Leu^{-}Aqt^{-}$)
			1x($2Leu^{+}Aqt^{+}$: $1Leu^{-}Aqt^{+}$: $1Leu^{-}Aqt^{-}$)
#26	7		2x($2Leu^{+}Aqt^{-}$: $2Leu^{-}Aqt^{-}$)
			5x($2Leu^{+}Aqt^{-}$: $1Leu^{-}Aqt^{+}$: $1Leu^{-}Aqt^{-}$)
#29	16	NPD	1x($2Leu^{+}Aqt^{+}$: $2Leu^{-}Aqt^{-}$)
			5x($2Leu^{+}Aqt^{+}$: $2Leu^{+}Aqt^{-}$)
			4x($2Leu^{-}Aqt^{+}$: $2Leu^{-}Aqt^{-}$)
			2x($2Leu^{+}Aqt^{+}$: $1Leu^{+}Aqt^{-}$: $1Leu^{-}Aqt^{-}$)
			3x($2Leu^{+}Aqt^{-}$: $1Leu^{+}Aqt^{+}$: $1Leu^{-}Aqt^{+}$)
			1x($4Leu^{+}Aqt^{-}$)
#30	11		11x($2Leu^{+}Aqt^{+}$: $2Leu^{+}Aqt^{-}$)
#31	10	PD	2x($2Leu^{+}Aqt^{-}$: $2Leu^{-}Aqt^{+}$)
		NPD	1x($2Leu^{+}Aqt^{+}$: $2Leu^{-}Aqt^{-}$)
		T	6x($1Leu^{+}Aqt^{+}$: $1Leu^{-}Aqt^{+}$: $1Leu^{+}Aqt^{-}$: $1Leu^{-}Aqt^{-}$)
			1x($2Leu^{+}Aqt^{-}$: $1Leu^{-}Aqt^{+}$: $1Leu^{-}Aqt^{-}$)
#32	11	PD	2x($2Leu^{+}Aqt^{-}$: $2Leu^{-}Aqt^{+}$)
		T	5x($1Leu^{+}Aqt^{+}$: $1Leu^{-}Aqt^{+}$: $1Leu^{+}Aqt^{-}$: $1Leu^{-}Aqt^{-}$)
			1x($2Leu^{+}Aqt^{-}$: $Leu^{-}Aqt^{-}$: $Leu^{-}Aqt^{+}$)
			1x($2Leu^{-}Aqt^{-}$: $Leu^{+}Aqt^{-}$: $Leu^{+}Aqt^{+}$)
			2x($2Leu^{-}Aqt^{-}$: $Leu^{+}Aqt^{-}$: $Leu^{+}Aqt^{+}$)
#37	11	PD	1x($2Leu^{+}Aqt^{-}$: $2Leu^{-}Aqt^{+}$)
		NPD	4x($2Leu^{+}Aqt^{+}$:$2Leu^{-}Aqt^{-}$)
		T	5x($1Leu^{+}Aqt^{+}$: $1Leu^{-}Aqt^{+}$: $1Leu^{+}Aqt^{-}$: $1Leu^{-}Aqt^{-}$)
			1x($2Leu^{+}Aqt^{-}$: $1Leu^{-}Aqt^{-}$: $1Leu^{-}Aqt^{+}$)
#39	9	NPD	1x($2Leu^{+}Aqt^{+}$: $2Leu^{-}Aqt^{-}$)
			4x($2Leu^{-}Aqt^{-}$: $2Leu^{-}Aqt^{+}$)
			1x($2Leu^{+}Aqt^{-}$: $1Leu^{+}$ Aqt^{+} : $1Leu^{-}Aqt^{+}$)
			1x($2Leu^{+}Aqt^{+}$: $1Leu^{+}$ Aqt^{-} : $1Leu^{-}$ Aqt^{-})
			2x($2Leu^{+}Aqt^{+}$: $2Leu^{+}Aqt^{-}$)
#40	13	PD	1x($2Leu^{+}Aqt^{-}$: $2Leu^{-}Aqt^{+}$)

		T	5x($1Leu^{+}Aqt^{+}$: $1Leu^{-}Aqt^{+}$: $1Leu^{+}Aqt^{-}$: $1Leu^{-}Aqt^{-}$) 2x($2Leu^{+}Aqt^{-}$: $1Leu^{-}Aqt^{+}$: $1Leu^{-}Aqt^{-}$) 1x($2Leu^{-}Aqt^{+}$: $Leu^{-}Aqt^{-}$: $Leu^{+}Aqt^{-}$) 1x($2Leu^{-}Aqt^{-}$: $Leu^{+}Aqt^{+}$: $Leu^{+}Aqt^{-}$) 1x($2Leu^{+}Aqt^{+}$: $Leu^{-}Aqt^{-}$: $Leu^{+}Aqt^{-}$) 1x($2Leu^{-}Aqt^{-}$: $Leu^{+}Aqt^{-}$: $Leu^{+}Aqt^{-}$) 1x($2Leu^{-}Aqt^{-}$: $Leu^{-}Aqt^{+}$: $Leu^{+}Aqt^{+}$)
#43	7	PD	2x($2Leu^{+}Aqt^{-}$: $2Leu^{-}Aqt^{+}$)
		NPD	1x($2Leu^{+}Aqt^{+}$: $2Leu^{-}Aqt^{-}$)
		T	4x($1Leu^{+}Aqt^{+}$: $1Leu^{-}Aqt^{+}$: $1Leu^{+}Aqt^{-}$: $1Leu^{-}Aqt^{-}$)
#44	10	PD	1x($2Leu^{+}Aqt^{-}$: $2Leu^{-}Aqt^{+}$)
		T	4x($1Leu^{+}Aqt^{+}$: $1Leu^{-}Aqt^{+}$: $1Leu^{+}Aqt^{-}$: $1Leu^{-}Aqt^{-}$) 2x($2Leu^{+}Aqt^{+}$: $2Leu^{-}Aqt^{+}$) 2x($2Leu^{+}Aqt^{+}$: $1Leu^{-}Aqt^{+}$: $1Leu^{-}Aqt^{-}$) 1x($2Leu^{-}Aqt^{-}$: $1Leu^{+}Aqt^{-}$: $1Leu^{+}Aqt^{+}$)
#45	11	PD	1x($2Leu^{+}Aqt^{-}$: $2Leu^{-}Aqt^{+}$)
		NPD	2x($2Leu^{+}Aqt^{+}$: $2Leu^{-}Aqt^{-}$)
		T	7x($1Leu^{+}Aqt^{+}$: $1Leu^{-}Aqt^{+}$: $1Leu^{+}Aqt^{-}$: $1Leu^{-}Aqt^{-}$) 1x($2Leu^{-}Aqt^{-}$: $1Leu^{+}Aqt^{+}$: $1Leu^{+}Aqt^{-}$)
#47	7	PD	1x($2Leu^{+}Aqt^{-}$: $2Leu^{-}Aqt^{+}$)
		NPD	4x($2Leu^{+}Aqt^{+}$:$2Leu^{-}Aqt^{-}$)
		T	1x($1Leu^{+}Aqt^{+}$: $1Leu^{-}Aqt^{+}$: $1Leu^{+}Aqt^{-}$: $1Leu^{-}Aqt^{-}$) 1x($2Leu^{+}Aqt^{-}$: $Leu^{-}Aqt^{-}$: $Leu^{-}Aqt^{+}$)
#48	12	PD	2x($2Leu^{+}Aqt^{-}$: $2Leu^{-}Aqt^{+}$) 7x($2Leu^{+}Aqt^{+}$: $2Leu^{+}$ Aqt^{-}) 2x($3Leu^{-}Aqt^{-}$:$1Leu^{-}Aqt^{+}$) 1x($2Leu^{-}Aqt^{-}$:$1Leu^{-}Aqt^{+}$: $1Leu^{+}Aqt^{+}$)
#49	10	PD	1x($2Leu^{+}Aqt^{-}$: $2Leu^{-}Aqt^{+}$)
		NPD	2x($2Leu^{+}Aqt^{+}$: $2Leu^{-}Aqt^{-}$)
		T	4x($1Leu^{+}Aqt^{+}$: $1Leu^{-}Aqt^{+}$: $1Leu^{+}Aqt^{-}$: $1Leu^{-}Aqt^{-}$) 2x($1Leu^{+}Aqt^{+}$: $1Leu^{+}Aqt^{-}$: $2Leu^{-}Aqt^{-}$) 1x($2Leu^{+}Aqt^{-}$:$2Leu^{-}Aqt^{-}$)

Centromere Linkage of *AQT*

Interestingly, #47 potential exhibited a pattern of meiotic segregation, which was indicative of centromeric localization of both insertion and *AQT* ($p < 0.01$). To explore this further, we have disrupted each of the yeast genes *met28*, *met3* and *met14*, linked to the centromeres of chromosomes IX, X and XI, respectively. Individual centromere linked gene was deleted using the plasmid containing a *KanMX* module (Longtine et al. 1998). *KanMX* was amplified using primers with 40 bp homology and 20 bp complimentary to the plasmid by PCR as a 1.6kb fragment. This PCR product was gel purified and transformed into *ubc4*Δ *aqt-wt* haploid to delete one centromere linked gene. Taking *MET3* gene for an example, *MET3* locates closely to the centromere of chromosome X, and transformation of PCR amplified *KanMX* module replaced gene *MET3* on chromosome X due to homologous recombination (Figure 3.3A). Transformants were plated on YPD for 1 day then velveteened onto G418 containing YPD. After 2-3 days, transformants that were resistant to G418 grew on the plate. Colony purified transformants were then confirmed by PCR (Figure 3.3B) and phenotypic assay (Figure 3.3C). Due the length difference between the WT gene and the *KanMX* module, PCR reactions using primers flanking the deletion locus to amplify a DNA fragment from the genomic DNA of deletion potentials was able to indicate whether the deletion was

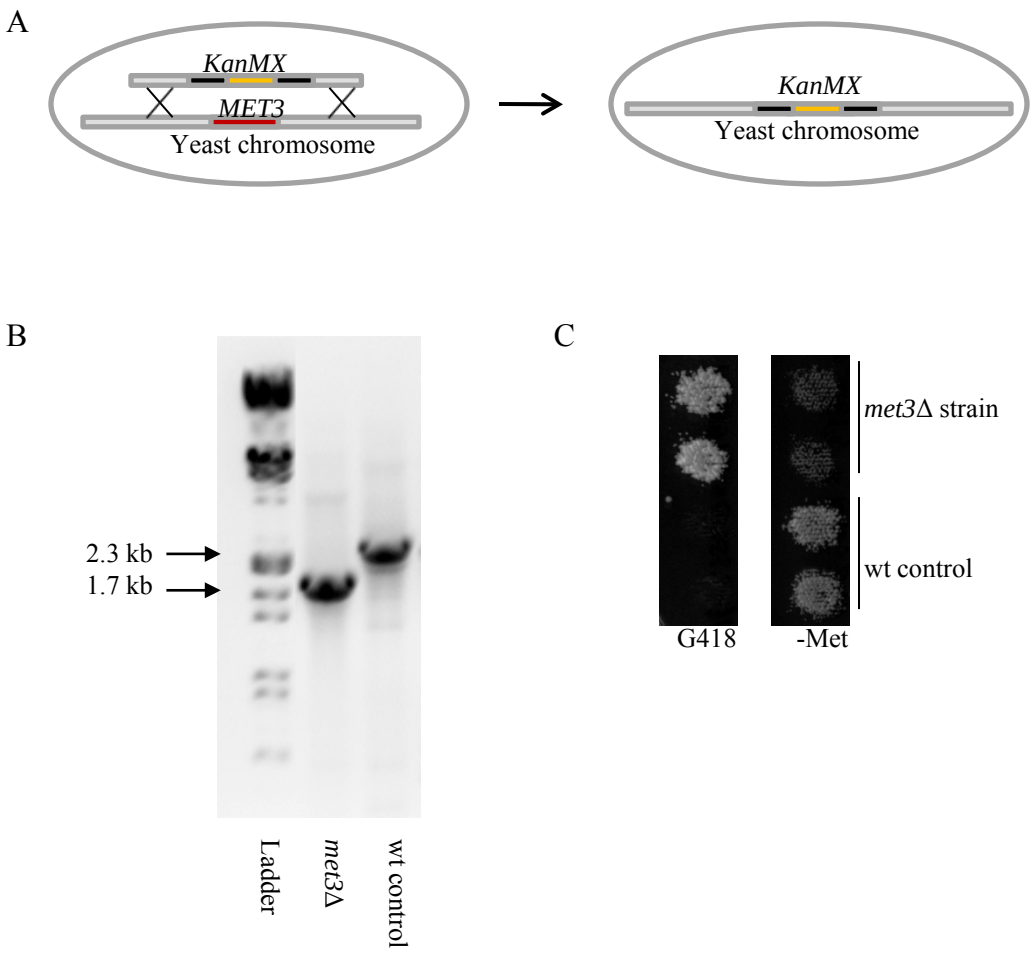

Figure 3.3 Construction of centromere-linked markers.
A – PCR-based gene deletion. Deletion cassette used for single gene deletions is PCR amplified from a plasmid bearing *KanMX* (gene for G418 resistance). Purified PCR fragment is transformed into yeast cells. Due to homologous recombination, gene to be deleted is replaced by the deletion cassette.
B – Identification of gene deletion by PCR. The example shown is identification of *met3*Δ. PCR is performed with genomic DNA using primers flanking the deletion locus. Correct deletion yields a 1.7kb PCR product, whereas the WT control is 2.3kb. The size difference enables the identification of deletion by PCR.
C – Identification of gene deletion by phenotypes. Given the example of *MET3*, which is involved in methionine synthesis, deletion does not grow on –Met medium, and grows on YPD containing G418.

successful. In the example shown in Figure 3, *MET3* is longer than the deletion module, therefore a shorter fragment was amplified in a deletion potential as compared to the WT control (Figure 3.3B). Genes specifically selected for the centromere-linked gene deletion were all involved in amino acid biosynthetic pathways. Phenotypically, correct deletion was expected to grow on YPD containing G418 and to become auxotrophic for that specific pathway (Figure 3.3C).

After both PCR and phenotypic assay confirmed the deletion to be correct, each deletion was crossed to the *AQT* strain, and resulting diploids, heterozygous by both *AQT* and respective deletion, were sporulated and dissected. If deletion and *AQT* are not linked to each other (on different chromosomes or distantly locate on the same chromosome) and *AQT* is not centromere linked, both deletion marker and *AQT* would follow random assortment, therefore tetratypes would be more frequently seen in such a case (Figure 3.4A).If deletion and *AQT* are linked to each other, crossingovers happening in between of those two genes are less likely. Parental ditype (two spores represent one parental strain) would be the predominant type of tetrads seen this case (Figure 3.4B). All experiments were performed in the *ubc4*Δ [PIN^+ PSI^+] background, enabling us to monitor *AQT* by phenotype. One typical tetrad representing each type of tetrads from the cross of *ubc4*Δ*met3*Δ and *ubc4*Δ *MET3 AQT* was shown in Figure 3.4C.

As shown in Table 3.2, combination of each deletion with *AQT* produced primarily parental (PD) and nonparental (NPD) ditypes, but essentially no tetratypes (T)

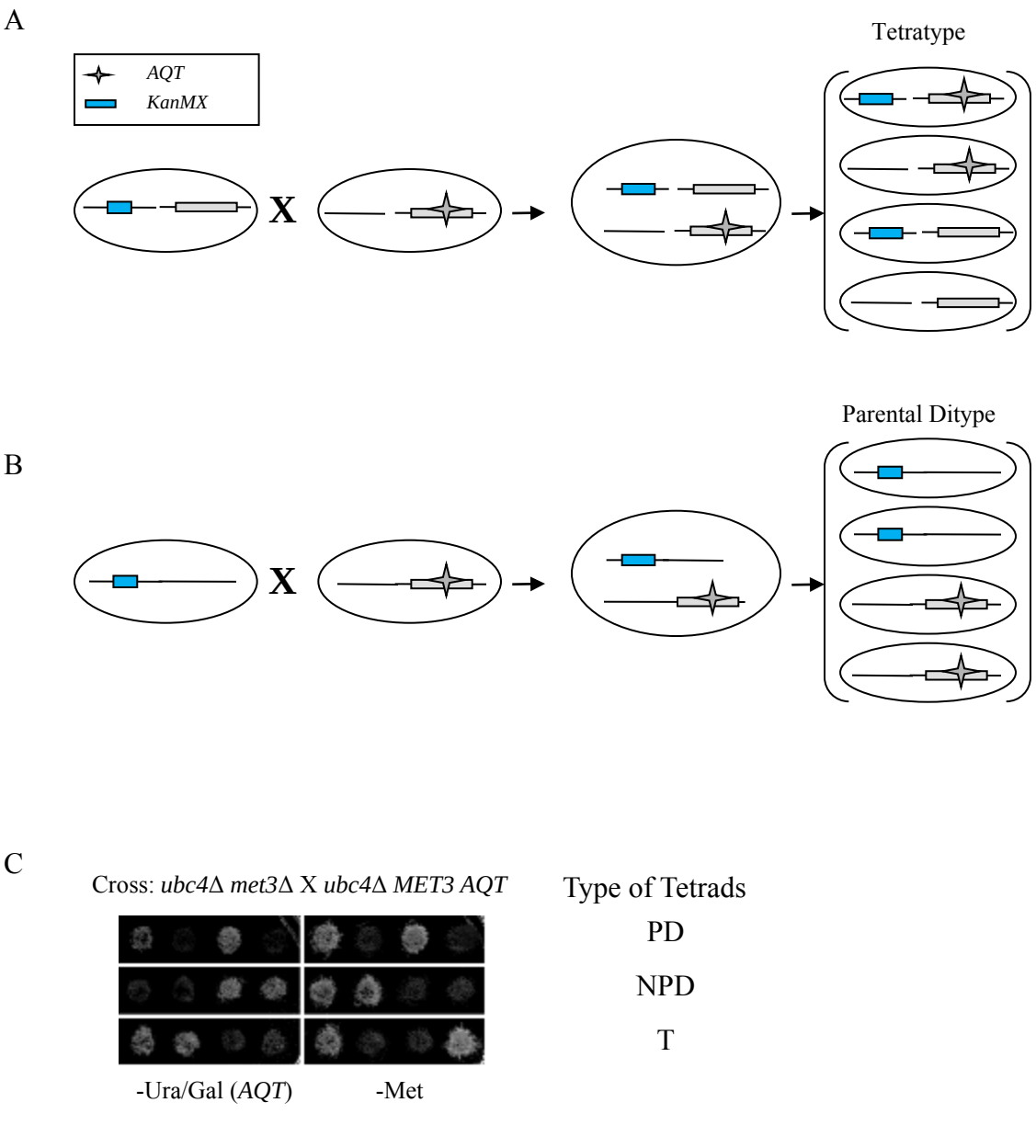

Figure 3.4 Centromeric linkage screening of *AQT* by tetrad analysis.
A and B – Strategy of locating *AQT* to a specific chromosome. Each strain with a specific centromere-linked marker is crossed to *AQT* strain of the opposite mating type. After sporulation and dissection, the predominant type of tetrads will be tetratype if there's no linkage between *AQT* and that specific chromosome, and *AQT* is not centromere linked (A). If *AQT* is centromere linked and also linked to the marker, parental ditype will be the most abundant tetrad type (B).
C – Tetrad analysis plate assay. *AQT* and *met3*Δ are assayed on –Ura/Gal and –Met media, respectively.

after sporulation and dissection. Apparently deletion and *AQT* did not follow the random assortment, which produces PD:NPD:T of 1:1:4 ratio. However, the approximately equal numbers of PD and NPD tetrads indicated the lack of linkage between *AQT* and deletion. In summary, the tetrad analysis data suggested that *AQT* is located on a different chromosome from the respective deletion, but is linked to the centromere of its own chromosome (for explanation of tetrad types, see Sherman 2002).

Table 3.2 Tetrad analysis of diploid *AQT* derivatives with individually labeled centromeres

Chromosome	**Number of full tetrads containing PolyQ plasmid**	**Phenotype**	
#9	16	PD	**8**x($2Met^-Aqt^-$: $2Met^+Aqt^+$)
		NPD	**7**x($2Met^+Aqt^-$: $2Met^-Aqt^+$)
		T	**1**x(1 Met^+Aqt^-: $1Met^-Aqt^+$: $1Met^-Aqt^-$: 1 Met^+Aqt^+)
#10	12	PD	**4**x($2Met^-Aqt^-$: $2Met^+Aqt^+$)
		NPD	**6**x($2Met^+Aqt^-$: $2Met^-Aqt^+$)
		T	**1**x(1 Met^+Aqt^-: $1Met^-Aqt^+$: $1Met^-Aqt^-$: 1 Met^+Aqt^+)
			1x($2Met^+Aqt^-$: $1Met^-Aqt^+$: $1Met^-Aqt^-$)
#11	13	PD	**6**x($2Met^-Aqt^-$: $2Met^+Aqt^+$)
		NPD	**6**x($2Met^+Aqt^-$: $2Met^-Aqt^+$)
			1x($2Met^+Aqt^-$: $1Met^-Aqt^+$: $1Met^-Aqt^-$)

***p*< 0.01 for all three dissections.**

Detection of Chromosome II Disomy in *AQT* strains by Tetrad Analysis

The next piece of information shedding light onto the molecular basis of *AQT* has come from the genetic cross in which the original *AQT* derivative, obtained in the strain bearing the *ubc4*Δ*::HIS3* disruption was crossed to the wild-type strain bearing the *ubc4*Δ*::KanMX* disruption, made with the bacterial gene *KanMX* that causes resistance to the antibiotic G418 in yeast. Originally, the disruption made in the *ubc4*Δ *aqt-wt* was targeting *HIS2* gene, which is linked to chromosome VI, with the same experimental procedure as deletions made in chromosome IX, X, XI. After sporulation and dissection, both *AQT* and *KanMX* markers segregated 2:2 as expected (Figure 3.5A). Surprisingly, majority of tetrads did show 3:1 or 4:0 segregation for the His^+ phenotype, indicating that the *KanMX* might have gone to the *ubc4* locus due to longer homology to the flanking sequence of the pre-existing *HIS3* module from the same set of the plasmids for gene deletion, and there were two copies of the *HIS3* allele in the *AQT* haploid. Notably, all *AQT* spores (76 total) obtained from tetrads with 2:2 ratio for *KanMX* were His^+, and all His^- spores were G418 sensitive and Aqt^- (See Table 3.3 for tetrad analysis data). Large proportion of tetratype and low proportion of parental ditype indicated high frequency of meiotic trisomy chromosome pairing events in diploid yeast cells (Loidl 1995). PCR

A

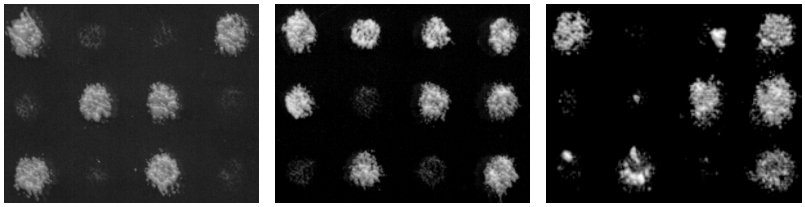

$His^+ : His^-$ Ratio	Number of Tetrads
(4:0)	13
(3:1)	23
(2:2)	2

B

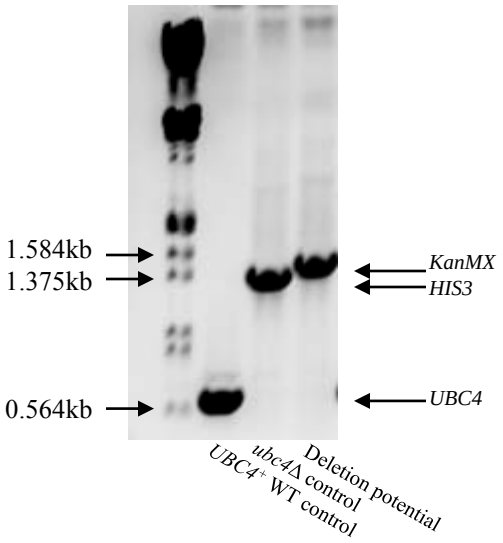

Figure 3.5 Discovery of chromosome II disomy in *AQT* strain.
A – Tetrad analysis showing unexpected segregation pattern. Tetrad analysis of a diploid obtained from mating of the *AQT* strain bearing the *ubc4Δ::HIS3* transplacement, to the strain bearing the *ubc4Δ::KanMX* transplacement, demonstrates presence of at least 2 copies of *HIS3* gene versus one copy of the *KanMX* gene. This can be concluded from the fact that majority of tetrads produce more than 2 His^+ spores, in contrast to the typically 2:2 segregation by G418 resistance caused by *KanMX*. All *AQT* spores in this cross were His^+.
B – Confirmation of *KanMX* replacement of *HIS3* at *ubc4Δ* locus by PCR. Due to the difference between *KanMX* module and *HIS3* module, deletion potential is confirmed to bear *ubc4Δ::KanMX* instead of the original *ubc4Δ::HIS3*.

reactions amplifying the *UBC4* gene confirmed that *KanMX* module replaced *HIS3* module in the deletion experiment (Figure 3.5B).

Table 3.3 Tetrad analysis of diploid *AQT* derivative revealing the chromosome II disomy

Number of full tetrads containing PolyQ plasmid	**Phenotype**	
40	PD	**3**x(2 $G418^r$ His^-Aqt^- : 2 $G418^s$ His^+Aqt^+)
	NPD	**11**x(2 $G418^s$ His^+Aqt^- : 2 $G418^r$ His^+Aqt^+)
	T	**22**x(1 $G418^r$ His^+Aqt^+ : 1 $G418^s$ His^+Aqt^- : 1 $G418^s$ His^+Aqt^+ : 1$G418^r$ His^-Aqt^-)
		1x(2$G418^r$ His^+Aqt^+ : 2$G418^s$ His^+Aqt^+)
		1x(1 $G418^r$ His^+Aqt^+ : 2 $G418^s$ His^+Aqt^- : 1$G418^r$ His^-Aqt^-)
		2x(1 $G418^s$ His^+Aqt^+ : 2 $G418^s$ His^+Aqt^- : 1$G418^r$ His^-Aqt^+)

The simplest scenario compatible with the ratios observed in the dissection and tetrad analysis is that *AQT* derivatives are disomics by chromosome II, containing the *UBC4* gene (and respectively, the *ubc4*Δ*:: HIS3* disruption). As chromosome segregation is controlled by a centromere, such a scenario would also explain the centromere linkage of *AQT*.

Confirmation of Chromosome II Disomy in *AQT* strains by Biochemical Techniques

To better detect the presence of an extra chromosome, the pulse field gel electrophoresis was conducted. All three *AQT* isolates together with their isogenicWT strain was colony purified and two colonies were taken from each strain to be tested. Indeed, separation of the yeast chromosomes using the Bio-Rad CHEF (Contour-clamped Homogeneous Electric Field) gel electrophoresis apparatus was followed by Southern blotting to P^{32}-labelled *SSA3* DNA probes. The results confirmed that each of three independent *AQT* derivatives contained an additional copy of the chromosome II band (Figure 3.6A). Unexpectedly, electrophoretic mobilities of duplicated chromosomes varied among *AQT* derivatives, and in the case of *AQT* isolate #2, the difference was detected between two isolates of one and the same *AQT* derivative.

Additionally, two tetrads from dissection of diploid heterozygous by *AQT* were also performed the pulse field gel electrophoresis and Southern blotting experiment described above. The parental strains were used as the controls, and two colonies were tested. Since all Aqt^+ spores showed two bands for chromosome II, apparently the extra-copy of chromosome II also co-segregated with *AQT* in tetrad analysis (Figure 3.6B). The variations in electrophoretic mobilities of chromosome II copies were also detected.

In order to detect whether there was fragment loss or duplication of chromosome II in *AQT* isolates, which may potentially explain the variability in the electrophoretic mobility, the Comparative Genomic Hybridization (CGH) assay was performed.

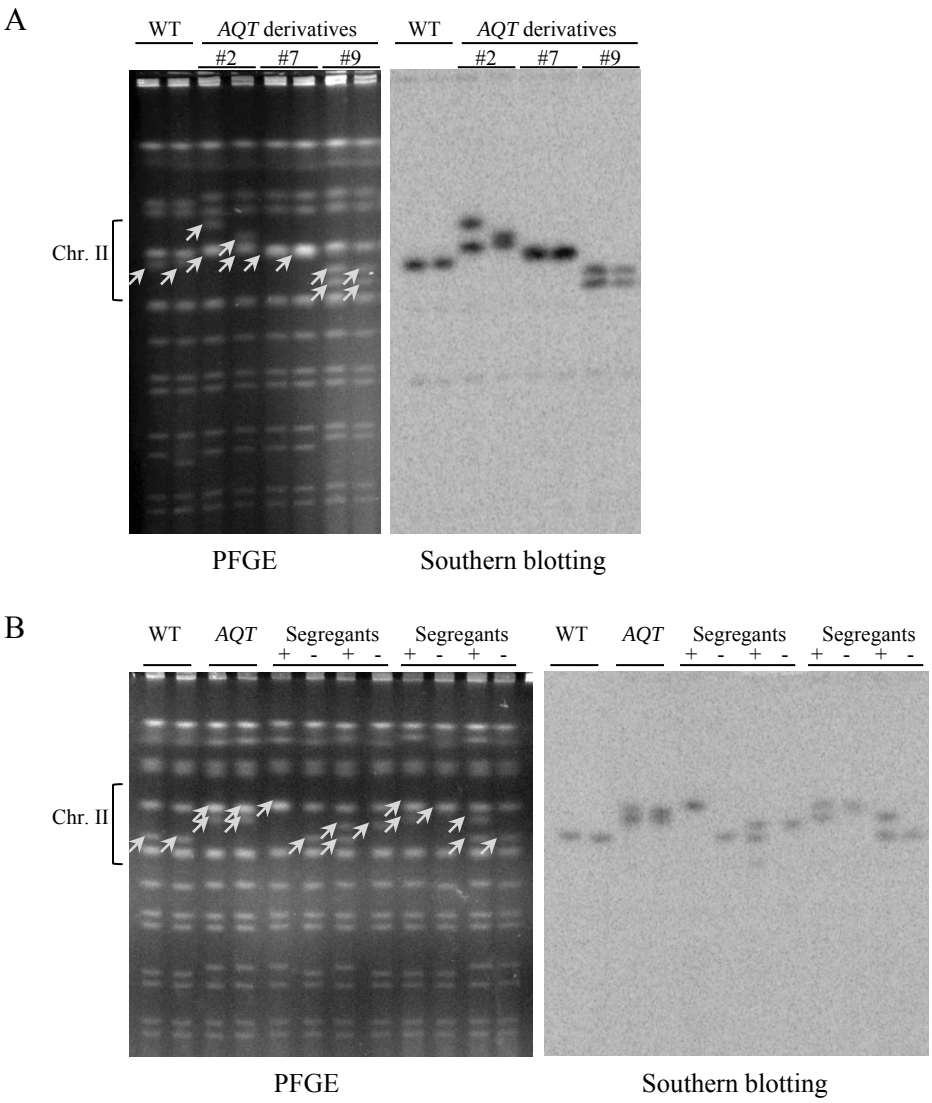

Figure 3.6 Confirmation of chromosome II disomy in *AQT* strain and derivatives by PFGE.

A – PFGE and Southern blotting of WT and *AQT* isolates. Chromosome fractionation by PFGE (left), followed by Southern blotting (right) demonstrates the presence of the extra copy of chromosome II in all *AQT* derivatives. Chromosome II bands are indicated by arrows on the CHEF gel, and visualized by hybridization to the labeled fragment of *SSA3* gene (located on chromosome II) on Southern blot. Per each independent *AQT* derivative (designated as *AQT2*, *AQT7* and *AQT9*) and wild-type control (WT), two isolates are tested. Note variation in chromosome II electrophoretic mobilities (see text for comments).

B – PFGE and Southern blotting of segregants from *AQT* heterozygous diploids. Two tetrads from dissection of diploid heterozygous by *AQT*/*aqt-wt* are tested together with the respective parental haploid strains. As indicated by arrows and the intensity of chromosome II bands in Southern blot, all Aqt^+ segregants tested are disomic by chromosome II.

However, the DNA microarray-based analysis confirmed that all *AQT* derivatives contained an extra copy of every piece of the coding material in chromosome II (Figure 3.7A, for CGH raw data, see APPENDIX B). This suggests that either variations in electrophoretic mobility are due to repetitive non-coding elements, or they reflect exchanges of material between non-homologous chromosomes.

Conclusions

Instead of a mutation in a single genetic locus as previously characterized, both classic genetic analysis and biochemistry based genome analysis data demonstrate that *AQT* is associated with an extra copy of chromosome II.

A

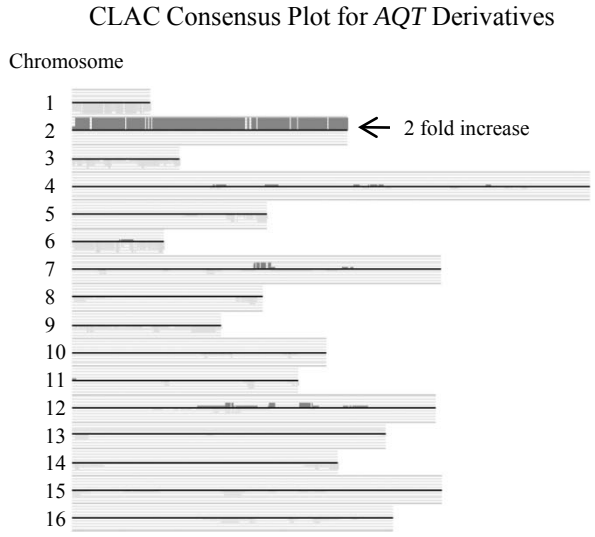

Figure 3.7 Confirmation of chromosome II disomy in *AQT* strain and derivatives by DNA microarray analysis.
A – CLAC consensus plot of *AQT* derivatives. Hybridization to a complete DNA microarray of the *S. cerevisiae* genome confirms that all the coding material of chromosome II is duplicated in the *AQT* strains. Comparison is performed using CGH-Miner.

CHAPTER 4

IDENTIFICATION OF *SUP45* AS A GENE RESPONSIBLE FOR *AQT*

Materials and Methods

Strains and Plasmids

AQT isolate #7 (GT574) was used in the serial deletion analysis identifying the gene responsible for *AQT* effects. The WT control strain was the isogenic *ubc4*Δ strain (GT349) in which the independent *AQT* isolates were derived from.

Plasmid pGSHU carrying a cassette containing the orthologous *URA3* gene from *Kluyveromyces lactis* and hygromycin resistant gene hyg^r as selectable/counter-selectable markers was used to insert into the extra chromosome II set points (Storici and Resnick 2006). Further deletions were conducted using a *LEU2* gene from plasmid vector pRS315 (Sikorski and Hieter 1989) as the selectable marker.

Methods

Deletion primers were generally 70 bp long, which consist of 50 bp homology to flank the sequence to be deleted and 20 bp complementary to ends of marker genes to be PCR amplified. Determination of the 50 by homology sequences were based on the BLAST search in SGD database aiming at a minimal number of homology within the

genome. By doing this, the efficiency of homology recombination based DNA replacement was increased.

Phusion High Fidelity PCR Master Mix (manufactured by New England BioLabs) was used to amplify the *KlURA3-hyg*^{r} cassette from the plasmid pGSHU and genomic DNA of deletion potentials.

Results

Serial Deletion Analysis of Chromosome II Extra Copy

With previous demonstrated chromosome II disomy in the *AQT* strain which was the cause of *AQT* effects, a hypothesis was proposed that a specific gene or few genes were responsible for the decreased polyglutamine toxicity in *AQT* strains. Base on the well developed PCR-based genomic DNA manipulation approaches, we decided to delete chromosomal fragments within the extra chromosome II in a serial division fashion to look for the gene responsible for the Aqt$^+$ phenotype.

One first step in the serial deletion analysis involved the insertion of the *KlURA3-hyg*^{r} cassette from pGSHU for selection/counter-selection into the set points. The set point for chromosome II left arm was at 190234-190383 (inside gene *PEP1*, 48kb from centromere) (Figure 4.1A). The set point for chromosome II right arm was at 519000-519449 (inside gene *IRA1*). Taking the chromosomal left arm deletion as an example, the *KlURA3-hyg*^{r} cassette from pGSHU was amplified and gel purified prior to

A

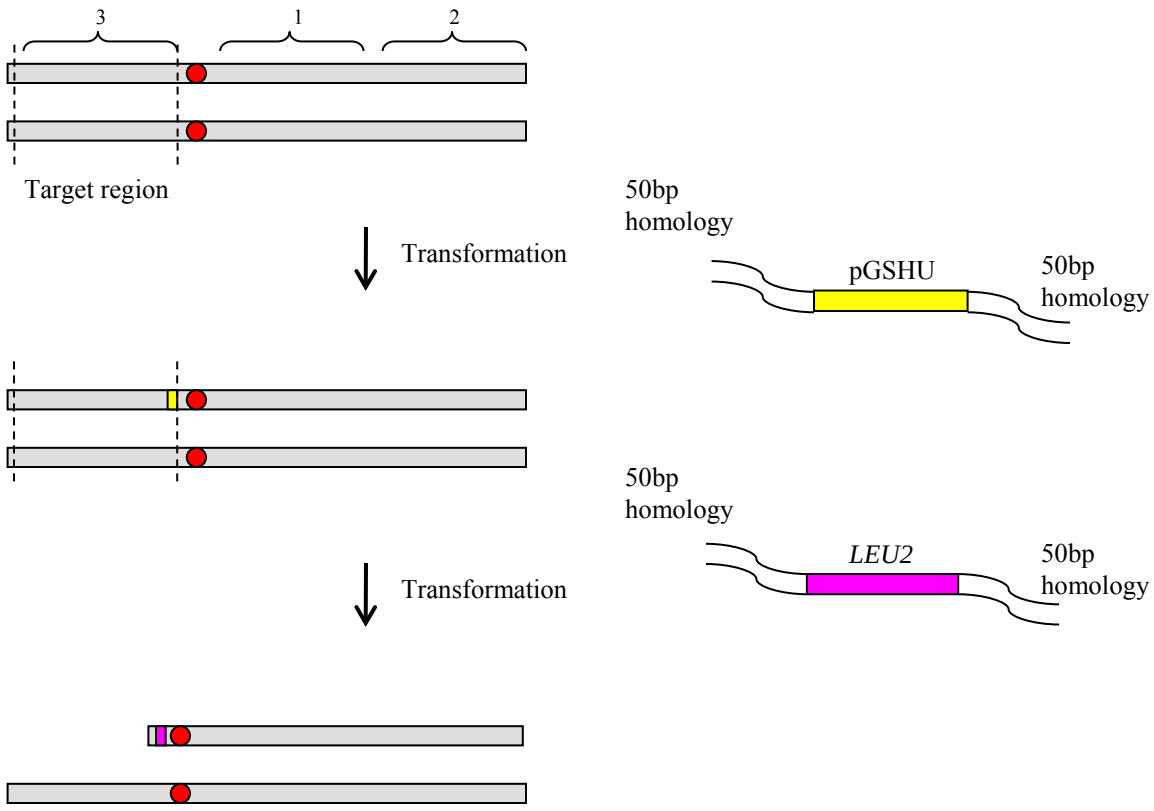

Figure 4.1 Illustration of serial deletion analysis.
A – Schematic view of fragment deletion with selectable markers. Deletion of region 3 (Rg3) on the extra chromosome II is shown as an example. The first step of deletion employs the insertion of selectable/counter-selectable markers from plasmid pGSHU, which contains *KlURA3* and *hyg*^{r} genes. The *KlURA3-hyg*^{r} cassette together with the target region is replaced by transformation of DNA fragment of *LEU2* gene and flanking 50bp homologous sequences.

transforming into the *AQT* haploid strain. *KlURA3* and *hyg*^{r}genes served as selectable markers in this step. The 2kb fragment containing *LEU2* gene amplified from vector pRS315 was then used to replace the large fragment including the *KlURA3-hyg*^{r} cassette inserted in the first step. The lost of resistance to hygromycin, auxotrophy of Uracil, and the prototrophy of Leucine indicated the replacement of *KlURA3-hyg*^{r} cassette by *LEU2* and the deletion in the extra chromosome II was achieved (Figure 4.1A). In addition to the phenotypic assay on plates selecting for the presence or absence of antibiotic resistant genes and auxotrophic markers, PCR reactions were conducted to confirm both insertion of the *KlURA3-hyg*^{r} cassette (Figure 4.2) and replacement by *LEU2* gene (Figure 4.3). To confirm the proper insertion of the *KlURA3-hyg*^{r} cassette, 3 PCR reactions were designed in the way that not only the insertion position was confirmed, but the presence of an unchanged chromosome II was also tested. The relative positions and directions of primers were shown in Figure 4.2A. Primers URA3.1 and SCE.2 were inside the *KlURA3-hyg*^{r} cassette, and primers ChkPL5' and ChkPL3' were outside of the insertion region. Only the correct insertions gave the expected length of DNA fragment for the PCR reactions locating the insertion position (Figure 4.2B). Primer pair ChkPL5'/3' was able to amplify the unmodified region from both the extra chromosome II of the insertion potential (I) and the chromosome II of the wild type control (WT).

Confirmation of the proper deletion of the large fragment of chromosome II followed a similar way of PCR design (Figure 4.3 A and B) after the screening process

A

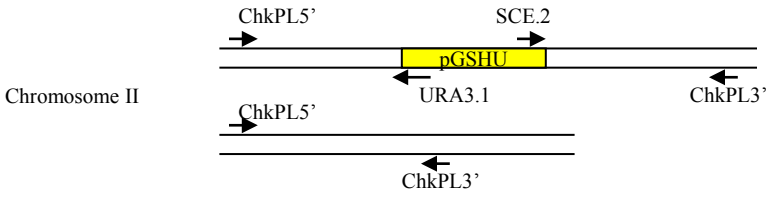

B

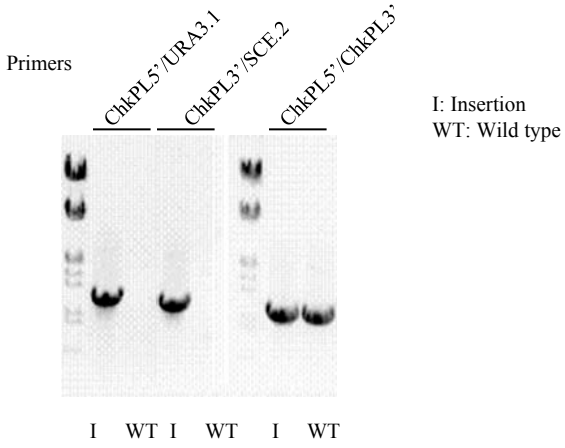

Figure 4.2 Confirmation of cassette insertion.
A – Schematic view of primers positions. A set of six primers are used to confirm the *KlURA3-hyg*^{r} cassette (pGSHU) insertion. PCR reactions using primer pairs ChkPL5'/URA3.1 and SCE.2/ChkPL3' are conducted to ensure the correct insertion location of the *KlURA3-hyg*^{r} cassette. Primer pair ChkPL5'/ChkPL3' are used to detect the presence of the other non-modified chromosome II.
B – PCR identification of insertion. PCR reactions were performed using 3 pairs of primers as described in (A). All bands are of expected sizes.

A

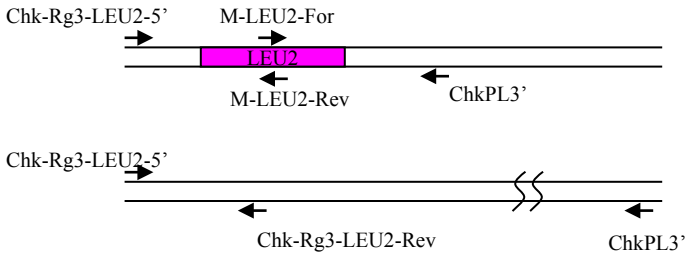

B

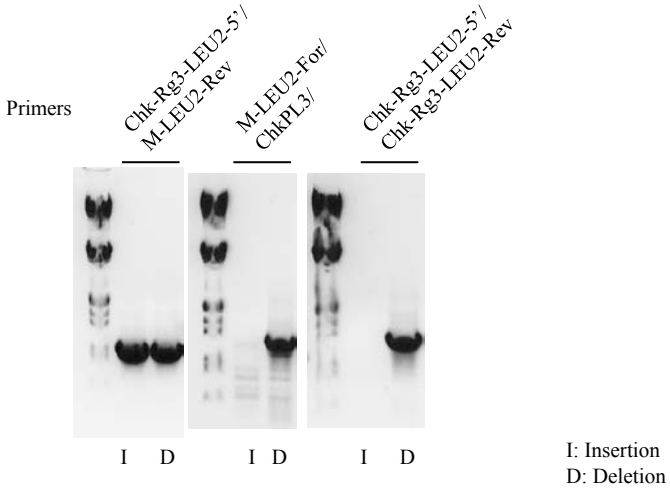

C

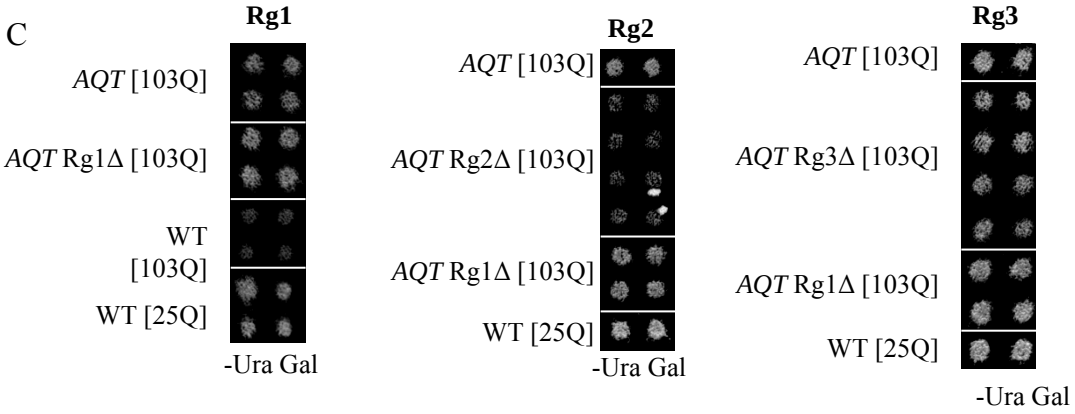

Figure 4.3 Confirmation of cassette proper deletion.
A – Schematic view of primers positions. Similar to the strategy of confirming *KlURA3-hyg*^{r} cassette insertion, proper deletion by *LEU2* deletion allele involves 3 PCR reactions.
B – PCR identification of deletion. All bands are of expected sizes.
C – Plate polyglutamine toxicity assay of region 1-3 deletions. Deletion of Rg2 eliminated the *AQT* effect, which remains in Rg1 and Rg3 deletion strains.

on plates. Due to the length of the target regions, deletion efficiency was significantly affected. Table 4.1 is the summary of deletion potentials obtained throughout the deletion identification process.

Table 4.1 Summary of number of deletion potentials obtained in Region 1-3 deletions

	Leu$^+$ Transformants	**Phenotypically Checked**	**Leu$^+$ Ura$^-$ (cassette loss)**	**Confirmed by PCR**
Region 1	974	974	15	1
Region 2	1200	1200	9	4
Region 3	2220	2220	8	2

The toxicity assay of *AQT* strain with Region 1, 2, and 3 individually deletion revealed that the gene responsible for *AQT* effects resided in Region 2 (Figure 4.3C).

Deletion of *SUP45* Gene Eliminates *AQT* Effects in [*PSI*$^+$] Background

As the serial deletion analysis confined *AQT* to the region of the chromosome II right arm, located between the positions 518877 and 779754 (Region 2) (Figure 4.4A), more extensive and detailing deletions were then made to this region. Utilizing the pre-existing set point, subregional Rg 2.1 and Rg 2.2 deletions were made. Both deletions were able to eliminate the *AQT* effect on polyQ toxicity, indicating the shorter region of

A

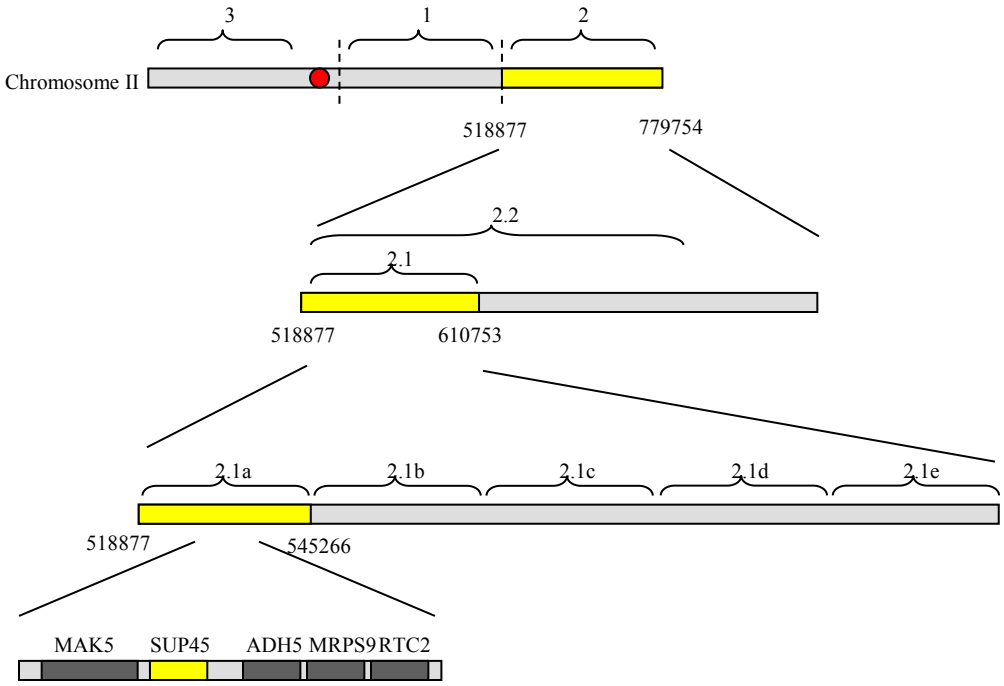

B

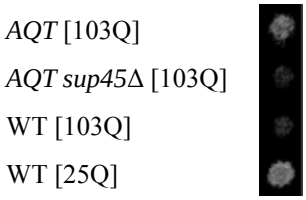

C

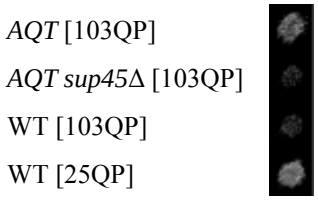

Figure 4.4 Identification of *SUP45* as a gene responsible for *AQT* in the [*PSI*$^+$] background.
A – Sequential deletion mapping of the chromosome II extra copy in the *AQT* strain. The *AQT7* derivative No. 7 was used in these experiments. Each numbered region corresponds to a respective deletion. Deletions eliminating the antitoxicity phenotype in the [*PSI*$^+$] background are shown as yellow boxes. All deletions were verified by PCR. Five ORFs located within the region 2.1a were each deleted individually; among those deletions, only deletion of *SUP45* eliminated *AQT* as shown on panels B and C.
B and C – Elimination of the antitoxic effect on 103Q (B) and 103QP (C) by the *sup45* deletion in *AQT* strain.

interest was from 518877-610753. Consequently, Rg 2.1 was divided into 5 smaller pieces, Rg 2.1a- Rg2.1e. Region 2.1a deletion, from 518877 to 545266 showing the Aqt^- phenotype was further analyzed until the search by serial deletions reached the region of 5 ORFs, including essential gene *SUP45*. Product of this gene, named Sup45 or eRF1, is a translation termination factor, working together with Sup35 (eRF3) (Stansfield et al. 1995). Individual ORF deletions were made within this region (from 528161 to 537490). Deletion of the extra copy of *SUP45* gene, located on the duplicated chromosome II in the *AQT* strain, eliminated the anti-toxicity effect on both 103Q (Figure 4.4B) and 103QP (Figure 4.4C).

Other Phenotypes Associated with Extra Copy of Chromosome II are Independent on *SUP45*

While *sup45* deletion eliminated amelioration of polyglutamine toxicity in the [PSI^+] *AQT ubc4*Δ strain, it has not influenced amelioration of temperature sensitivity (see Figure 4.5A). WT, *AQT*, and *AQT* with *sup45*Δ strains were grew in YPD for 1 day, then counted by hemacytometer to determine the cell concentration of each sample. Cell concentrations were then equilibrated according to the cell counts, and serial decimal dilution was conducted for each sample prior to the transfer to YPD plates by an 8-channel pipettor. Duplicated YPD plates were incubated at 30°C and 39°C, respectively,

for 2 days. The temperature sensitivity eliminated by *AQT* did not recover in the *AQT* strain with *sup45* deletion (Figure 4.5A).

In addition to the characteristics of *AQT* strain, such as temperature resistance at 39°C and anti-Sup35 toxicity effect, the ability to invade agar was observed in both wild type and *ubc4*Δ strains, but not in *AQT* strain. Deletion of *sup45* in *AQT* strain did not affect the loss of agar invading capability (Figure 4.5B).

These data (Figure 4.5) indicate that some phenotypes, associated with the chromosome II disomy, are caused by extra dosage of some other gene(s), located on chromosome II instead of *SUP45*.

Conclusions

The strategy of making serial deletions in the extra chromosome II looking for the gene responsible for *AQT* effect on the polyglutamine toxicity succeeded after at least 5 rounds of deletion and toxicity assay. Large quantities of deletion potentials were screened to identify the correct deletion.

Even with the ability to from aggresome, 103QP still caused toxicity in the [PIN^+ PSI^+] prion background. The ability of *sup45*Δ in *AQT* strain to eliminate the anti-polyglutamine toxicity for both 103Q and 103QP indicated the shared mechanism or pathway of 103Q and 103QP toxicity in the [PIN^+ PSI^+] cells.

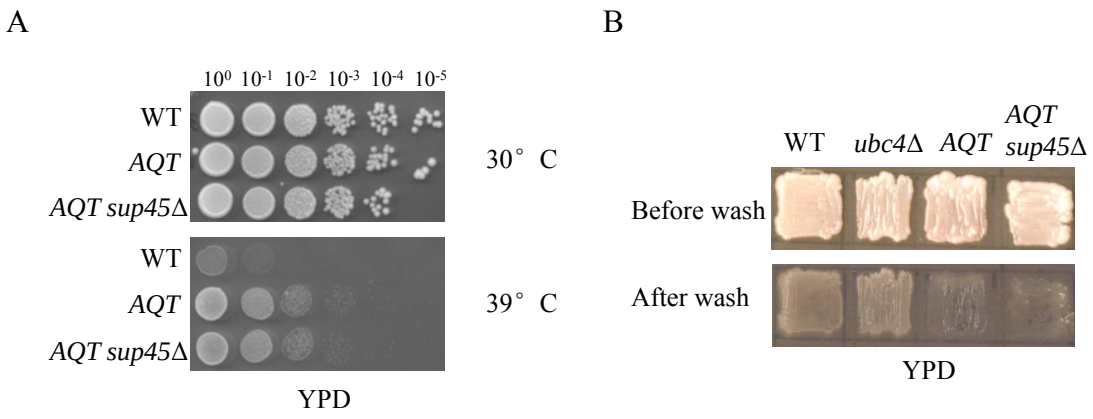

Figure 4.5 *SUP45* independent phenotypes associated with chromosome II disomy. A – Temperature resistance at 39° C in *AQT* strain was not affected by *sup45* deletion. Serial of decimal dilution was made in 96-well plates. Multi-channel pipetteor was used to transfer 5µl of culture to place onto YPD plates. Two identical plates were incubated at either 30° C or 39° C for two days before the plates were scanned.
B – The invasive phenotype of the wild-type and *ubc4*Δ strains was eliminated by *AQT*. However, deletion of *sup45* doesn't affect the phenotype of lack of agar invasion. Cells were patched on a YPD plate and incubated at 30° C for 2 days. The plate was scanned before and after gentle wash of 3 min under running water.

Some characteristics of *AQT* strains, at least the temperature resistance and the loss of agar invading ability, are associated with chromosome II disomy, indicating the involvement of genes other than *SUP45* in those phenotypes.

CHAPTER 5

ROLE OF RELEASE FACTORS IN [*PSI*$^+$]-DEPENDENT POLYGLUTAMINE TOXICITY

Materials and Methods

Strains and Plasmids

WT *UBC4*$^+$ strain used in this study was GT81-1C. The *AQT UBC4*$^+$ strain (segregant GT1665-3A) was obtained from dissection of GT1665, which was made by crossing GT81-1D with GT574 (*AQT* isolate #7). Since all *AQT* isolates were *ubc4*Δ::*HIS3*, the *AQT UBC4*$^+$ segregant was isolated from the tetrads of all 4 His$^+$ spores, resulting the presence of one allele of WT *UBC4* and one allele of *ubc4*Δ*::HIS3*. The heterozygosity of *UBC4*/*ubc4*Δ in the *AQT UBC4*$^+$ haploid strain was confirmed by PCR. GT574 was used as the *AQT* strain and GT349 was the respective WT *ubc4*Δ control.

The *SUP45* plasmid constructs included the centromeric plasmids bearing wild type or mutant (*sup45-103*) alleles of *SUP45* gene under its endogenous promoter (a gift of G. Zhouravleva); plasmid CEN-SUP45ΔC19, bearing the deletion of 19 C-terminal codons in *SUP45* (a gift of D. Bedwell); the centromeric plasmid bearing the *SUP45*Δ*C5* allele that lacks 5 C-terminal codons and causes only slight impairment of Sup45 function; the galactose-inducible *SUP45* plasmid, containing the *SUP45* cDNA under the

control of *GAL1* promoter. The CEN-SUP35C plasmid contained the *SUP35C* region under the endogenous *SUP35* promoter. Plasmid pCUP-Sup35NM-DsRed overexpressed Sup35NM domain and red fluorescent protein under the control of *CUP1* promoter. The plasmid overexpressing *UBC4* was a gift of M. Hochstrasser. Plasmids for the β-galactosidase assay were a gift of M. Tuite.

Methods

SDS-PAGE experiments were all done in the 10% acrylamide gel with 0.1% SDS. The amount of total protein loaded was equalized for all samples according to the Bradford assay, and confirmed by loading control protein Ade2p or Coomassie staining.

SDD-AGE experiments were done following the standard protocol (Halfmann and Lindquist 2008) with minor modifications. The capillary transfer stack was assembled from bottom to top: 9 pieces of thick blotting paper, 4 pieces of thin blotting paper, 1 piece of pre-wet thin blotting paper, the nitrocellulose membrane, agarose gel, 3 pieces of pre-wet thin blotting paper, the wick (3 pieces of wide pre-wet thin blotting paper), 1 pieces of pre-wet thin blotting paper, agarose gel casting tray and a bottle of 200 ml water.

For fluorescent microscopy experiments including the immunofluorescent microscopy, see Chapter 2 Methods.

Results

Level of Sup45p is Increased in *AQT* Strain

As discussed in Chapter 4, *SUP45* was identified as the gene responsible for *AQT* effect. We decided to further analyze the levels of Sup45p in the *AQT* strain. Western blot was performed to protein total lysate isolated from haploid *AQT* strain and the isogenic WT as control. Ade2 protein served as the loading control. Western blot analysis confirmed that the *AQT* derivative contains more Sup45 protein, compared to the isogenic wild type strain (Figure 5.1A). Moreover, when compared between $UBC4^{+}$ and *ubc4*Δ background, the increase of Sup45p level was more profound in *ubc4*Δ background (Figure 5.1 B), which is 2.5 fold as opposed to 1.5 fold in the $UBC4^{+}$. Thus, presence of the extra-copy of *SUP45* gene leads to increased levels of Sup45 protein in a partly ubc4Δ-dependent fashion, and is responsible for the anti-toxic (Aqt^{+}) phenotype in the [PSI^{+}] background.

Increased Expression of Sup45p in WT and *Ubc4*Δ Strains Leads to Decreased PolyQ/QP Toxicity

Next, we tested if increase in the Sup45 levels, produced by the means other than duplication of chromosome II, would also ameliorate the [PSI^{+}]-dependent polyglutamine toxicity. Indeed, introduction of the centromeric plasmid bearing the *SUP45* gene under its own (Figure 5.2A) or galactose-inducible (Figure 5.2B) promoter (in a latter case, under inducing conditions) ameliorated toxicity of both 103Q and 103QP. Anti-toxic

A

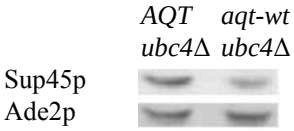

B

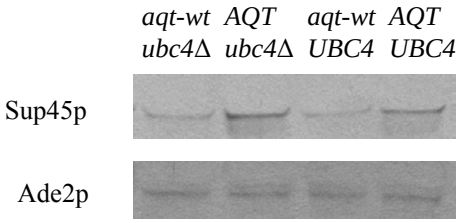

C

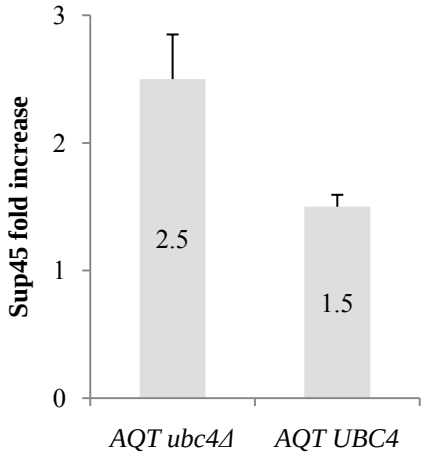

Figure 5.1 Level of Sup45p is increased in *AQT* strains.
A – Levels of Sup45 protein are elevated in *AQT ubc4*Δ strain, compared to WT *ubc4*Δ strain (Ade2 protein is used as the loading control).
B – Increase in Sup45 protein levels is more profound in the *AQT ubc4*Δ strain, compared to the isogenic *AQT* strain, bearing the wild type *UBC4* gene (*UBC4*$^{+}$) on one of the copies of chromosome II.
C – Bar graph of Sup45p level is shown relative to the isogenic non-*AQT* control in both *UBC4*$^{+}$and *ubc4*Δ backgrounds. At least 3 measurements with independent cultures were performed in each case; error bars correspond to standard deviations.

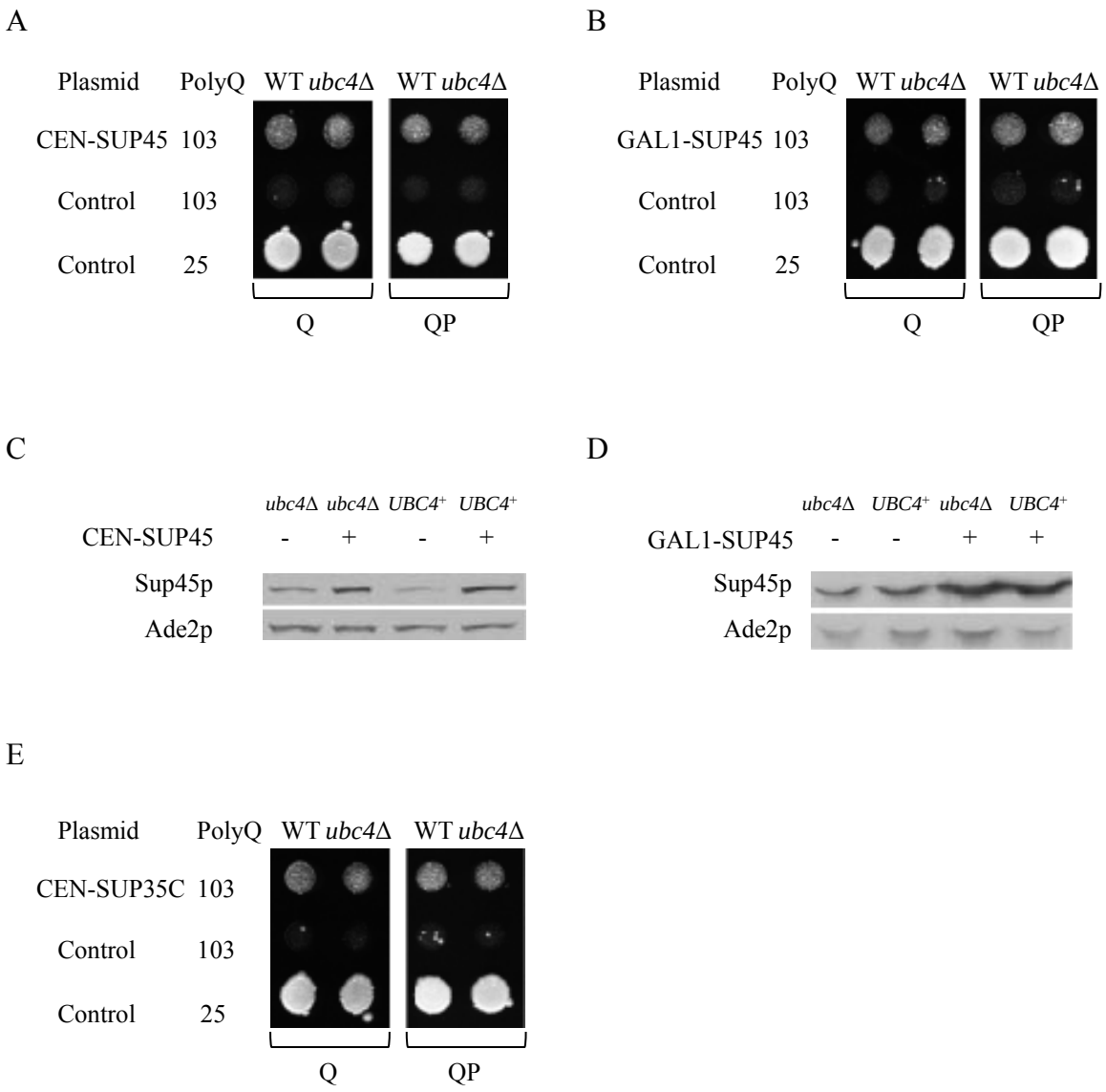

Figure 5.2 Modulation of polyglutamine toxicity by the plasmid-borne release factor genes.
A and B – Plasmid-borne extra copy of *SUP45* gene under endogenous (A) or galactose-inducible P_{GAL} (B) ameliorates toxicity of 103Q and 103QP in both wild type (WT) and *ubc4*Δ [*PSI*$^+$] strains.
C and D – Centromeric plasmids with *SUP45* gene under endogenous (C) or galactose-inducible P_{GAL} (D) promoters increase levels of Sup45 protein in both wild type (WT) and *ubc4*Δ strains. Cultures were grown in liquid -Ura -Leu glucose (C) or -Ura -Leu galactose/raffinose (D) medium. Ade2 protein is shown as a loading control.
E – Expression of the Sup35 derivative lacking the prion and middle domains (Sup35C) decreases 103Q and 103QP toxicity in both wild type (WT) and *ubc4*Δ strains. *SUP35* gene was under control of the endogenous *SUP35* promoter.

effect of plasmid-borne *SUP45* was clearly detected in both *ubc4*Δ and *UBC4*$^{+}$ backgrounds, indicating that it was less sensitive to the presence of Ubc4 protein, compared to the chromosomal extra copy. For both plasmids, Sup45 overproduction was confirmed by protein analysis (Figure 5.2C and D).

Overexpression of Sup35C Decreases PolyQ/QP Toxicity

Remarkably, when an extra copy of the altered *SUP35* gene, coding for the Sup35 protein that lacks the N-terminal (prion) and middle domains and is therefore unable to be incorporated into the [*PSI*$^{+}$] prion aggregates (*SUP35C*) was introduced into the cells, the polyglutamine toxicity of both 103Q and 103QP in the [*PSI*$^{+}$] strain was also ameliorated (Figure 5.2E).

Function of Sup45p is Required for *AQT* Effect

However, antitoxicity caused by a centromeric plasmid bearing the *SUP45* derivative (*SUP45*Δ*C5*), that is missing the C-terminal 5 amino acids but remains functional (Chernoff et al. 1992), was partially dependent on *ubc4*Δ (Figure 5.3A). Ability of the extra-copy of *SUP45* to ameliorate polyglutamine toxicity was abolished by a deletion of 19 C-terminal amino acids (Figure 5.3B), that impairs Sup45 function in translation and interaction with Sup35 (Kallmeyer et al. 2006), or by the missense mutation *sup45-103*, T62C (Figure 5.3C) that also impairs Sup45 function in translation

A

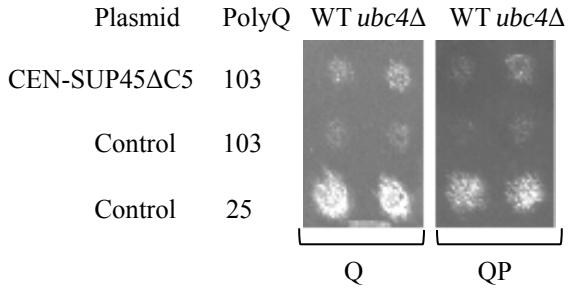

B

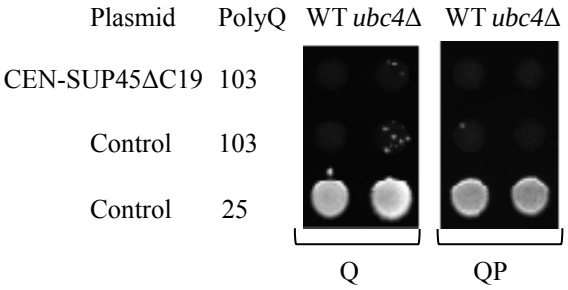

C

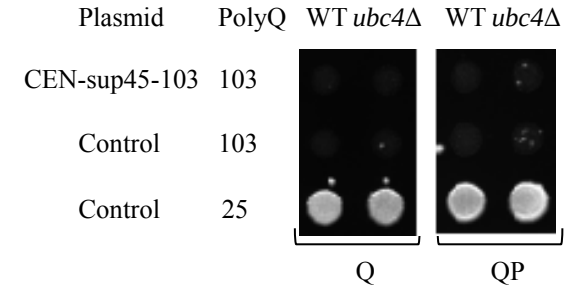

Figure 5.3 Functionally impaired Sup45 is not able to cause *AQT* effect.
A – Plasmid expressing the *SUP45* allele with a short C-terminal deletion, *SUP45ΔC5* (that only slightly impairs Sup45 protein function) from the endogenous *SUP45* promoter, ameliorates 103Q and 103QP toxicity in partially *ubc4*Δ-dependent fashion. B and C – Plasmids, expressing the *SUP45* alleles with either a longer C-terminal deletion, *SUP45*Δ*C19* (that abolishes Sup45 function and interaction with Sup35) (B) or missense mutation *sup45-103*, T62C (that impairs Sup45 function) (C) from the endogenous *SUP45* promoter, do not ameliorate 103Q and 103QP toxicity.

termination (Moskalenko et al. 2004). Thus, Sup45 ability to ameliorate toxicity depends on the same sequence elements that control its function in translational machinery.

Aggregation Pattern of Sup35 and PolyQ/QP in *AQT* Strain

As both polyglutamines and prion form of Sup35 form SDS-resistant polymers in the yeast cells, we have checked if patterns of their aggregation are influenced by the presence of an extra copy of *SUP45*. Both 103Q and 103QP proteins exhibit a broad range of distribution of the SDS-resistant polymers by size, as demonstrated by semi-denaturing agarose gel electrophoresis (SDD-AGE), with 103QP containing more protein in the higher molecular weight (MW) fraction (Figure 5.4A). This result confirms that aggresome, formed by 103QP, contains insoluble protein aggregates, in contrast to the juxtanuclear quality control compartment (JUNQ) observed in the yeast cells with the defect of ubiquitin-proteasome system (Bagola and Sommer 2008). Neither 103Q nor 103QP polymer distribution was significantly affected by *AQT* (Figure 5.4A). In the wild type [PSI^+] cells, lacking 103Q or 103QP, Sup35 prion polymers were distributed within a narrower range of sizes, compared to polyglutamines (Figure 5.4B). However, in the presence of either 103Q or 103QP, size range of the Sup35 polymers was increased and higher MW polymers were accumulated, suggesting that some Sup35 could be associated with 103Q (or 103QP) polymers, therefore partly following their distribution. Notably, the range of the Sup35 polymer size distribution became narrower in the presence of *AQT*,

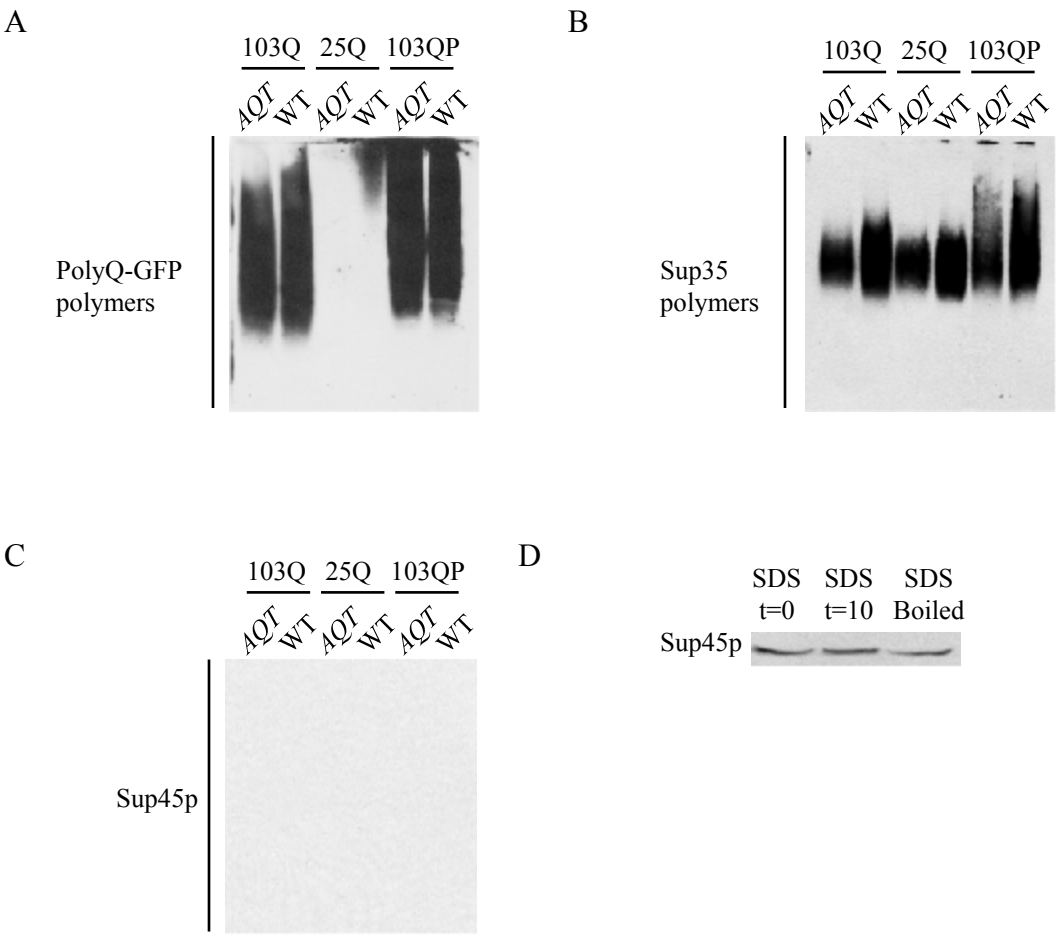

Figure 5.4 Polymer fractionation assay by SDD-AGE.
A and B – Fractionation of the polyQ/QP-GFP (A) and Sup35 (B) polymers by sizes in the *ubc4*Δ [*PSI*$^{+}$] strains either with (*AQT*) or without (WT) *AQT*. Polymers were separated by SDD-AGE (see Chapter 2 Methods). Filter obtained from one and the same gel was reacted to either GFP (A) or Sup35C (B) antibodies. Ploygluta mines alter distribution of Sup35 ploymers, and this effect is counteracted by *AQT*. Experiment has been repeated with 3 independent cultures per each combination, each time with the same result.
C – No Sup45 polymers were detected by SDD-AGE.
D – Sup45 is dissociated from aggregates in 2% SDS.

and the high MW fraction, which depends on 103Q/QP, disappeared (Figure 5.4B). This suggests that extra dosage of Sup45 somewhat counteracts increase in size of Sup35 polymers and possibly, their interaction with polyglutamines. As expected, Sup45 protein itself does not convert into the SDS-resistant polymers (Figure 5.4C). An additional piece of information on lack of SDS-resistant polymers of Sup45p was obtained from western blot. Length of 2% SDS treatment and pre-loading sample boiling didn't not affect the solubility of Sup45p in SDS-PAGE (Figure 5.4D).

Colocalization of Sup35/Sup35NM Aggregates and PolyQ/QP

Immunofluorescence microscopy data show that while most of the cytologically detected Sup35 aggregates are distinct from 103Q (or 103QP) aggregates, colocalization of some Sup35 with 103Q or 103QP was detected in essentially every cell containing both types of aggregates in both WT and *AQT* strains (Figure 5.5A). Unexpectedly, Sup45 was also observed as aggregates similar to the sizes and distribution of those Sup35 aggregates in the immunofluorescence microscopy. Partial colocalization of Sup45 with 103Q or 103QP was also detected the same as for Sup35 (Figure 5.5B), which was very likely due to the presence of interaction between Sup35 and Sup45 instead of Sup45 aggregates. When Sup35NM, tagged with DsRed, was overproduced in the [PSI^+] strain also expressing 103QP, most of Sup35 was eventually assembled into one large deposit, either partially or completely overlapping with the 103QP aggresome (Figure 5.5C).

A

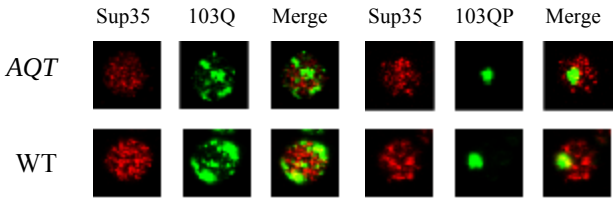

B

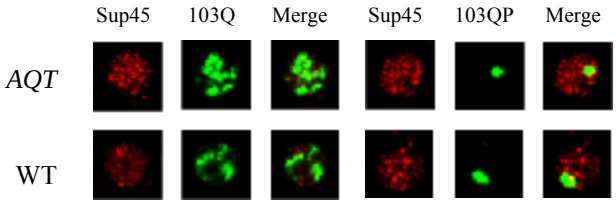

C

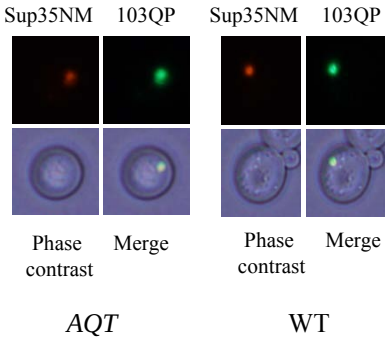

Figure 5.5 Colocalization of [*PSI*$^+$] and polyglutamines.
A – Some (but not all) of Sup35 aggregates, visualized by secondary immunofluorescence (red) in the *ubc4*Δ [*PSI*$^+$] strain, colocalize with 103Q or 103QP aggregates, visualized by GFP tag (green).
B – Sup45, seen in aggregates (red) in the *ubc4*Δ [*PSI*$^+$] strain in immunofluorescence microscopy, partially colocalize with 103Q or 103QP .
C – Overexpressed Sup35NM-DsRed (red) forms large clumps in the [*PSI*$^+$] cells, that overlap with the 103QP-GFP aggresome (green) in both *AQT* and WT strains.

Moreover, this sequestration was not affected by an extra copy of *SUP45* (Figure 5.5C and Table 5.1), however, it was expected, as Sup35NM-DsRed construct does not contain a major region of interaction with Sup45, located within Sup35C (Wang et al. 2001).

Table 5.1 Summary table of colocalization of Sup35NM and 103QP aggregates

Sample	Overlapped	Partial Overlapped	Distant	Total
AQT No.1	24	11	7	42
AQT No.2	30	8	5	43
WT No.1	26	8	7	41
WT No.2	28	8	12	48

Two independent colonies were taken from *AQT* and WT strains for the colocalization detection, respectively. There was no significant difference between *AQT* and WT.

Effects of Polyglutamines and *AQT* on Sup35 and Sup45 Aggregation

We have also checked effects of polyglutamines and gene dosage on patterns of Sup45 aggregation. Sequestration of Sup45 by the Sup35 prion aggregates is known to contribute to cytotoxicity of overproduced Sup35 in [PSI^+] strains (Vishveshwara et al. 2009). Although we could not detect aggregate-associated Sup45 by SDD-AGE (Figure

5.4C), apparently because it is not converted into an amyloid form and is therefore released after SDS treatment (Figure 5.4D), centrifugation analysis demonstrates that presence of either [*PSI*$^+$] prion or 103Q protein results in the shift of a fraction of Sup45 protein to the pelletable (aggregate-associated) form, with both factors together having an additive effect (Figure 5.6A). Effect of 103Q in the [*psi*$^-$] strain is probably mediated by its ability to promote aggregation of Sup35 even in a non-prion form, as reported previously (Urakov et al. 2010) and confirmed by us (Figure 5.6A). 103QP did not exhibit any observable effect on Sup45 aggregation on its own. However, it promoted Sup35 aggregation in [*psi*$^-$] and further increased Sup45 aggregation in the presence of [*PSI*$^+$]. Remarkably, proportion of the pelletable versus soluble Sup45 was decreased in the *AQT* (disomic) [*PSI*$^+$] strain expressing 103Q or 103QP, compared to the identical strain not possessing disomy (Figure 5.6B). This shows that increase in level of Sup45 counteracts its sequestration by aggregates.

Termination Readthrough in the Strains Expressing Polyglutamines

As our data point to sequestration of release factors as a mechanism of polyglutamine toxicity, we have checked if polyglutamines increase translational readthrough of stop codons. For this purpose, the chimeric constructs bearing a stop codon between the *PGK1* and *lacZ* ORFs have been employed. Surprisingly, no increase

A

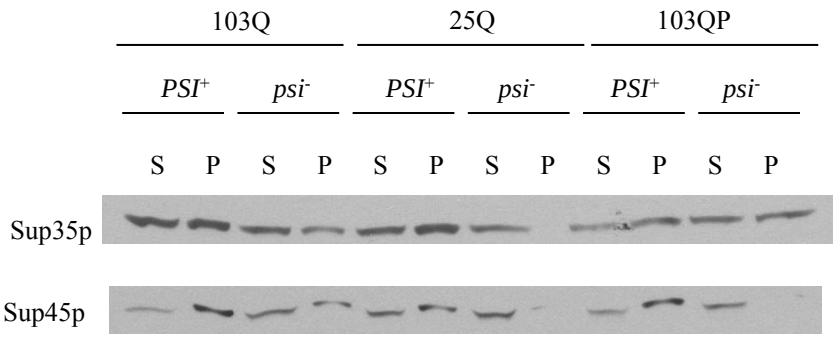

B

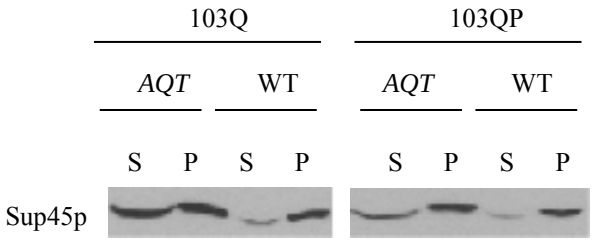

Figure 5.6 Modulation of polyglutamine toxicity by the plasmid-borne release factor genes.
A – Expression of 103Q promotes aggregation of Sup35 and Sup45, whereas expression of 103QP promotes only Sup35, in the *ubc4*Δ [*psi*$^-$] strain, and increases aggregate-associated fraction of Sup45 in the *ubc4*Δ [*PSI*$^+$] strain, as detected by an increase in the pellet (P) versus supernatant (S) fraction in comparison to the respective strain expressing 25Q, as determined by centrifugation analysis, followed by Western blotting.
B – Proportion of soluble (supernatant, S) versus aggregate-associated (pellet, P) Sup45 is significantly increased in *AQT ubc4*Δ [*PSI*$^+$] strain, compared to the identical non-*AQT* (WT) strain, as determined by centrifugation analysis, followed by Western blotting.

in translational readthrough (measured by β-galactosidase activity) has been detected in the presence of 103Q (Table 5.2).

Table 5.2. Readthrough of stop codon UGA in the absence and presence of 103Q.

PolyQ	Readthrough (%)
25Q	0.43 ± 0.07
103Q	0.32 ± 0.15

Cultures were grown in -Ura -Trp glucose medium to reach early stationary phase. Cells were washed 3 times before being transferred to -Ura -Trp glactose/raffinose medium for 24 hours induction. Three independent cultures were tested. $p > 0.05$.

These data suggest that either damage to translational machinery, caused by the aggregation and sequestration of release factors in the presence of polyglutamines, is so severe that translation is arrested and not proceeding beyond the stop codon, or cytotoxicity is related to non-translational functions of release factors (see Discussion for more detail).

Discussion

Amelioration of [*PSI*$^+$]-dependent cytotoxicity by expression of the non-prionogenic derivative of Sup35 (Sup35C), or by extra-dosage of the Sup35

functional partner, Sup45, indicates that toxicity results from sequestration of release factor(s) by polyglutamine aggregates. Possibly Sup35, containing QN-rich domain, is sequestered directly, while Sup45 is sequestered via its interaction with Sup35. Indeed, ability of polyglutamines to facilitate aggregation of endogenous QN-rich proteins even in a non-prion strain has been reported previously (Derkatch et al. 2004; Urakov et al. 2010), and it was shown that Sup35 prion aggregates cause toxicity via sequestering Sup45 when Sup35 is overproduced at high levels in the [*PSI*$^+$] strain (Vishveshwara et al. 2009). In agreement with these data, *AQT* (*i. e.*, extra copy of *SUP45*) ameliorates both polyglutamine toxicity and toxicity of excess Sup35 in the [*PSI*$^+$] cells. There is probably a competition for Sup35/Sup45 complex between polyglutamine aggregates and functional sites at which Sp35/Sup45 complex is supposed to act,, therefore increased abundance of Sup45, for example in result of disomy by the chromosome containing a respective gene (as in *AQT* derivatives), not only increases a proportion of non-sequestered Sup45 but also partly counteracts sequestration of Sup35, that can be seen as a change in size distribution of the Sup35 polymers. Hence this is the antitoxic effect of excess Sup45.

On surface, two observations contradict such a simplistic model. First, in the cells that do not overproduce Sup35, only a small fraction of Sup35 aggregates are colocalized with cytologically detectable polyglutamine aggregates, and this colocalization is not completely abolished in the *AQT* strain (Figure 5.5A). However, we don't know which

fraction of Sup35 remains functional in the [*PSI*$^+$] strains. Although it is clear that some fraction should retain function, as Sup35 is an essential protein and its complete elimination is lethal (Dagkesamanskaya and Ter-Avanesyan 1991), it remains unknown whether functional component is represented by the residual non-aggregated Sup35, smaller oligomers, or both. If functional Sup35 constitutes only a small fraction of total Sup35 protein in the [*PSI*$^+$] cells, sequestration of this fraction by polyglutamines and its release in the presence of excess Sup45 would be difficult to detect cytologically, but these changes would still have profound physiological consequences. At least, change in the distribution of Sup35 polymers by size in the presence of polyglutamines, which is reversed in the strains bearing extra-copy of *SUP45* (Figure 5.4B), clearly shows that certain alterations of Sup35 aggregation patterns, making them less similar to polyQ aggregation patterns, coincide with the antitoxic phenotype.

Another complication is that sequestration of release factors by polyglutamines does not appear to further increase the stop codon readthrough in the [*PSI*$^+$] cells (Table 5.2). One possibility is that complete absence of release factors from the translational machinery damages it to such an extent that not only termination but also translation through the stop codon becomes impossible. Another possibility is that toxicity is related to non-translational functions of Sup35/45. Indeed, it has been reported that the immediate consequence of the severe shortage of a release factor in yeast is a cytoskeleton defect leading to cell death (Valouev et al. 2002).

Relevance of yeast data to human polyglutamine disorders.

Involvement of translational machinery in HD has been suspected from some results in mammalian systems (King et al. 2008). It remains unknown if polyglutamines can sequester the human homologs of Sup35 and Sup45 (respectively, eRF3 and eRF1), as mammalian ortholog of Sup35, eRF3, does not have a QN-rich domain. However, our results could be relevant to mammalian systems in a more general way. About 40% of variation in the age of HD onset in case of the same length of polyglutamine repeat is due to genetic variation (Wexler et al. 2004). Our work provides potential explanation for such a variation by demonstrating that changes in the abundance of the sequestered protein(s), occurring via alteration of either gene dosage or gene expression, can modulate polyglutamine toxicity. Non-genetic component of variations in polyglutamine toxicity can be explained by differences in the composition of other aggregated proteins (*e. g.* endogenous self-perpetuating aggregates or prions) present in the cell. Our results show that prion composition of the cell not only drives polyglutamine toxicity but also determines a pathway via which polyglutamines influence cell physiology, as proteins already associated with the other aggregates are more likely to be sequestered by polyglutamines. Mammalian cells contain a variety of proteins with the prion-like QN-rich domains, and machinery for propagation of the QN-rich protein aggregates exists in mammals. It is entirely possible that either organisms or tissues (or both) differ by the aggregate composition, and this in turn influences their susceptibility to

polyglutamine disorders. Composition of endogenous aggregates may also modulate which proteins are sequestered by polyglutamines, as proteins associated with other QN-rich aggregates are more likely to be sequestered, like Sup45 in the cells containing the Sup35 prion. This could explain why different groups are coming out with different conclusions in regard to both mechanisms of polyglutamine toxicity and contributions of different types of polyglutamine aggregates.

Conclusions

Levels of Sup45p in *UB4*$^{+}$ and *ubc4*Δ WT strains are indeed increased due to the increased dosage of *SUP45*. However, presence of WT *UBC4*$^{+}$ controls the level of Sup45 in a more stringent way, resulting in a less profound increase of Sup45p as compared to that in *ubc4*Δ background.

Excess of the termination factor Sup45 or presence of non-prion derivative of the termination factor Sup35 (Sup35C) ameliorates polyQ/QP toxicity.

Function of Sup45, including stop codon recognition and ability to interact with Sup35, is required for ameliorating polyQ/QP toxicity.

Pattern of polyQ/QP polymer distribution is not affected by *AQT*.

Presence of polyQ/QP polymer broadens the range of sizes of Sup35 polymer, indicating the sequestration of Sup35 by polyQ/QP aggregates.

Sup35, when not overproduced, forms numerous small aggregates, and partly colocalizes with polyQ/QP aggregates. Sup45 was observed to colocalize with polyQ/QP in a similar fashion. *AQT* did not affect the partial colocalization of Sup35 and polyQ/QP, or Sup45 and polyQ/QP, respectively.

The single aggregate per cell formed by overexpressed Sup35 colocalized with aggresome formed by 103QP.

Both presence of [*PSI*$^{+}$] and 103Q are able to promote Sup45 aggregation/ sequestration. Sup45 is released to the supernatant fraction in *AQT* strain with either 103Q or 103QP

CHAPTER 6

EFFECT OF CHROMOSOME II EXTRA COPY ON [*PSI*$^+$]-INDEPENDENT POLYGLUTAMINE TOXICITY

Materials

Strains and Plasmids

Strains used in the studies discussed in this chapter are in [*PIN*$^+$ *psi*$^-$] prion background. The WT (GT386) and *AQT* (GT676) are the [*PIN*$^+$ *psi*$^-$] strains cured by overexpressing Hsp104 in the respective [*PIN*$^+$ *PSI*$^+$] strains GT349 (WT) and GT574 (*AQT* No. 7). [*PIN*$^+$ *psi*$^-$] strains with deletions on the extra chromosome II in *AQT* strain were obtained initially from the serial deletion analysis in [*PIN*$^+$ *PSI*$^+$], and [*PSI*$^+$] was cured by overexpressing Hsp104.

The Hsp104 plasmid construct used to cure [*PSI*$^+$] was pLH105 (#198), in which *HSP104* was fused to the GPD promoter (*TDH3* promoter).

Methods

Various techniques were used to detect the *AQT* effect on polyglutamine toxicity in [*PIN*$^+$ *psi*$^-$] background. These techniques included serial dilution spotting of cultures growing in -Ura/Gal (103Q induction culture) at various time points, and additional passages from -Ura/Gal onto -Ura/Gal to enlarge the growth difference between strains.

[*PSI*$^+$] curing using GPD-HSP104 plasmid was done by passing on YPD for two passages, and colony purification to lose the plasmid. Loss of [*PSI*$^+$] was then confirmed by lack of growth on -Ade agar plates.

Results

Effect of *AQT* on Polyglutamine Toxicity in [*PIN*$^+$] Strains

While original *AQT* isolates were all obtained in [*PIN*$^+$ *PSI*$^+$] background and confirmed to retain both prions, we were interested to know if *AQT* would cause a similar effect in the absence of [*PSI*$^+$] as well. [*psi*$^-$] *AQT* strain together with the isogenic WT strain was grown to late logarithmic phase in -Ura/Glu medium. Cells were counted using the hemacytometer after 3 times of wash. The induction culture was started with cell concentration of 10^6 cells/ml. Culture was taken from the inoculum and at 24 hr from the induction medium and spotted onto -Ura for viability test. *AQT* was clearly seen to decrease 103Q toxicity after 24 hours as compared to the WT (Figure 6.1A).

We also checked if presence of [*PSI*$^+$] in *AQT* and its derivatives affected the ability of invading agar plates. Similar to the phenotype observed in [*PSI*$^+$] (Figure 4.5B), loss of agar invasion was seen in both *AQT* and *AQT sup45*Δ strains as opposed to the isogenic WT (Figure 6.1B). Hence either [*PSI*$^+$] nor *SUP45* was responsible for the lack of the capability of agar invasion.

A

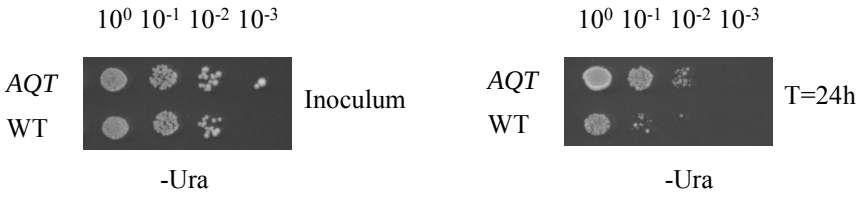

B

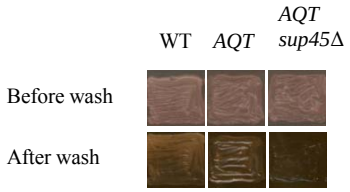

Figure 6.1 Effect of *AQT* in [*PIN*$^+$ *psi*$^-$] background.
A – *AQT* strain ameliorates 103Q toxicity in the [*PIN*$^+$ *psi*$^-$] background. Cultures were grown in liquid -Ura glucose medium for 1 day, and washed 3 times prior to the induction of 103Q in -Ura galactose/raffinose medium. The induction started with the cell concentration of 10^6 cells/ml. Cultures were taken for dilution spotting from the inoculum and after induction of 24 h.
B – *AQT* eliminates the agar invading ability in [*PIN*$^+$ *psi*$^-$] background. Deletion of *sup45* in the *AQT* strain dose not affect the lack of ability to invade agar plates.

*AQT sup45*Δ [*psi*$^-$] strain was tested in polyQ toxicity assay to determine whether or not *SUP45* was the reason for *AQT* effect in [*psi*$^-$] background. Unfortunately, deletion of *sup45* did not exhibit increase of toxicity even after three passages on -Ura/Gal (Figure 6.2A). Additionally, excess Sup35C and Sup45 were introduced into *UBC4*$^+$ WT and *ubc4*Δ WT strains, respectively. No amelioration of polyQ toxicity was detected by plate toxicity assay (Figure B and C), indicating that polyglutamine toxicity in [*psi*$^-$] strain is not due to the toxicity through translation termination, an additional mechanism was involved in a [*PIN*$^+$] dependent manner, and a gene other than *SUP45* on chromosome II was responsible for the *AQT* effect.

Mapping the Chromosome II Region Responsible for [*PIN*$^+$]-Dependent Polyglutamine Toxicity

Utilizing the previously generated chromosome II disomic strains with various regional deletions, I created the complete [*psi*$^-$] set of deletion strains by overexpressing Hsp104. Preliminary deletion mapping data confined amelioration of [*PIN*$^+$]-dependent component of poly-Q toxicity to the region 3 of chromosome II (Figure 6.3A). Additional deletions within region 3 were depicted in Figure 6.3A. Toxicity assay performed with sub-regional deletions made in region 3 confined the location of responsible gene to Rg3.2 excluding Rg3.1 (Figure 6.3B). This region corresponds to the nucleotide positions 102568 to 148377, containing 29 ORFs. This potential region was further divided into

A

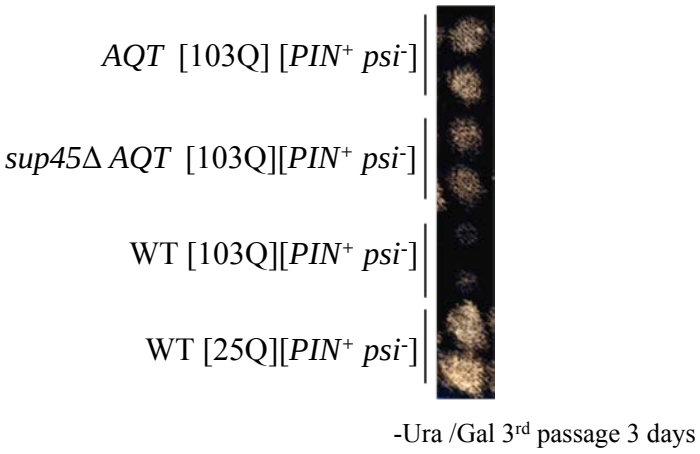

B

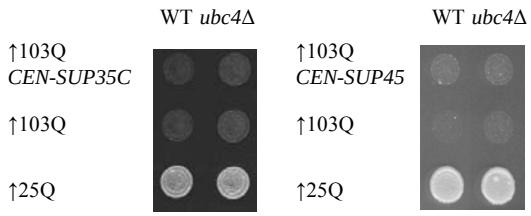

Figure 6.2 *SUP45* is NOT the gene responsible for *AQT* effects in [*PIN*+ *psi*-] background.
A – Deletion of *sup45* does not eliminate the anti-polyglutamine toxicity in [*PIN*+ *psi*-] background. Plate is scanned after 3 days of the third passage on –Ura/Gal.
B and C – Introduction of plasmid-borne Sup35C (B) and Sup45 (C) does not decrease polyglutamine toxicity in [*PIN*+ *psi*-] background.

A

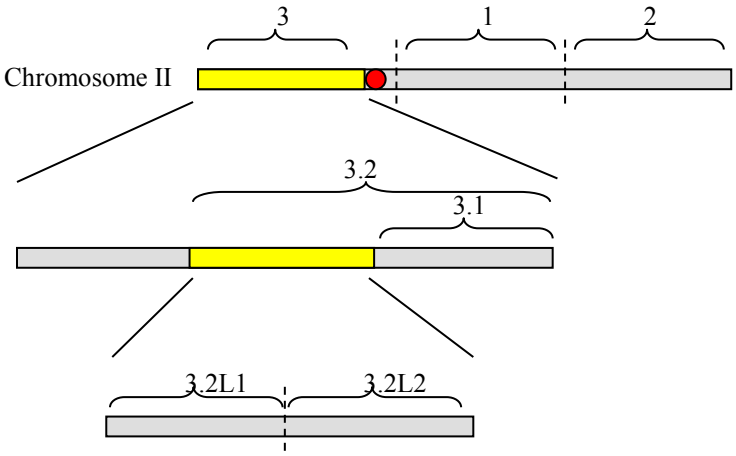

B

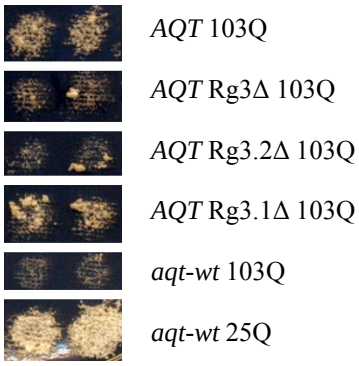

Figure 6.3 Mapping for [*PIN*$^+$] dependent polyglutamine toxicity.
A and B– Chromosomal deletions made in region 3 of the extra chromosome II (A). Serial deletions made for identifying the gene responsible for *AQT* in [*PIN*$^+$ *PSI*$^+$] background are cured of [*PSI*$^+$] by Hsp104 overexpression. Toxicity assay has suggested that Rg3 contains the *AQT* gene(s) in [*psi*$^-$] background (B). There are two shorter deletions made in Rg3, Rg3.1 and Rg3.2. Polyglutamine is toxic to Rg3.2 rather than Rg3.1, indicating the middle region of Rg3 (yellow box) contains the [*PIN*$^+$]-dependent *AQT* gene. This middle region is further divided into Rg3.2L1 and Rg3.2L2, of which the analysis is yet to be finished.

Rg3.2L1 and Rg3.2L2. Identification of ORF responsible for this effect is currently underway.

Discussion

The data demonstrate that different yeast prions promote polyglutamine toxicity by different mechanisms, namely sequestration of the cytoskeletal components, resulting in the effect of endocytosis, in case of Rnq1 prion [*PIN*$^+$] (Meriin et al. 2003; Meriin et al. 2007), and sequestration of the release factors in case of Sup35 prion, [*PSI*$^+$] (this work). Additive action of both prions on 103Q toxicity in the absence of P-rich region suggests that effects of [*PIN*$^+$] and [*PSI*$^+$] are at least partly independent of each other. Chromosome II disomy ameliorates both [*PSI*$^+$]-dependent (via extra-dosage of *SUP45*) and [*PIN*$^+$]-dependent (via *SUP45*-unrelated pathway) components of polyQ toxicity. However, some level of interference between two sequestration pathways cannot be excluded, taking into account the strong anti-toxic effect of the individual overproduction of Sup45 or Sup35C in the strain bearing both [*PIN*$^+$] and [*PSI*$^+$] prions.

CHAPTER 7

EFFECT OF ARGININE BIOSYNTHETIC PATHWAY ON POLYGLUTAMINES AND [*PSI*$^+$] PRION

Materials and Methods

Strains and Plasmids

Segregant GT532-9A is the Aqt$^+$ spore obtained from dissection of the diploid heterozygous by *AQT* (No. 2 isolate), which served as the *AQT* haploid [*PSI*$^+$] strain. Deletions of *arg* genes were all made in GT532-9A.

The centromeric plasmid bearing a WT *ARG4* gene under its endogenous promoter was constructed by inserting PCR amplified fragment Chr VIII 139675-141920 from genomic DNA, which contains 518 bp upstream and 336 bp downstream of *ARG4* gene, into vector pRS315.

Methods

Pulse filed gel electrophoresis was done using the same protocol and parameter settings as described in Chapter 3. However, instead of using P^{32}-labelled probes, Southern blotting detecting chromosome VIII was done using the Amersham Random Prime Labeling Kit from GE Healthcare. *ARG4* genomic fragment was used as the probe template.

Results

Effect of Loss of One Copy of Chromosome VIII in the Diploid *AQT* Strain

One Aqt$^-$ derivative of the diploid homozygous by ubc4Δ and heterozygous by AQT1/aqt1-wt was obtained from the transposon mutagenesis screening (Figure 7.1A). Interestingly, dissection of this Aqt$^-$ diploid derivative on YPD gave a ratio of 2:2 by spore viability (Figure 7.1B), indicating a chromosome loss happened to this derivative. Loss of that specific chromosome therefore resulted in the loss of *AQT* phenotype. In order to test which chromosome had lost, we performed pulse-field gel electrophoresis experiment to separate yeast chromosomes on agarose gel (Figure 7.1C left). Probing with chromosome VIII specific probes indicated monosomy of chromosome VIII in the Aqt- derivative of Aqt+ diploid (Figure 7.1C right). Next, we checked whether or not chromosome VIII contained a gene that was able to affect polyglutamine toxicity. As mentioned in Chapter 3, a few centromere linked genes were disrupted to locate the *AQT* gene due to the centromere linkage of *AQT* indicated by tetrad analysis. *ARG4* gene, which is close to the centromere of chromosome VIII, was also deleted to determine the linkage between *AQT* and *CEN8*. Tetrad analysis demonstrated that genes *AQT* and *ARG4* are not linked to each other (for tetrad analysis data see Table 7.1).

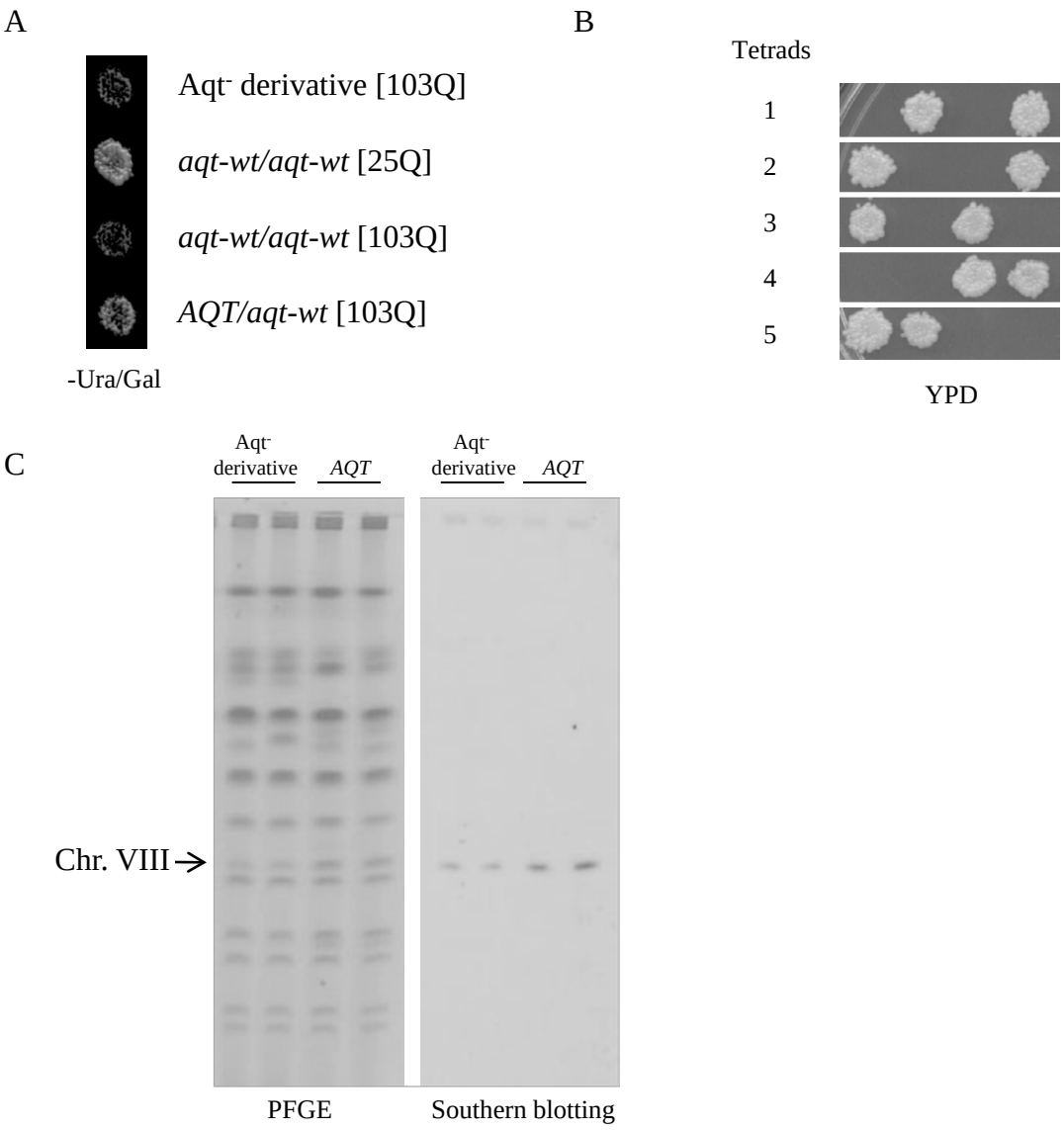

Figure 7.1 Chromosome VIII monosomic potential from transposon mutagenesis library screening.
A – Aqt- derivative shows decreased *AQT* effect after transposon mutagenesis library screening. The Aqt- derivative is one of the potentials obtained from the initial screening discussed in Chapter 3.
B – Indication of monosomy in tetrad analysis. Dissection of the Aqt- derivative shows viability ratio of 2:2.
C – Confirmation of chromosome VIII monosomy by PFGE and Southern blotting. Both original *AQT* diploid and the Aqt- derivative are tested in duplicates (two independent colonies). Chromosome VIII on the CHEF gel is indicated by an arrow. *ARG4* gene is amplified and used as the template to produce Chr VIII specific probes. The chromosome VIII band intensity in Southern blot supports the presence of chromosome VIII monosomy in this Aqt- derivative.

Table 7.1 Tetrad analysis of diploid cross *arg4*Δ *AQT* X *ARG4 aqt-wt*.

Number of full tetrads containing PolyQ plasmid	**Phenotype**		**Total number of dissected tetrads**
48	PD	**29**x(2Arg-Aqt- : 2Arg+Aqt+)	100
	NPD	**14**x(2Arg-Aqt- : 2Arg+Aqt-)	
	T	**5**x(2Arg-Aqt- : 1Arg+Aqt+ :1Arg+ Aqt-)	

Note: Toxic effect of *arg4*Δ on 103Q is discussed in the following section.

Effects of *Arg4* Deletion on Polyglutamine Toxicity

When the haploid *arg4*Δ *AQT* was crossed with *ARG4* aqt-wt, the dissection was expected to yield all three types of tetrads (parental ditype, non parental ditype and tetratype), and 2:2 segregation pattern of both Arg^+ and Aqt^+ (Figure 7.2A). However, all Arg^- spores were Aqt^-. Taking together with the appearance of all 4 Aqt^- (PD) and 3 Aqt^- (T) spores in a tetrad (Figure 7.2B), *arg4*Δ was able to mask the effect of *AQT*. Surprisingly, deletion of *arg4* gene further increased polyQ toxicity in the *ubc4*Δ *aqt1-wt* haploid strain (Figure 7.2C). Additionally, increase of toxicity was also observed in *UBC4 aqt1-wt* strain, indicating effect of increased toxicity by *arg4*Δ was independent on deletion of *UBC4* (Figure 7.2D).

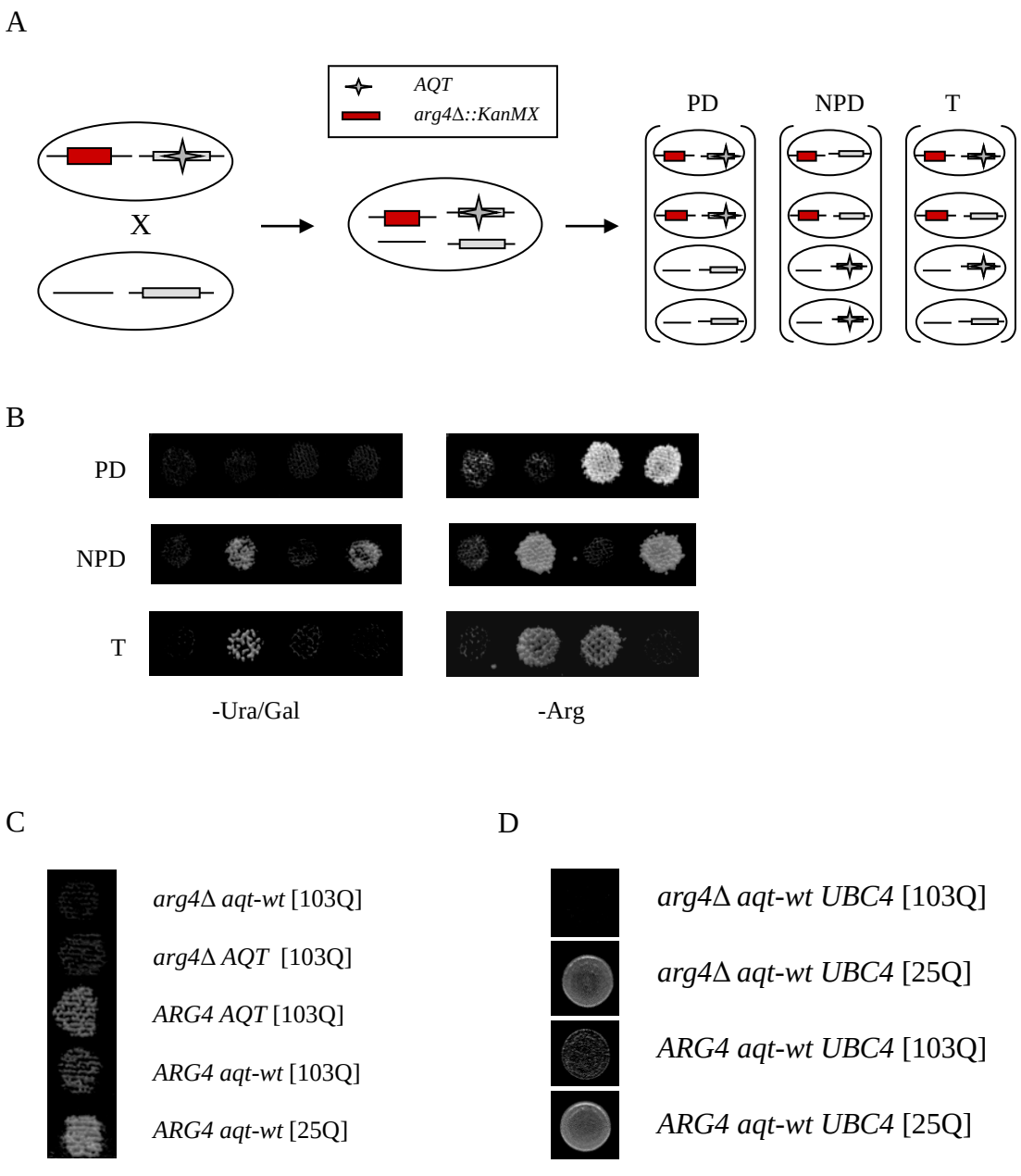

Figure 7.2 Deletion of *ARG4* gene inhibits the effects of *AQT.*
A – Illustration of tetrad dissection of diploid *arg4*Δ *AQT* X *ARG4 aqt-wt*. All three tetrad types are expected if *ARG4* and *AQT* are not linked.
B – Phenotypes of different types of tetrads in tetrad analysis.
C – Deletion of *ARG4* gene in both WT and *AQT* strains increased polyglutamine toxicity.
D – Effect of *arg4*Δ does not depend on $UBC4^{+}$.

To test whether or not the increased toxicity was simply due to *arg4*Δ rather than modified regulation of genes next to *ARG4*, I constructed *ARG4* gene with 500bp upstream and 300bp downstream flanking regions into yeast centromeric vector pRS315. Introduction of a wild type copy of *ARG4* into the *arg4*Δ *aqt-wt* and *arg4*Δ *AQT* haploid strains restored the level of toxicity effect as seen in controls (Figure 7.3 A and B).

Effects of *Arg4* Deletion on [*PSI*$^+$] Phenotypic Expression

The *ade1-14* allele was used to indicate the presence of absence of [*PSI*$^+$] prion due to the cellular function of Sup35 as the translation termination factor. When most of Sup35 is in the [*PSI*$^+$] prion form, recognition of the premature stop codon in *ade1-14* allele is significantly affected, and the readthrough results in the translation of Ade1 protein and the growth on -Ade medium. When Sup35 is in soluble form in [*psi*$^-$] strain, no complete Ade1 protein is made, therefore there's no growth on -Ade medium. Deletion of *arg4* gene did not only increased the polyglutamine toxicity in an *AQT* -independent manner, but also inhibited the [*PSI*$^+$] phenotypic expression on -Ade medium (Figure 7.4A). The lack of growth on -Ade of *arg4*Δ strain was not due to the curing of [*PSI*$^+$]. The presence of [*PSI*$^+$] prion was detected by crossing *arg4*Δ strain with WT [*psi*$^-$] strain (Figure 7.4B). The resulting diploid was able to grow on -Ade medium, indicating the *arg4*Δ strain was indeed [*PSI*$^+$]. *ARG4* gene codes for

A

*ARG4 aqt-wt ubc4*Δ [103Q]

*arg4*Δ *aqt-wt ubc4*Δ [103Q]

*arg4*Δ *aqt-wt ubc4*Δ [103Q] [*ARG4*]

*ARG4 aqt-wt ubc4*Δ [25Q]

B

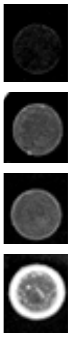

*arg4*Δ *AQT ubc4*Δ [103Q]

*arg4*Δ *AQT ubc4*Δ [103Q][*ARG4*]

*ARG4 AQT ubc4*Δ [103Q]

*ARG4 aqt-wt ubc4*Δ [25Q]

Figure 7.3 Complementation assay by introducing plasmid-borne *ARG4*.
A – Introduction of plasmid CEN-ARG4 in *arg4*Δ *aqt-wt* strain eliminates the increased polyglutamine toxicity.
B – Introduction of plasmid CEN-ARG4 in *arg4*Δ *AQT* strain eliminates the increased polyglutamine toxicity.

A

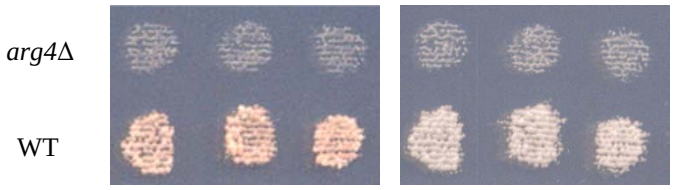

B

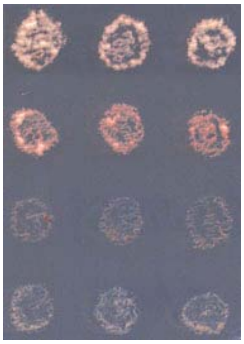

C

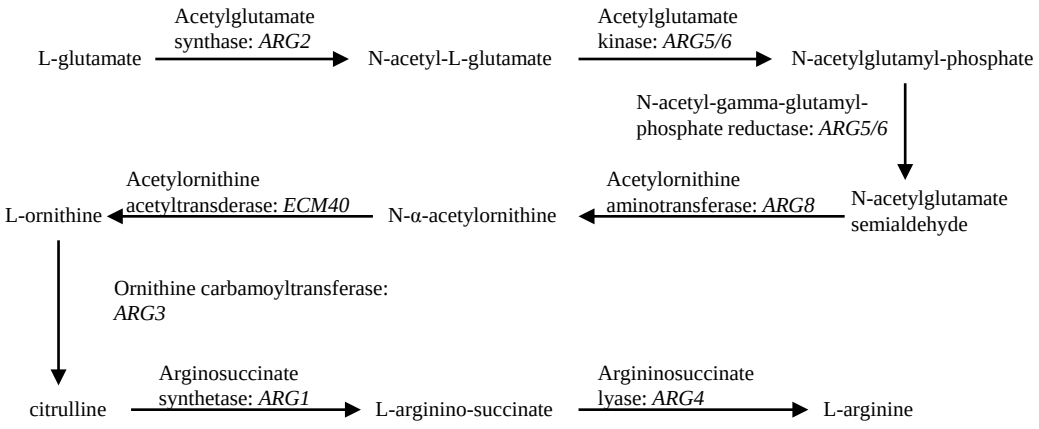

Figure 7.4 Deletion of *ARG4* inhibits the manifestation of [*PSI*$^+$].
A – Loss of phenotypic expression of [*PSI*$^+$] in *arg4*Δ strain.
B – Genetic crossing revealed the presence of [*PSI*$^+$]. *Arg4*Δ haploid is crossed to [*psi*$^-$] *ARG4* strain of the opposite mating type. Resulting diploid is able to grow on –Ade plate.
C– Arginine biosynthesis pathway. *ARG4* gene codes for argininosuccinate lyase, which catalyze the last step in arginine biosynthesis in yeast.

argininosuccinate lyase, which is responsible for catalyzing the last reaction in the arginine biosynthesis pathway (Figure 7.4C).

Effects of Other *Arg* Deletions on Polyglutamine Toxicity and [*PSI*$^+$] Phenotypic Expression

Arginine biosynthesis pathway has been well studied (Henry et al. 1984). Gene for argininosuccinate lyase is conserved in a variety of species including *Escherichia coli*, *Saccharomyces*, algae, rat and human (Yu and Howell 2000). We further deleted genes *ARG1* and *ARG8* along this pathway. Deletion of *arg1* behaved very similarly to *arg4*Δ in polyQ toxicity assay whereas *arg8*Δ didn't have much additive effect (Figure 7.5A). All three *arg* deletions were able to block the manifestation of [*PSI*$^+$] on -Ade medium (Figure 7.5B). With extra Arginine in the medium, growth of *arg* deletions was increased but still much worse than controls (Figure 7.5C).

Accumulation of red pigment in cells is another phenotypic expression of lack of [*PSI*$^+$]. We tested all three *arg* deletions with WT on YPD. Only *arg4* exhibited slightly darker red color (Figure 7.5D).

Deletions of *arg* genes were crossed with *UBC4*$^+$ WT strain to generate *UBC4 arg1*Δ, *UBC4 arg4*Δ, and *UBC4 arg8*Δ, respectively. *UBC4 arg8*Δ were able to grow as opposed to *UBC4 arg1*Δ and *UBC4 arg4*Δ strains (Figure 7.5E).

Are Effects of Arginine Biosynthetic Pathway Related to Polyamine Biosynthesis?

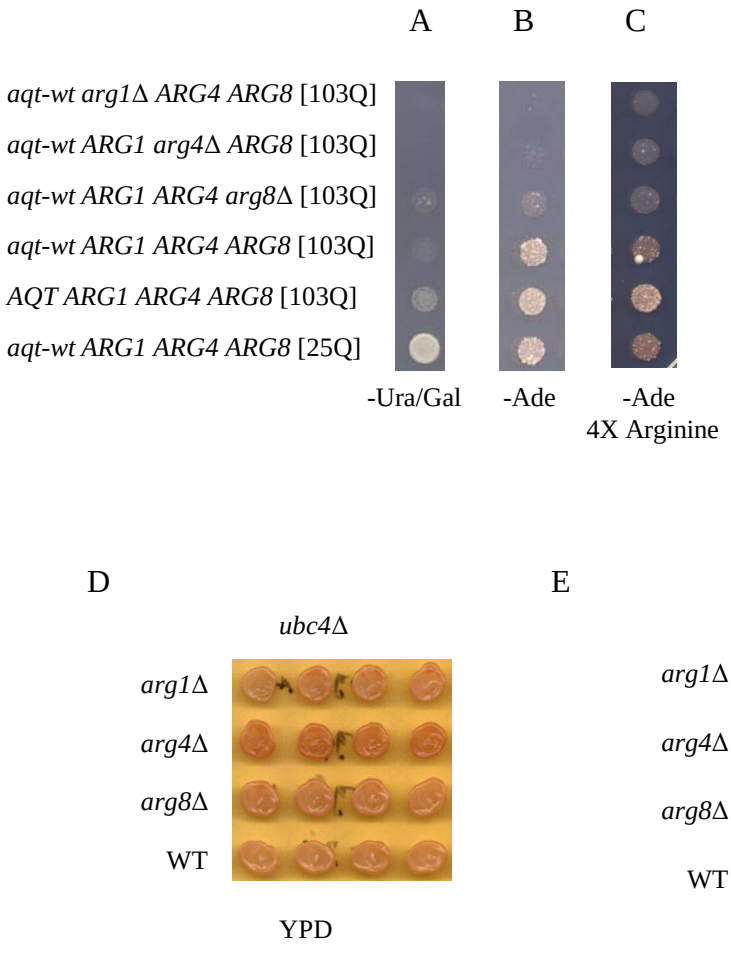

Figure 7.5 Effects of *Arg* deletions on polyglutamine toxicity and [*PSI*$^+$].
A – Polyglutamine toxicity assay of *Arg* deletions. *arg1*Δ *and arg4*Δ increases polyglutamine toxicity, whereas *arg8*Δ does not have the effect as the other two deletions
B– All three *arg* deletions inhibit manifestation of [*PSI*$^+$]
C – Extra arginine partially restores phenotypic expression of [*PSI*$^+$]. 4X arginine was added into the –Ade medium.
D – Color assay of *arg* deletions. *Arg4*Δ shows a darker red color when compared to other *arg* deletions as well as the WT control.
E – In the presence of *UBC4* WT, *arg8*Δ exhibits partial suppression of [*PSI*$^+$] phenotypic expression.

Ornithine decarboxylase relates Arginine biosynthesis intermediate, ornithine, to polyamine biosynthesis (Tabor and Tabor 1984). Expanded polyglutamine proteins promoted spermine synthesis and led to increase of polyglutamine aggregation and cell death. Moreover, cell death was inhibited when there was an ornithine decarboxylase antagonist (Colton et al. 2004). We then hypothesized that in the yeast model deficiency of Arg1p and Arg4p resulted in the accumulation of ornithine, thus stimulating polyamine biosynthesis (Figure 7.6A). We started testing this hypothesis by deleting *SPE1* gene, coding for ornithine decarboxylase. Deletion of *spe1* did not affect polyglutamine toxicity (Figure 7.6B). However, [*PSI*$^{+}$] phenotypic expression was suppressed by *spe1*Δ (Figure 7.6C).

Discussions

We have shown that monosomy of chromosome VIII increases polyglutamine toxicity in diploid heterozygous by *AQT*. Deletion of *ARG4* that is located on chromosome VIII increases polyQ toxicity by the mechanism unrelated to *AQT* or *ubc4*Δ. The increase of polyglutamine toxicity is exclusively due to loss of the Arg4 protein in the *arg4*Δ strain rather than deletion induced modification of *ARG4* neighbor genes. These findings indicate that effect of *ARG4* on polyglutamine toxicity is dosage-dependent.

A

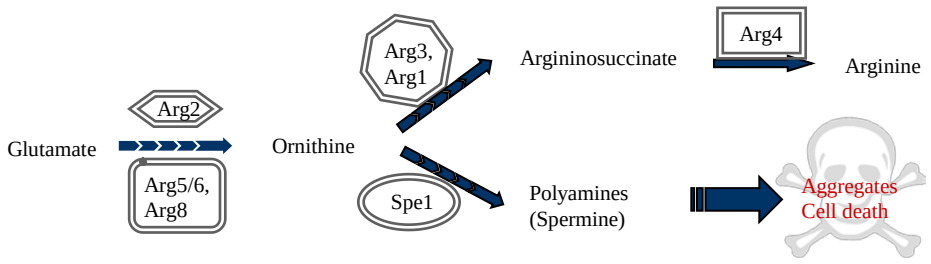

B

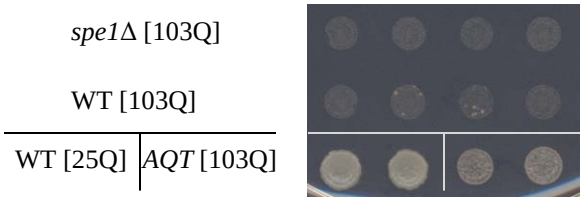

C

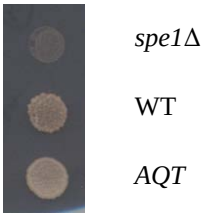

Figure 7.6 Relation between Arginine biosynthesis and polyamine biosynthesis.
A – Schematic view of argine and polyamine biosynthesis pathways. Ornithine connects argine and polyamine synthesis in yeast. The hypothesis is that the increase of level of polyamine due to the imbalance created by loss of Arg1 or Arg4 may result in the increase in polyglutamine toxicity, and eventually cell death.
B and C – Effect of *spe1*Δ on polyglutamine toxicity and [*PSI*$^{+}$] manifestation. No obvious effect of deletion of *spe1* is observed in polyQ toxicity assay. However, *spe1*Δ does inhibit the phenotypic expression of [*PSI*$^{+}$].

Deletion of *arg8* involved in steps before ornithine synthesis as well as deletion of *spe1* did not increase polyglutamine toxicity. Whereas, deletion of genes *arg1* and *arg4* controlling steps after ornithine caused even severe polyglutamine toxicity. These data indicated that ornithine was likely involved in the increased polyQ toxicity, however not through polyamine biosynthesis. On the other hand, deletions of genes involved in Arginine and Polyamine biosynthesis were all able to affect [PSI^{+}] phenotypic expression, indicating factors utilizing Arginine and/or Spermine might be responsible.

GENERAL CONCLUSIONS

- PolyQ or polyQP are toxic in the presence of [*PSI*$^+$], a prion form of translation termination factor Sup35.
- Effects of Anti-polyQ-toxicity (*AQT*) strains result from disomy by chromosome II.
- The extra copy of *SUP45* gene on duplicated chromosome II is responsible for *AQT* in [*PSI*$^+$] background.
- Increased level of Sup45p is more strictly controlled in the presence of WT Ubc4.
- Excess of the termination factor Sup45 or non-prion derivative of the termination factor Sup35 (Sup35C) ameliorates polyQ/QP toxicity.
- Function of Sup45 is required for *AQT* effect.
- Sup35/Sup35NM aggregates colocalize with polyglutamine aggregates.
- Size range of Sup35 polymers is broadened in the presence of 103Q or 103QP, and *AQT* strain is able to reduce the size of Sup35 polymers.
- Sup45 is sequestered to aggregates in the presence of polyglutamine or [*PSI*$^+$] prion.
- Phenotypes, such as lack of agar invasion and temperature resistance, are not associated with excess Sup45.

- Chromosome II disomy is responsible for *AQT* effect in [*PIN*$^{+}$ *psi*$^{-}$] background. However, the mechanism is independent on *SUP45*.
- Gene(s) within chromosome II nucleotide positions 102568 and 148377 is responsible for *AQT* in [*PIN*$^{+}$ *psi*$^{-}$].
- Chromosome VIII disomy and deletions of *arg4* and *arg1* cause polyglutamine toxicity independent on Sup45.
- Phenotypic expression of [*PSI*$^{+}$] is suppressed by deletions of *arg1*, *arg4*, *arg8*, and *spe1*.

APPENDIX A

LIST OF STRAINS IN NUMERICAL ORDER

Yeast strains used in this study were listed in the table below.

Table A.1 List of strains in numerical order

Strain	Genotype
GT81-1C	*MAT a ade1-14 his3-Δ200 or 11,15 leu2-3,112 lys2 trp1-Δ ura3-52* [*PSI*$^{+}$ *PIN*$^{+}$]
GT349	*MAT a ade1-14 Δubc4::HIS3 his3-Δ200 or 11.15 leu2-3,112 lys2 trp1-Δ ura3-52* [*PSI*$^{+}$ *PIN*$^{+}$]
GT409	*MAT a ade1-14 his3-Δ200 or 11,15 leu2-3,112 lys2 trp1-Δ ura3-52* [*psi*$^{-}$ *pin*$^{-}$]
GT532-9A	*MAT a ade1-14 Δubc4::HIS3 his3-Δ200(or -11, 15) leu2-3,112 lys2 trp1-Δ* [*#607 URA*] *ura3-52* [*PSI*$^{+}$ *PIN*$^{+}$]
GT532	*ade1-14/ade1-14 Δubc4::HIS3/ubc4::HIS3 his3-Δ200(or -11, 15)/ his3-Δ200(or -11, 15) leu2-3,112/leu2-3,112 lys2/lys2 trp1-Δ/trp1-Δ ura3-52/ura3-52* [*pYES2-103Q*] [*PSI*$^{+}$ *PIN*$^{+}$]
GT534	*ade1-14/ade1-14 Δubc4::HIS3/ubc4::HIS3 his3-Δ200(or -11, 15)/ his3-Δ200(or -11, 15) leu2-3,112/leu2-3,112 lys2/lys2 trp1-Δ/trp1-Δ ura3-52/ura3-52* [*pYES2-103Q*] [*PSI*$^{+}$ *PIN*$^{+}$]
GT573	*MAT a ade1-14 Δubc4::HIS3 his3-Δ200 or 11.15 leu2-3,112 lys2 trp1-Δ ura3-52* [*PSI*$^{+}$ *PIN*$^{+}$] *(antitoxic papilla 2a')*
GT574	*MAT a ade1-14 Δubc4::HIS3 his3-Δ200 or 11.15 leu2-3,112 lys2 trp1-Δ ura3-52* [*PSI*$^{+}$ *PIN*$^{+}$] *(antitoxic papilla 7a')*
GT575	*MAT a ade1-14 Δubc4::HIS3 his3-Δ200 or 11.15 leu2-3,112 lys2 trp1-Δ ura3-52* [*PSI*$^{+}$ *PIN*$^{+}$] *(antitoxic papilla 9a')*
GT1161	*MAT a Δarg4::KanMX6 ade1-14 Δubc4::HIS3 his3-Δ200(or -11, 15) leu2-3,112 lys2 trp1-Δ ura3-52* [*PSI*$^{+}$ *PIN*$^{+}$]

Table A.1 List of strains in numerical order (continuation)

GT1162	*a/α Δarg4::KanMX6/ARG4 ade1-14/ ade1-14 Δubc4::HIS3/UBC4 his3-Δ200 or 11,15/ his3-Δ200 or 11,15 leu2-3,112/ leu2-3,112 lys2/ lys2 trp1-Δ/ trp1-Δ ura3-52/ ura3-52* [PSI^+ PIN^+]
GT1163	*MAT a Δarg4::KanMX6 ade1-14 Δubc4::HIS3 his3-Δ200(or -11, 15) leu2-3,112 lys2 trp1-Δ ura3-52* [*pYES2-103Q*] [PSI^+ PIN^+]
GT1164	*MAT a Δarg4::KanMX6 ade1-14 Δubc4::HIS3 his3-Δ200(or -11, 15) leu2-3,112 lys2 trp1-Δ ura3-52* [*pYES2-103Q*] [PSI^+ PIN^+]
GT1202	*MAT a Δmet28::KanMX6 ade1-14 Δubc4::HIS3 his3-Δ200(or -11, 15) leu2-3,112 lys2 trp1-Δ ura3-52* [PSI^+ PIN^+]
GT1203	*MAT a Δmet3::KanMX6 ade1-14 Δubc4::HIS3 his3-Δ200(or -11, 15) leu2-3,112 lys2 trp1-Δ ura3-52* [PSI^+ PIN^+]
GT1204	*MAT a Δmet14::KanMX6 ade1-14 Δubc4::HIS3 his3-Δ200(or -11, 15) leu2-3,112 lys2 trp1-Δ ura3-52* [PSI^+ PIN^+]
GT1205	*a/α Δmet28::KanMX6/MET28 aqt1-wt/AQT1-2 ade1-14/ ade1-14 Δubc4::HIS3/Δubc4::HIS3 his3-Δ200 or 11,15/ his3-Δ200 or 11,15 leu2-3,112/ leu2-3,112 lys2/ lys2 trp1-Δ/ trp1-Δ ura3-52/ ura3-52* [PSI^+ PIN^+]
GT1206	*a/α Δmet3::KanMX6/MET3 aqt1-wt/AQT1-2 ade1-14/ ade1-14 Δubc4::HIS3/Δubc4::HIS3 his3-Δ200 or 11,15/ his3-Δ200 or 11,15 leu2-3,112/ leu2-3,112 lys2/ lys2 trp1-Δ/ trp1-Δ ura3-52/ ura3-52* [PSI^+ PIN^+]
GT1207	*a/α Δmet14::KanMX6/MET14 aqt1-wt/AQT1-2 ade1-14/ ade1-14 Δubc4::HIS3/Δubc4::HIS3 his3-Δ200 or 11,15/ his3-Δ200 or 11,15 leu2-3,112/ leu2-3,112 lys2/ lys2 trp1-Δ/ trp1-Δ ura3-52/ ura3-52* [PSI^+ PIN^+]
GT1219	*MAT a ade1-14 Δubc4::KanMX6 his3-Δ200(or -11, 15) leu2-3,112 lys2 trp1-Δ ura3-52* [PSI^+ PIN^+]
GT1221	*MAT a ade1-14 Δubc4::HIS3 his3-Δ200(or -11, 15) leu2-3,112 lys2 ura3-52* [PSI^+ PIN^+]
GT1223	*MAT a Δarg1::KanMX6 ade1-14 Δubc4::HIS3 his3-Δ200(or -11, 15) leu2-3,112 lys2 trp1-Δ ura3-52* [PSI^+ PIN^+]
GT1224	*MAT a Δarg8::KanMX6 ade1-14 Δubc4::HIS3 his3-Δ200(or -11, 15) leu2-3,112 lys2 trp1-Δ ura3-52* [PSI^+ PIN^+]

Table A.1 List of strains in numerical order (continuation)

GT1277	*a/α Δarg1::KanMX6/ARG1 aqt1-wt/aqt1-wt ade1-14/ ade1-14 Δubc4::HIS3/UBC4 his3-Δ200 or 11,15/ his3-Δ200 or 11,15 leu2-3,112/ leu2-3,112 lys2/ lys2 trp1-Δ/ trp1-Δ ura3-52/ ura3-52* [*#874*] [PSI^+ PIN^+]
GT1278	*a/α Δarg8::KanMX6/ARG8 aqt1-wt/aqt1-wt ade1-14/ ade1-14 Δubc4::HIS3/UBC4 his3-Δ200 or 11,15/ his3-Δ200 or 11,15 leu2-3,112/ leu2-3,112 lys2/ lys2 trp1-Δ/ trp1-Δ ura3-52/ ura3-52* [*#874*] [PSI^+ PIN^+]
GT1279	*a/α Δarg1::KanMX6/ARG1 aqt1-wt/aqt1-wt ade1-14/ ade1-14 Δubc4::HIS3/Δubc4::HIS3 his3-Δ200 or 11,15/ his3-Δ200 or 11,15 leu2-3,112/ leu2-3,112 lys2/ lys2 trp1-Δ/ trp1-Δ ura3-52/ ura3-52* [*#874*] [PSI^+ PIN^+]
GT1280	*a/α Δarg8::KanMX6/ARG8 aqt1-wt/aqt1-wt ade1-14/ ade1-14 Δubc4::HIS3/Δubc4::HIS3 his3-Δ200 or 11,15/ his3-Δ200 or 11,15 leu2-3,112/ leu2-3,112 lys2/ lys2 trp1-Δ/ trp1-Δ ura3-52/ ura3-52* [*#874*] [PSI^+ PIN^+]
GT1281	*MAT α ade1-14 Δubc4::KanMX6/Δubc4::HIS3 AQT1-2 his3-Δ200(or -11, 15) leu2-3,112 lys2 trp1-Δ ura3-52* [*#874*] [PSI^+ PIN^+]
GT1282	*MAT a ade1-14 Δubc4::KanMX6/Δubc4::HIS3 AQT1-2 his3-Δ200(or -11, 15) leu2-3,112 lys2 trp1-Δ ura3-52* [*#874*] [PSI^+ PIN^+]
GT1283	*MAT α ade1-14 Δspe1::KanMX6 Δubc4::HIS3 aqt1-wt his3-Δ200(or -11, 15) leu2-3,112 lys2 trp1-Δ ura3-52* [*#874*] [PSI^+ PIN^+]
GT1299	*a/α Δspe1::KanMX6/SPE1 aqt1-wt/aqt1-wt ade1-14/ ade1-14 Δubc4::HIS3/UBC4 his3-Δ200 or 11,15/ his3-Δ200 or 11,15 leu2-3,112/ leu2-3,112 lys2/ lys2 trp1-Δ/ trp1-Δ ura3-52/ ura3-52* [*#874*] [PSI^+ PIN^+]
GT1305	*a/α Δspe1::KanMX6/SPE1 AQT1-2/aqt1-wt ade1-14/ ade1-14 Δubc4::HIS3/Δubc4::HIS3 his3-Δ200 or 11,15/ his3-Δ200 or 11,15 leu2-3,112/ leu2-3,112 lys2/ lys2 trp1-Δ/ trp1-Δ ura3-52/ ura3-52* [PSI^+ PIN^+]
GT1343	*MAT a ade1-14 Δpep1::pGSHU cassette Δubc4::HIS3 his3-Δ200 or 11.15 leu2-3,112 lys2 trp1-Δ ura3-52* [PSI^+ PIN^+]
GT1344	*MAT a ade1-14 Δpep1::pGSHU cassette Δubc4::HIS3 his3-Δ200 or 11.15 leu2-3,112 lys2 trp1-Δ ura3-52* [PSI^+ PIN^+]

Table A.1 List of strains in numerical order (continuation)

GT1349	*MAT a ade1-14 Δira1::pGSHU cassette Δubc4::HIS3 his3-Δ200 or 11.15 leu2-3,112 lys2 trp1-Δ ura3-52* [PSI^+ PIN^+]
GT1350	*MAT a ade1-14 Δira1::pGSHU cassette Δubc4::HIS3 his3-Δ200 or 11.15 leu2-3,112 lys2 trp1-Δ ura3-52* [PSI^+ PIN^+]
GT1443	*a/α ade1-14/ade1-14 Δubc4::HIS3/ubc4::HIS3 his3-Δ200(or -11, 15)/ his3-Δ200(or -11, 15) leu2-3,112/leu2-3,112 lys2/lys2 trp1-Δ/trp1-Δ ura3-52/ura3-52* [PSI^+ PIN^+]
GT1452	*a/α ade1-14/ade1-14 Δubc4::HIS3/ubc4::HIS3 his3-Δ200(or -11, 15)/ his3-Δ200(or -11, 15) leu2-3,112/leu2-3,112 lys2/lys2 trp1-Δ/trp1-Δ ura3-52/ura3-52, PEP1/Δpep1::pGSHU cassette* [PSI^+ PIN^+]
GT1465	*MAT a ade1-14 Δola1-Δira1::LEU2 Δubc4::HIS3 his3-Δ200 or 11.15 leu2-3,112 lys2 trp1-Δ ura3-52* [PSI^+ PIN^+]
GT1466	*MAT a ade1-14 Δ ira1-Δsnf5::LEU2 Δubc4::HIS3 his3-Δ200 or 11.15 leu2-3,112 lys2 trp1-Δ ura3-52* [PSI^+ PIN^+]
GT1467	*MAT a ade1-14 Δ boi1-Δpep1::LEU2 Δubc4::HIS3 his3-Δ200 or 11.15 leu2-3,112 lys2 trp1-Δ ura3-52* [PSI^+ PIN^+]
GT1471	*MAT a ade1-14 Δ ira1-Δmsi1::LEU2 Δubc4::HIS3 his3-Δ200 or 11.15 leu2-3,112 lys2 trp1-Δ ura3-52* [PSI^+ PIN^+]
GT1472	*MAT a ade1-14 Δ ira1-Δert1::LEU2 Δubc4::HIS3 his3-Δ200 or 11.15 leu2-3,112 lys2 trp1-Δ ura3-52* [PSI^+ PIN^+]
GT1473	*MAT a ade1-14 Δ kip1-Δpep1::LEU2 Δubc4::HIS3 his3-Δ200 or 11.15 leu2-3,112 lys2 trp1-Δ ura3-52* [PSI^+ PIN^+]
GT1474	*MAT a ade1-14 Δ apl3-Δpep1::LEU2 Δubc4::HIS3 his3-Δ200 or 11.15 leu2-3,112 lys2 trp1-Δ ura3-52* [PSI^+ PIN^+]
GT1490	*MAT a ade1-14 csh1Δ::pGSHU CSH1 Δubc4::HIS3 his3-Δ200 or 11.15 leu2-3,112 lys2 trp1-Δ ura3-52* [PSI^+ PIN^+]
GT1491	*MAT a ade1-14 YBR184WΔ::pGSHU YBR184W Δubc4::HIS3 his3-Δ200 or 11.15 leu2-3,112 lys2 trp1-Δ ura3-52* [PSI^+ PIN^+]
GT1492	*MAT a ade1-14 Δ ira1-Δapd1::LEU2 Δubc4::HIS3 his3-Δ200 or 11.15 leu2-3,112 lys2 trp1-Δ ura3-52* [PSI^+ PIN^+]
GT1493	*MAT a ade1-14 Δ apd1-Δcsh1::LEU2 Δubc4::HIS3 his3-Δ200 or 11.15*

Table A.1 List of strains in numerical order (continuation)

	leu2-3,112 lys2 trp1-Δ ura3-52 [PSI^+ PIN^+]
GT1494	*MAT a ade1-14 Δ csh1-Δnpl4::LEU2 Δubc4::HIS3 his3-Δ200 or 11.15 leu2-3,112 lys2 trp1-Δ ura3-52* [PSI^+ PIN^+]
GT1495	*MAT a ade1-14 Δ npl4-Δybr184w::LEU2 Δubc4::HIS3 his3-Δ200 or 11.15 leu2-3,112 lys2 trp1-Δ ura3-52* [PSI^+ PIN^+]
GT1496	*MAT a ade1-14 Δ ybr184w-Δmsi1::LEU2 Δubc4::HIS3 his3-Δ200 or 11.15 leu2-3,112 lys2 trp1-Δ ura3-52* [PSI^+ PIN^+]
GT1544	*MAT a ade1-14 Δ ira1-Δmak5::LEU2 Δubc4::HIS3 his3-Δ200 or 11.15 leu2-3,112 lys2 trp1-Δ ura3-52* [PSI^+ PIN^+]
GT1546	*MAT a ade1-14 Δ mak5-Δrtc2::LEU2 Δubc4::HIS3 his3-Δ200 or 11.15 leu2-3,112 lys2 trp1-Δ ura3-52* [PSI^+ PIN^+]
GT1547	*MAT a ade1-14 Δ rtc2-Δara1::LEU2 Δubc4::HIS3 his3-Δ200 or 11.15 leu2-3,112 lys2 trp1-Δ ura3-52* [PSI^+ PIN^+]
GT1553	*MAT a ade1-14 Δ sup45-Δadh5::LEU2 Δubc4::HIS3 his3-Δ200 or 11.15 leu2-3,112 lys2 trp1-Δ ura3-52* [PSI^+ PIN^+]
GT1555	*MAT a ade1-14 Δ SUP45/sup45::LEU2 Δubc4::HIS3 his3-Δ200 or 11.15 leu2-3,112 lys2 trp1-Δ ura3-52* [PSI^+ PIN^+]
GT1559	*MAT a/α Δubc4::HIS3/ Δubc4::HIS3 ade1-14/ade1-14 leu2-3, 112/leu2-3, 112 his3-Δ200(or -11, 15)/his3-Δ200(or -11, 15) lys2/lys2 trp1-Δ/trp1-Δ ura3-52/ura3-52* [PSI^+ PIN^+]
GT1564	*MAT a/α SUP45/Δsup45::HygR ade1-14/ade1-14 leu2-3, 112/leu2-3, 112 his3-Δ200(or -11, 15)/his3-Δ200(or -11, 15) lys2/lys2 trp1-Δ/trp1-Δ ura3-52/ura3-52* [PSI^+ PIN^+]
GT1564-1C	*MAT α Δsup45::HygR ade1-14 leu2-3, 112 his3-Δ200(or -11, 15) lys2 trp1-Δ ura3-52* [psi^- PIN^+] [*#1160*]
GT1564-3B	*MATα Δsup45::HygR ade1-14 leu2-3, 112 his3-Δ200(or -11, 15) lys2 trp1-Δ ura3-52* [psi^- PIN^+] [*#1162*]
GT1568	*MAT a ade1-14 Δ sup45::LEU2 Δubc4::HIS3 his3-Δ200 or 11.15 leu2-3,112 lys2 trp1-Δ ura3-52* [psi^- PIN^+]
GT1576	*MAT a/α SUP45/Δsup45::HygR ade1-14/ade1-14 leu2-3, 112/leu2-3, 112 his3-Δ200(or -11, 15)/his3-Δ200(or -11, 15) lys2/lys2 trp1-Δ/trp1-Δ ura3-52/ura3-52* [*#1160 CEN-LEU2-SUP45*] [PSI^+ PIN^+]

Table A.1 List of strains in numerical order (continuation)

GT1577	*MAT a/α UBC4/ Δubc4::HIS3 SUP45/Δsup45::HygR ade1-14/ade1-14 leu2-3, 112/leu2-3, 112 his3-Δ200(or -11, 15)/his3-Δ200(or -11, 15) lys2/lys2 trp1-Δ/trp1-Δ ura3-52/ura3-52* [*#1160 CEN-LEU2-SUP45*] [PSI^+ PIN^+]
GT1577-1B	*MATα Δubc4::HIS3 Δsup45::HygR ade1-14 leu2-3, 112 his3-Δ200(or -11, 15) lys2 trp1-Δ ura3-52* [*#1160 CEN-LEU2-SUP45*] [PSI^+ PIN^+]
GT1578	*MATa/α UBC4/ Δubc4::HIS3 SUP45/Δsup45::HygR ade1-14/ade1-14 leu2-3, 112/leu2-3, 112 his3-Δ200(or -11, 15)/his3-Δ200(or -11, 15) lys2/lys2 trp1-Δ/trp1-Δ ura3-52/ura3-52* [*#1160 CEN-LEU2-SUP45*] [psi^- PIN^+]
GT1578-1C	*MATα Δubc4::HIS3 Δsup45::HygR ade1-14 leu2-3, 112 his3-Δ200(or -11, 15) lys2 trp1-Δ ura3-52* [*#1160 CEN-LEU2-SUP45*] [psi^- PIN^+]
GT1579	*MATa/α SUP45/Δsup45::HygR ade1-14/ade1-14 leu2-3, 112/leu2-3, 112 his3-Δ200(or -11, 15)/his3-Δ200(or -11, 15) lys2/lys2 trp1-Δ/trp1-Δ ura3-52/ura3-52* [*#1162 CEN-URA3-SUP45*] [PSI^+ PIN^+]
GT1580	*MATa/α UBC4/ Δubc4::HIS3 SUP45/Δsup45::HygR ade1-14/ade1-14 leu2-3, 112/leu2-3, 112 his3-Δ200(or -11, 15)/his3-Δ200(or -11, 15) lys2/lys2 trp1-Δ/trp1-Δ ura3-52/ura3-52* [*#1162 CEN-URA3-SUP45*] [PSI^+ PIN^+]
GT1581	*MATa/α UBC4/ Δubc4::HIS3 SUP45/Δsup45::HygR ade1-14/ade1-14 leu2-3, 112/leu2-3, 112 his3-Δ200(or -11, 15)/his3-Δ200(or -11, 15) lys2/lys2 trp1-Δ/trp1-Δ ura3-52/ura3-52* [*#1162 CEN-URA3-SUP45*] [psi^- PIN^+]
GT1603	*MATa/α Δubc4::HIS3/ Δubc4::HIS3 SUP45/Δsup45::HygR ade1-14/ade1-14 leu2-3, 112/leu2-3, 112 his3-Δ200(or -11, 15)/his3-Δ200(or -11, 15) lys2/lys2 trp1-Δ/trp1-Δ ura3-52/ura3-52* [psi^- PIN^+]
GT1604	*MAT a ade1-14 Δola1-Δira1::LEU2 Δubc4::HIS3 his3-Δ200 or 11.15 leu2-3,112 lys2 trp1-Δ ura3-52* [psi^- PIN^+]
GT1605	*MAT a ade1-14 Δ ira1-Δsnf5::LEU2 Δubc4::HIS3 his3-Δ200 or 11.15 leu2-3,112 lys2 trp1-Δ ura3-52* [psi^- PIN^+]
GT1606	*MAT a ade1-14 Δ boi1-Δpep1::LEU2 Δubc4::HIS3 his3-Δ200 or 11.15 leu2-3,112 lys2 trp1-Δ ura3-52* [psi^- PIN^+]

Table A.1 List of strains in numerical order (continuation)

GT1607	*MAT a ade1-14 Δ ira1-Δmsi1::LEU2 Δubc4::HIS3 his3-Δ200 or 11.15 leu2-3,112 lys2 trp1-Δ ura3-52* [*psi⁻ PIN⁺*]
GT1608	*MAT a ade1-14 Δ ira1-Δert1::LEU2 Δubc4::HIS3 his3-Δ200 or 11.15 leu2-3,112 lys2 trp1-Δ ura3-52* [*psi⁻ PIN⁺*]
GT1609	*MAT a ade1-14 Δ kip1-Δpep1::LEU2 Δubc4::HIS3 his3-Δ200 or 11.15 leu2-3,112 lys2 trp1-Δ ura3-52* [*psi⁻ PIN⁺*]
GT1610	*MAT a ade1-14 Δ apl3-Δpep1::LEU2 Δubc4::HIS3 his3-Δ200 or 11.15 leu2-3,112 lys2 trp1-Δ ura3-52* [*psi⁻ PIN⁺*]
GT1611	*MAT a ade1-14 Δ ira1-Δapd1::LEU2 Δubc4::HIS3 his3-Δ200 or 11.15 leu2-3,112 lys2 trp1-Δ ura3-52* [*psi⁻ PIN⁺*]
GT1612	*MAT a ade1-14 Δ apd1-Δcsh1::LEU2 Δubc4::HIS3 his3-Δ200 or 11.15 leu2-3,112 lys2 trp1-Δ ura3-52* [*psi⁻ PIN⁺*]
GT1613	*MAT a ade1-14 Δ csh1-Δnpl4::LEU2 Δubc4::HIS3 his3-Δ200 or 11.15 leu2-3,112 lys2 trp1-Δ ura3-52* [*psi⁻ PIN⁺*]
GT1614	*MAT a ade1-14 Δ npl4-Δybr184w::LEU2 Δubc4::HIS3 his3-Δ200 or 11.15 leu2-3,112 lys2 trp1-Δ ura3-52* [*psi⁻ PIN⁺*]
GT1615	*MAT a ade1-14 Δ ybr184w-Δmsi1::LEU2 Δubc4::HIS3 his3-Δ200 or 11.15 leu2-3,112 lys2 trp1-Δ ura3-52* [*psi⁻ PIN⁺*]
GT1616	*MAT a ade1-14 Δ ira1-Δmak5::LEU2 Δubc4::HIS3 his3-Δ200 or 11.15 leu2-3,112 lys2 trp1-Δ ura3-52* [*psi⁻ PIN⁺*]
GT1617	*MAT a ade1-14 Δ mak5-Δrtc2::LEU2 Δubc4::HIS3 his3-Δ200 or 11.15 leu2-3,112 lys2 trp1-Δ ura3-52* [*psi⁻ PIN⁺*]
GT1618	*MAT a ade1-14 Δ rtc2-Δara1::LEU2 Δubc4::HIS3 his3-Δ200 or 11.15 leu2-3,112 lys2 trp1-Δ ura3-52* [*psi⁻ PIN⁺*]
GT1619	*MAT a ade1-14 Δ sup45-Δadh5::LEU2 Δubc4::HIS3 his3-Δ200 or 11.15 leu2-3,112 lys2 trp1-Δ ura3-52* [*psi⁻ PIN⁺*]
GT1620	*MATa/α Δubc4::HIS3/ Δubc4::HIS3 SUP45/Δsup45::HygR ade1-14/ade1-14 leu2-3, 112/leu2-3, 112 his3-Δ200(or -11, 15)/his3-Δ200(or -11, 15) lys2/lys2 trp1-Δ/trp1-Δ ura3-52/ura3-52* [*#1160 CEN-LEU2-SUP45*] [*PSI⁺ PIN⁺*]
GT1665	*a/α ade1-14/ade1-14 leu2-3, 112/leu2-3, 112 his3-Δ200(or -11, 15)/his3-Δ200(or -11, 15) lys2/lys2 trp1-Δ/trp1-Δ ura3-52/ura3-52*

Table A.1 List of strains in numerical order (continuation)

	ubc4Δ/ubc4Δ/UBC4 trisomic ChrII [*#874*] [PSI^+ PIN^+]
OT147	*MATα his5*
OT148	*MATa his5*

APPENDIX B

LIST OF PLASMIDS IN NUMERICAL ORDER

Plasmids used in this study were listed in the table below.

Table B.1 List of plasmids in numerical order

No.	Protein	Plasmid	Marker/Type	Promoter	Reference
3	N/A	pRS316-GAL	URA3/CEN	*GAL1*	(Liu et al. 1992)
39	N/A	YEp13	LEU2/2μ	N/A	(Rose and Broach 1990)
96	N/A	pRS316	URA3/CEN	N/A	(Sikorski and Hieter 1989)
189	N/A	pRS315	LEU2/CEN	N/A	(Sikorski and Hieter 1989)
191	Sup45DelC5	YEp13-SUP1	LEU2/2μ	*SUP35*	(Chernoff et al. 1992)
210	Sup35C	pRS315-SUP35 del3ATG	LEU2/CEN	*SUP35*	J. Hoffman
275	β-galactosidase	pUKC815	URA3/2μ	*PGK*	(Firoozan et al. 1991)
278	β-galactosidase w/ UGA stop codon	pUKC819	URA3/2μ	*PGK*	(Firoozan et al. 1991)
303	Sup45	pGAL-SUP45 Library	URA3/CEN	*GAL1-10*	G. Newnam
564	Ubc4	pTRP-UBC4	TRP1/2μ	*GAL1*	Dr. Braun
659	Htt-25Q	pYES-Q25trp	TRP1/2μ	*GAL1*	(Wang et al. 2009)
660	Htt-103Q	pYES-Q103trp	TRP1/2μ	*GAL1*	(Wang et al. 2009)

Table B.1 List of plasmids in numerical order (continuation)

872	Htt-25Q	pYES2-25Q	URA3/2µ	*GAL1*	(Meriin et al. 2002)
873	Htt-25QP	pYES2-25QP	URA3/2µ	*GAL1*	(Meriin et al. 2007)
874	Htt-103Q	pYES2-103Q	URA3/2µ	*GAL1*	(Meriin et al. 2002)
875	Htt-103QP	pYES2-103QP	URA3/2µ	*GAL1*	(Meriin et al. 2007)
1058	Arg4	pRS315_ARG4	LEU2/CEN	*ARG4*	This study
1059	Arg4	CEN-AL	LEU2/CEN	*ARG4*	This study
1068	N/A	pFL35	TRP1/2µ	N/A	(Bonneaud et al. 1991)
1086	N/A	pGSHU	Hyg^R URA3 /NA	N/A	(Storici and Resnick 2006)
1087	Ump1	pRS316-GAL-UMP1	URA3/CEN	*GAL1*	This study
1090	Ump1	pRS315-UMP1	LEU2/CEN	*UMP1*	This study
1100	Sup35NM	pCUP-Sup35NM-DsRed	LEU2/CEN	*CUP*	This study
1150	Sup45	pRS315-SUP45-ADH5	LEU2/CEN	*SUP45*	This study
1151	Sup45	pRS315-GAL-SUP45cDNA	LEU2/CEN	*GAL1*	This study
1159	Sup45DelC5	pRS414-SUP45CDel	TRP1/CEN	*SUP45*	(Vishveshwara et al. 2009)
1160	Sup45	pRS315-SUP45	LEU2/CEN	*SUP45*	(Le Goff et al. 2002)
1161	Sup45 Missense	pRS315-SUP45-103	LEU2/CEN	*SUP45*	(Moskalenko et al. 2004)
1162	Sup45	pRS316-SUP45	URA3/CEN	*SUP45*	(Le Goff et al. 2002)

Table B.1 List of plasmids in numerical order (continuation)

1163	Sup45Del C19	pDB843-SUP45-DelC19	LEU2/CEN	*SUP45*	(Kallmeyer et al. 2006)

APPENDIX C

LIST OF PRIMERS

Primers used in this study were synthesized by IDT or Invitrogen and were DNA oligonucleotides without specific additional modifications. Dry primers were resuspended in the ddH_2O to the concentration of 250 μM as the stock. The list of primers is in the table below.

Table C.1 List of primers in numerical order

Number	Primer	Sequence
554	10_MET3_F	ACTATTACACTTCATTTACCACCCTCTGATCTA GATTTTCCGGATCCCCGGGTTAATTAA
555	9_MET28_R	GTGAGTCAAGGCCGGGCAGCCAATGACTAAG AACACGAGGGAATTCGAGCTCGTTTAAAC
556	9_MET28_F	ACGTTTCGCGGGCTACCTGCCCATGTTCCGTCT CTTAATGCGGATCCCCGGGTTAATTAA
557	10_MET3_R	GTACAATATGTGAAATAGGTTCATCCGCTGAC TCTAGCTGGAATTCGAGCTCGTTTAAAC
558	11_MET14_F	TGTACAGTAATCGGTCAAATTACAAATGCTTA CGGATGATCGGATCCCCGGGTTAATTAA
559	11_MET14_R	CAAGAAAAGTTGGAATTATTTCTCCAAGCACA CTGTACACGAATTCGAGCTCGTTTAAAC
686	PRSQZ	CGACGGGATCCCCCTTAACG
687	9_MET28_ChF	CGACAGTTCCATGTCGCGAG
688	9_MET28_ChR	AAGGGGTACTGAGTGCACGT
689	10_MET3_ChF	AGATGCTCAGAATACCCGTC
690	10_MET3_ChR	GCGGTCGATCATGAATTTTG

Table C.1 List of primers in numerical order (continuation)

691	11_MET14_ChF	TCTATGAGCGAGGCCACTGG
692	11_MET14_ChR	TGCGTATCCGTTAATGTCGT
693	F_pRS315_ARG4	CTGGGATCCTATTTAGTCTCATGGCCATT
694	R_pRS315_ARG4	ATCCTCTAGACTGTCAGAGACTGTTCCTT
695	Chk9_MET28_F	TTGATCAATGCGGAGTGGGA
696	Chk9_MET28_R	GTACTGAGTGCACGTGACTT
697	HIS2_Chk_Fwd	GATCCAAAGCCGTTCTAGAT
698	HIS2_Chk_Rvs	ATTTGAGTAGCTCGTCAAGG
699	HIS2_Del_Rvs	CGATCAAGTGGTCAACCTCAACTTTCACACGT ACTGTTTGCGGATCCCCGGGTTAATTAA
700	HIS2_Del_Fwd	ATGTTGAACTTCCAGATGCGGCCGAGTCGGCG AGCAAACAGAATTCGAGCTCGTTTAAAC
701	ARG1_Del_For	GCAGTTGCGAGACCCAGACTGGCACTGTCTCA ATAGTATAGAATTCGAGCTCGTTTAAAC
702	ARG1_Del_Rev	TACCCTTATACAGTCTAACCCTGACAGTACCG TTAACGCTCGGATCCCCGGGTTAATTAA
703	ARG8_Del_Rev	TTTTTGATGACCTCGGTGGGTGGTTCGACGAA CTCAGCACGAATTCGAGCTCGTTTAAAC
704	ARG8_Del_For	GGATTCGATATGGTTGCCAGCTCGCTATGTGA CTCACTTACGGATCCCCGGGTTAATTAA
705	ARG1_Chk_Rev	CGGATCGTACAACTTTTCAG
706	ARG1_Chk_For	GCCGTATGGAAGAGTCATTT
707	ARG8_Chk_Rev	TCAAGGTATGAAAGACGCAC
708	ARG8_Chk_For	GCTCATAGCAATCGCGAAAT
709	HIS2_NEW_ChF	AAACGTCTGGAGGAATGACT
710	HIS2_NEW_ChR	TAAAAGCGCGGAAACATGAG

Table C.1 List of primers in numerical order (continuation)

711	F_pRS315_UBP6	AGCTCTAGACGGTGGTGTCTTAATGGTT
712	R_pRS315_UBP6	TTAAGGATCCATGGGGGTGCCAAAGGTAAA
713	HIS2-M	GGAATGGAGATCGAAAGTTG
714	G418-M	ATCAGGTGCGACAATCTATC
715	SLA1_Del_F	CCTATAAAATCTTAAAATACATTAATCTAGAA TCCAAACGGCGGATCCCCGGG
716	SLA1_Del_R	GACAGAGTGTGTTATATACAAAAGAGCTAGA GTATGACGAATTCGAGCTCGTT
717	SPE1_Del_F	TTTGTGTACAATGGCGTACAGTGGTGGACAGG AAAAATGCGAATTCGAGCTCGTTTAAAC
718	SPE1_Del_R	CTGAGACAGTAGAGAATTGATACATGGATAAC TGAATCTCCGGATCCCCGGGTTAATTAA
719	SPE1_Chk_F	AATTCGTCCCCGAACGCAAC
720	SPE1_Chk_R	ATGGCGTACAGTGGTGGACA
721	pRS315_UMP1_F	ATGTTCTAGATATCACTGGCGCTGTATGGCCG
722	pRS315_UMP1_R	CACCGGAGGGGCCCGGAAGGTAAAAGCTCAA GGA
723	pRS316-GAL_UMP1_F	CACCAAGCTTATGAATATCGTCCCACAAGA
724	pRS316-GAL_UMP1_R	GAAATCTAGAGCAATTTTTAAATGCCTAATTG
725	SLA1-M-Rev	CCAGAGAACTCCTAGATGAA
726	SLA1-M-For	TTCATCTAGGAGTTCTCTGG
727	ChF_Arg4	ACTCATTGGCAGAATCCCGA
728	ChR_Arg4	TTGACTGCGGACCTGAACTT
729	ChkPL5’	TCACCAAGCACTGAGCGTCC
730	ChkPL3’	CTAACTACGGACTGGGGCAA

Table C.1 List of primers in numerical order (continuation)

731	ChkPR5’	CATAGCTCTCGCAGAGAAGA
732	ChkPR3’	CAGTCGATGTCTCTAACACC
733	SCE.2	CTGTTCGATGTTCAGTTCGA
734	URA3.1	TTCAATAGCTCATCAGTCGA
735	P.IL	AGAATTCCGGCGGTTGGAGTGGAACCCTCCCG TGTGTAAAACATATTTTGTTCGTACGCTGCAG GTCGAC
736	P.IISL	TGAAAGGAACGATGATTGCCTCACTTTACCCT CTATCTAGGCGTCGTAACTAGGGATAACAGGG TAATCCGCGCGTTGGCCGATTCAT
737	P.IR	AAAATAGTAAGCTCAGACCAACTGTGTGCGGA AGCCTCAACTGCTAGAGATTCGTACGCTGCAG GTCGAC
738	P.IISR	AGACATATGTACCCGATGATACCACCACGTTC TTGGCCCTAATTTTCAAGTAGGGATAACAGGG TAATCCGCGCGTTGGCCGATTCAT
743	Rg3-LEU2-5’	AAAATCGCCCACACGCGTGCCCGAAGTTAGCA CTCCACAGTTGCAAGATGCAACAAGTAATTGG TTGTTT
744	Rg3-LEU2-3’	TGAAAGGAACGATGATTGCCTCACTTTACCCT CTATCTAGGCGTCGTAACCTACGTCGTTAAGG CCGTTT
745	Rg1-LEU2-5’	CGAATGGATAGTTAGCTGGGTTACCCAATGGA CATCTAGTGATGGCTTGGCAACAAGTAATTGG TTGTTT
746	Rg1-LEU2-3’	AGACATATGTACCCGATGATACCACCACGTTC TTGGCCCTAATTTTCAAGCTACGTCGTTAAGG CCGTTT
747	Chk-Rg3-LEU2-5’	AGCACTCCACAGTTGCAAGA
748	Chk-Rg1-LEU2-5’	TTACCCAATGGACATCTAGT
756	Chk-Rg1-LEU2-Rev	TAGCATTGCTCAGAGTTAGA

Table C.1 List of primers in numerical order (continuation)

757	Chk-Rg3-LEU2-Rev	TCCGGATTCCGTCCTCTTAT
758	M-Leu2-Rev	TCACTATCCCAAGCGACACC
759	Rg1-FrL-5’	TAAGTGGTGGGACGTATGCC
760	Rg1-FrL-3’	TGTCCATTGGGTAACCCAGC
761	Rg1-HiL-5’	TAGGGCCAAGAACGTGGTGG
762	Rg1-HiL-3’	TGCAACAAGGGCTTTGTCAC
763	M-LEU2-For	TGGTGTCGCTTGGGATAGTG
764	Rg3-Seq-5’	AAACGAATGGAGGACGAGC
765	Rg1-Seq-5’	ACTGGATCAACGTCACCCTC
768	Rg2-LEU2-5’	AATGAGACTCTTATTTCCGAAGGACCGACATC AATTAACAGAGACACAGCCAACAAGTAATTG GTTGTTT
769	Rg2-LEU2-3’	CTGCAATTGTTGTGGTGTGAGGCTCTGATACA GCTGTTGCGGAATTTGCGCTACGTCGTTAAGG CCGTTT
770	Chk-Rg2-LEU2-3’	CGTTTGCGGTGGCGGTGAAG
771	Chk-Rg3.1-LEU2-5’	GAAAGTGTGTTTCCGTTGCC
772	Chk-Rg3.2-LEU2-5’	GTGCTGCCACTTCAGACTCC
773	Chk-Rg2.1-LEU2-3’	ACAGCGACGGAACAGCGGTG
774	Chk-Rg2.2-LEU2-3’	GCGTGAACTGTTCGAGATTG
775	Rg3.1-LEU2-5’	GATCCGTCGGATGAAGCTATCAGCAATTCTGT GACAGCCTTATGTTCCCTCAACAAGTAATTGG TTGTTT
776	Rg3.2-LEU2-5’	GCTCTCTGATAGTGAGGACGATGATCCTGCAG TCAACGATCCCAAGAGGCCAACAAGTAATTGG TTGTTT
777	Rg2.1-LEU2-3’	CCAAGAAGATGGGTTAGTCAAGCTATGGGATA CCTCCTGCGAAGAAACTACTACGTCGTTAAGG

Table C.1 List of primers in numerical order (continuation)

		CCGTTT
778	Rg2.2-LEU2-3’	CTGGAATACCGAATAGAGAGCTCCCAATGAACATACAACCGGACCTTCCACTACGTCGTTAAGGCCGTTT
788	Chk-2.1a-3’	AATCCCGCATCGTTTATCCC
789	Chk-2.1b-5’	TGGCTATATTCGGAGGAGGC
790	Chk-2.1b-3’	TGGTCCCGAGCACAGCCAAG
791	Chk-2.1c-5’	CAAGGCAGTGCGAAGCGGTG
792	Chk-2.1c-3’	GTGGAGGTACACGGGTATGC
793	Chk-2.1d-5’	CCATAGCTTGTCGATTGCTC
794	Chk-2.1d-3’	AGGACGATGCTAAAGTTGCC
795	Chk-2.1e-5’	CCTAATGCGATACGTCTTCC
796	Chk-Npl4-Del-P.I	CGACTCCCAGTTATTGTTCC
797	Chk-Npl4-Del-P.II	TTGTGCGTACCTCTTTCCTG
798	Chk-Ubs1-Del-P.I	AGTTCCGAGAACATTCTGCC
799	Chk-Ubs1-Del-P.II	CAGAGGCTAATCTCATTGGC
800	IntP.Ibc	ATCCCAGAACAGTGGGTAAAAGGGAGGCAGAAGTGCATTGATTTACATCCTTCGTACGCTGCAGGTCGAC
801	IntP.IIbc	GGGGTGCCTTGGAACAGAGCCCATCACATCATTTGACACTCCTGTAGGCGCCGCGCGTTGGCCGATTCAT
802	IntP.Ide	GCTATTCAACTTTTGAAGTCCGAAGCAGCACAGTTTACGCTACTGCGTGATTCGTACGCTGCAGGTCGAC
803	IntP.IIde	TCCATAAGCCGGTAAGAATAGTCCTGTTATAGCTGATACTACCTTGTACACCGCGCGTTGGCCGATTCAT
804	2.1a-3’	CGAGGCAGGCATCATGCTGCCAATCGATTTGA

Table C.1 List of primers in numerical order (continuation)

		GAGGTGGGGACAACGAAGCTACGTCGTTAAG GCCGTTT
805	2.1b-5’	CTTCGTTGTCCCCACCTCTCAAATCGATTGGCA GCATGATGCCTGCCTCGCAACAAGTAATTGGT TGTTT
806	2.1b-3’	GGGGTGCCTTGGAACAGAGCCCATCACATCAT TTGACACTCCTGTAGGCGCTACGTCGTTAAGG CCGTTT
807	2.1c-5’	ATCCCAGAACAGTGGGTAAAAGGGAGGCAGA AGTGCATTGATTTACATCCCAACAAGTAATTG GTTGTTT
808	2.1c-3’	GCTGCTAGGCATCAAACAAGGCATCCTAATGT AAGCAAGTATAGCGAACACTACGTCGTTAAGG CCGTTT
809	2.1d-5’	TGTTCGCTATACTTGCTTACATTAGGATGCCTT GTTTGATGCCTAGCAGCCAACAAGTAATTGGT TGTTT
810	2.1d-3’	TCCATAAGCCGGTAAGAATAGTCCTGTTATAG CTGATACTACCTTGTACACTACGTCGTTAAGG CCGTTT
811	2.1e-5’	GCTATTCAACTTTTGAAGTCCGAAGCAGCACA GTTTACGCTACTGCGTGACAACAAGTAATTGG TTGTTT
812	Npl4-Del-P.I	CACAGCAGATTCTATTAGTAACTTCCATTCGTC TGGAGAGAGTATCTGCATTCGTACGCTGCAGG TCGAC
813	Npl4-Del-P.II	TTGGCGGGTAATAAGATGCGTCTACCCATTTT AAGGAACGCCCTCGTAACCCGCGCGTTGGCCG ATTCAT
814	Ubs1-Del-P.I	CATCAATCTAACGTTGCCTTTGTCGTGATTTTG TGCGAGGAGGCGATATATTCGTACGCTGCAGG TCGAC
815	Ubs1-Del-P.II	ACTACCGCGATTATCGTTCGTTTCATCTGGACA TGCCAACGTTCTTGACCCCGCGCGTTGGCCGA TTCAT

Table C.1 List of primers in numerical order (continuation)

816	Chk-IRA1-5’	GGCTGGGAAACCATGCTTGG
817	Chk-IRA1-3’	CCCTCTAAGCGAGCCGACAC
818	Mid-IRA1-5’	ATTCGCCTGTCCTAGTGTTG
819	Chk-MAK5-5’	CCGCTGTATTAGTGGTATCG
820	Chk-MAK5-3’	GGTATTGGTGCCATGCTGCG
821	Del-IRA1-5’	AACCTTGCAATCATTATACTTTACACAAATCTC TACGTTTAAGAAGCAAGCACACAATGG
822	Del-IRA1-3’	TAAAGTCAAGTGATCATCTTTTGCCCTGCAAA TAGAGCTTCTGTTTAGCTTGCCTCGTCC
823	Del-MAK5-5’	TTTCACCTCACAAACCCGCCTCAAGGTTAGTT AGTCCGTAAAGAAGCAAGCACACAATGG
824	Del-MAK5-3’	ACATAGTGGGTTTAGAGGACCGTGTATATTAC GTAGAAAACTGTTTAGCTTGCCTCGTCC
825	Del-IRA1-S2-5’	CTTGAAAATTAGGGCCAAGAACGTGGTGGTAT CATCGGGTAAGAAGCAAGCACACAATGG
826	Del-IRA1-S2-3’	ATTTGAGCACTCTGAAAAGAACCTGGGCATTT CAAATCATCTGTTTAGCTTGCCTCGTCC
827	Del-IRA1-S3-5’	ATGATTTGAAATGCCCAGGTTCTTTTCAGAGT GCTCAAATAAGAAGCAAGCACACAATGG
828	Chk-IRA1-S2-3’	TTGATACCAGAGCAAGCATC
829	Hyg-For	GCCTCGCTCCAGTCAATGAC
830	Hyg-Rev	GTCATTGACTGGAGCGAGGC
831	Del-RTC2-5’	ACGTAATAGCCTCAAGCGAGCATCCCTAAATT TCTGCCATAAGAAGCAAGCACACAATGG
832	Del-RTC2-3’	TCTGGGCTATAGCCGATGCGCATATGAGTAAG TTTGAGTTCTGTTTAGCTTGCCTCGTCC
833	Del-ARA1-5’	GAGGGGGATATCAAGCATCTGGACTTATTTGC ACTATCTCAAGAAGCAAGCACACAATGG

Table C.1 List of primers in numerical order (continuation)

834	Del-ARA1-3’	GTCCAAGTTTGGTCCGTTACCAGTAAACTCTG GAAGGATGCTGTTTAGCTTGCCTCGTCC
835	Del-TBS1-5’	AAGTATCTGAAATACATACGCGCGCGTATGCA TATGTATTAAGAAGCAAGCACACAATGG
836	Del-TBS1-3’	GATTACAAGCCCAGCAGGAGTTGTGTGAATGA ATATGGATCTGTTTAGCTTGCCTCGTCC
837	Chk-RTC2-5’	TTCCTCTCACCCGCAAAGC
838	Chk-RTC2-3’	CGTGTCAGCAAAGGGCATCG
839	Chk-ARA1-5’	CTACCCTTACCTCCGCCTGG
840	Chk-ARA1-3’	TTAGCTTCGCTGCTTGATGC
841	Chk-TBS1-5’	TGGGACGAAGTGGACAGATC
842	Chk-TBS1-3’	AGCCACTGCCCAAAGTCTAC
859	Chk-IRA1-S3-5’	ACATCAGCAGGAGAACACGC
860	Chk-SUP45-5’	AGATTAGCAGGCGAACTGGC
861	Chk-SUP45-3’	CAATCTGTCGCTACCGCATG
862	Chk-ADH5-3’	CTTACGCACGCAGTTGCTAG
873	Del-SUP45-5’	TTTTCTACGTAATATACACGGTCCTCTAAACCC ACTATGTAAGAAGCAAGCACACAATGG
874	Del-SUP45-3’	TTAATTCATTTCGGCTTGTCTCCTTATTAAGAC TACAGAACTGTTTAGCTTGCCTCGTCC
875	Del-ADH5-3’	ATGTCCACCGGTTCTCGCAAAGTACAGAATCA CTCGCTATCTGTTTAGCTTGCCTCGTCC
911	Chk-Rg3.2X-5’	CGCTGCTCGTCCTGGGTGA
912	Chk-Rg3.2X-3’	GCTACGCTGGTTGAGTGGAAG
913	Chk-Rg3.2XI-3’	GAGAGTGGAATAACGGGTCG
914	Chk-Rg3.2XII-5’	GTATGCCCAAGACCAGTCGG

Table C.1 List of primers in numerical order (continuation)

915	Rg3.2X-Del-5’	ACAATCAACGACAGTTCGCGCTTCCCTCACTA AATATGGCCAACAAGTAATTGGTTGTTT
916	Rg3.2X-Del-3’	TTTATACATTCGACAATGTACTTCGCCAGGGG ACCGGCCGCTACGTCGTTAAGGCCGTTT
917	Rg3.2XI-3’	AAGATCCTTACATTACACGGCGTGCGACAGAC TCGAACCACTACGTCGTTAAGGCCGTTT
918	Rg3.2XII-5’	TGGTTCGAGTCTGTCGCACGCCGTGTAATGTA AGGATCTTCAACAAGTAATTGGTTGTTT
919	Chk-Rg3.2XI-Rev	CGACCAGAACCCGTGGTATG
920	Chk-Rg3.2XII-For	CAACTGGCTAAGGTGAACGG

APPENDIX D

CGH DATA OF *AQT* DERIVATIVES

The microarray experiment was performed by our collaborator, Dr. Piotr Mieczkowski (University of North Carolina). For the data of the CGH analysis of *AQT* derivatives provided by Dr. Mieczkowski, see the separate file attached.

REFERENCES

Bagola K, Sommer T. 2008. Protein quality control: on IPODs and other JUNQ. *Curr Biol* **18**: R1019-1021.

Bondzi C, Brunner AM, Munyikwa MR, Connor CD, Simmons AN, Stephens SL, Belt PA, Roggero VR, Mavinakere MS, Hinton SD et al. 2011. Recruitment of the oncoprotein v-ErbA to aggresomes. *Mol Cell Endocrinol* **332**: 196-212.

Bonneaud N, Ozier-Kalogeropoulos O, Li GY, Labouesse M, Minvielle-Sebastia L, Lacroute F. 1991. A family of low and high copy replicative, integrative and single-stranded S. cerevisiae/E. coli shuttle vectors. *Yeast* **7**: 609-615.

Caviston JP, Holzbaur EL. 2009. Huntingtin as an essential integrator of intracellular vesicular trafficking. *Trends Cell Biol* **19**: 147-155.

Chernoff YO, Galkin AP, Lewitin E, Chernova TA, Newnam GP, Belenkiy SM. 2000. Evolutionary conservation of prion-forming abilities of the yeast Sup35 protein. *Mol Microbiol* **35**: 865-876.

Chernoff YO, Inge-Vechtomov SG, Derkach IL, Ptyushkina MV, Tarunina OV, Dagkesamanskaya AR, Ter-Avanesyan MD. 1992. Dosage-dependent translational suppression in yeast Saccharomyces cerevisiae. *Yeast* **8**: 489-499.

Chernoff YO, Newnam GP, Kumar J, Allen K, Zink AD. 1999. Evidence for a protein mutator in yeast: role of the Hsp70-related chaperone ssb in formation, stability, and toxicity of the [*PSI*$^{+}$] prion. *Mol Cell Biol* **19**: 8103-8112.

Chin LS, Olzmann JA, Li L. 2010. Parkin-mediated ubiquitin signalling in aggresome formation and autophagy. *Biochem Soc Trans* **38**: 144-149.

Colton CA, Xu Q, Burke JR, Bae SY, Wakefield JK, Nair A, Strittmatter WJ, Vitek MP. 2004. Disrupted spermine homeostasis: a novel mechanism in polyglutamine-mediated aggregation and cell death. *J Neurosci* **24**: 7118-7127.

Dagkesamanskaya AR, Ter-Avanesyan MD. 1991. Interaction of the yeast omnipotent suppressors SUP1(SUP45) and SUP2(SUP35) with non-mendelian factors. *Genetics* **128**: 513-520.

Davies SW, Turmaine M, Cozens BA, DiFiglia M, Sharp AH, Ross CA, Scherzinger E, Wanker EE, Mangiarini L, Bates GP. 1997. Formation of neuronal intranuclear inclusions underlies the neurological dysfunction in mice transgenic for the HD mutation. *Cell* **90**: 537-548.

Derkatch IL, Uptain SM, Outeiro TF, Krishnan R, Lindquist SL, Liebman SW. 2004. Effects of Q/N-rich, polyQ, and non-polyQ amyloids on the de novo formation of the [*PSI*$^+$] prion in yeast and aggregation of Sup35 in vitro. *Proc Natl Acad Sci U S A* **101**: 12934-12939.

DiFiglia M, Sapp E, Chase KO, Davies SW, Bates GP, Vonsattel JP, Aronin N. 1997. Aggregation of huntingtin in neuronal intranuclear inclusions and dystrophic neurites in brain. *Science* **277**: 1990-1993.

Duennwald ML, Jagadish S, Giorgini F, Muchowski PJ, Lindquist S. 2006. A network of protein interactions determines polyglutamine toxicity. *Proc Natl Acad Sci U S A* **103**: 11051-11056.

Firoozan M, Grant CM, Duarte JA, Tuite MF. 1991. Quantitation of readthrough of termination codons in yeast using a novel gene fusion assay. *Yeast* **7**: 173-183.

Garcia-Mata R, Gao YS, Sztul E. 2002. Hassles with taking out the garbage: aggravating aggresomes. *Traffic* **3**: 388-396.

Gokhale KC, Newnam GP, Sherman MY, Chernoff YO. 2005. Modulation of prion-dependent polyglutamine aggregation and toxicity by chaperone proteins in the yeast model. *J Biol Chem* **280**: 22809-22818.

Halfmann R, Lindquist S. 2008. Screening for amyloid aggregation by Semi-Denaturing Detergent-Agarose Gel Electrophoresis. *J Vis Exp*.

Hands SL, Wyttenbach A. 2010. Neurotoxic protein oligomerisation associated with polyglutamine diseases. *Acta Neuropathol* **120**: 419-437.

Hay DG, Sathasivam K, Tobaben S, Stahl B, Marber M, Mestril R, Mahal A, Smith DL, Woodman B, Bates GP. 2004. Progressive decrease in chaperone protein levels in a mouse model of Huntington's disease and induction of stress proteins as a therapeutic approach. *Hum Mol Genet* **13**: 1389-1405.

Henry SA, Klig LS, Loewy BS. 1984. The genetic regulation and coordination of biosynthetic pathways in yeast: amino acid and phospholipid synthesis. *Annu Rev Genet* **18**: 207-231.

Inge-Vechtomov SG, Tikhodeev ON, Karpova TS. 1988. Selective systems for obtaining recessive ribosomal suppressors in saccharomycete yeasts. *Genetika* **24**: 1159-1165.

Inge-Vechtomov SG, Zhouravleva GA, Chernoff YO. 2007. Biological roles of prion domains. *Prion* **1**: 228-235.

Johnston JA, Ward CL, Kopito RR. 1998. Aggresomes: a cellular response to misfolded proteins. *J Cell Biol* **143**: 1883-1898.

Kallmeyer AK, Keeling KM, Bedwell DM. 2006. Eukaryotic release factor 1 phosphorylation by CK2 protein kinase is dynamic but has little effect on the efficiency of translation termination in Saccharomyces cerevisiae. *Eukaryot Cell* **5**: 1378-1387.

King MA, Hands S, Hafiz F, Mizushima N, Tolkovsky AM, Wyttenbach A. 2008. Rapamycin inhibits polyglutamine aggregation independently of autophagy by reducing protein synthesis. *Mol Pharmacol* **73**: 1052-1063.

Kopito RR. 2000. Aggresomes, inclusion bodies and protein aggregation. *Trends Cell Biol* **10**: 524-530.

Krobitsch S, Lindquist S. 2000. Aggregation of huntingtin in yeast varies with the length of the polyglutamine expansion and the expression of chaperone proteins. *Proc Natl Acad Sci U S A* **97**: 1589-1594.

Kumar A, Snyder M. 2001. Genome-wide transposon mutagenesis in yeast. *Curr Protoc Mol Biol* **Chapter 13**: Unit13 13.

La Spada AR, Taylor JP. 2010. Repeat expansion disease: progress and puzzles in disease pathogenesis. *Nat Rev Genet* **11**: 247-258.

Laney JD, Hochstrasser M. 2003. Ubiquitin-dependent degradation of the yeast Mat(alpha)2 repressor enables a switch in developmental state. *Genes Dev* **17**: 2259-2270.

Le Goff C, Zemlyanko O, Moskalenko S, Berkova N, Inge-Vechtomov S, Philippe M, Zhouravleva G. 2002. Mouse GSPT2, but not GSPT1, can substitute for yeast eRF3 in vivo. *Genes Cells* **7**: 1043-1057.

Lemoine FJ, Degtyareva NP, Lobachev K, Petes TD. 2005. Chromosomal translocations in yeast induced by low levels of DNA polymerase a model for chromosome fragile sites. *Cell* **120**: 587-598.

Liu H, Krizek J, Bretscher A. 1992. Construction of a GAL1-regulated yeast cDNA expression library and its application to the identification of genes whose overexpression causes lethality in yeast. *Genetics* **132**: 665-673.

Loidl J. 1995. Meiotic chromosome pairing in triploid and tetraploid Saccharomyces cerevisiae. *Genetics* **139**: 1511-1520.

Longtine MS, McKenzie A, 3rd, Demarini DJ, Shah NG, Wach A, Brachat A, Philippsen P, Pringle JR. 1998. Additional modules for versatile and economical PCR-based gene deletion and modification in Saccharomyces cerevisiae. *Yeast* **14**: 953-961.

Lunkes A, Lindenberg KS, Ben-Haiem L, Weber C, Devys D, Landwehrmeyer GB, Mandel JL, Trottier Y. 2002. Proteases acting on mutant huntingtin generate

cleaved products that differentially build up cytoplasmic and nuclear inclusions. *Mol Cell* **10**: 259-269.

Mangiarini L, Sathasivam K, Seller M, Cozens B, Harper A, Hetherington C, Lawton M, Trottier Y, Lehrach H, Davies SW et al. 1996. Exon 1 of the HD gene with an expanded CAG repeat is sufficient to cause a progressive neurological phenotype in transgenic mice. *Cell* **87**: 493-506.

Meriin AB, Zhang X, Alexandrov IM, Salnikova AB, Ter-Avanesian MD, Chernoff YO, Sherman MY. 2007. Endocytosis machinery is involved in aggregation of proteins with expanded polyglutamine domains. *FASEB J* **21**: 1915-1925.

Meriin AB, Zhang X, He X, Newnam GP, Chernoff YO, Sherman MY. 2002. Huntington toxicity in yeast model depends on polyglutamine aggregation mediated by a prion-like protein Rnq1. *J Cell Biol* **157**: 997-1004.

Meriin AB, Zhang X, Miliaras NB, Kazantsev A, Chernoff YO, McCaffery JM, Wendland B, Sherman MY. 2003. Aggregation of expanded polyglutamine domain in yeast leads to defects in endocytosis. *Mol Cell Biol* **23**: 7554-7565.

Moskalenko SE, Zhuravleva GA, Soom M, Shabel'skaia SV, Volkov KV, Zemlianko OM, Philippe M, Mironova LN, Inge-Vechtomov SG. 2004. Characterization of missense mutations in the SUP45 gene of Saccharomyces cerevisiae encoding translation termination factor eRF1. *Genetika* **40**: 599-606.

Muchowski PJ, Schaffar G, Sittler A, Wanker EE, Hayer-Hartl MK, Hartl FU. 2000. Hsp70 and hsp40 chaperones can inhibit self-assembly of polyglutamine proteins into amyloid-like fibrils. *Proc Natl Acad Sci U S A* **97**: 7841-7846.

Narayanan V, Mieczkowski PA, Kim HM, Petes TD, Lobachev KS. 2006. The pattern of gene amplification is determined by the chromosomal location of hairpin-capped breaks. *Cell* **125**: 1283-1296.

Olzmann JA, Li L, Chin LS. 2008. Aggresome formation and neurodegenerative diseases: therapeutic implications. *Curr Med Chem* **15**: 47-60.

Olzmann JA, Li L, Chudaev MV, Chen J, Perez FA, Palmiter RD, Chin LS. 2007. Parkin-mediated K63-linked polyubiquitination targets misfolded DJ-1 to aggresomes via binding to HDAC6. *J Cell Biol* **178**: 1025-1038.

Ravikumar B, Vacher C, Berger Z, Davies JE, Luo S, Oroz LG, Scaravilli F, Easton DF, Duden R, O'Kane CJ et al. 2004. Inhibition of mTOR induces autophagy and reduces toxicity of polyglutamine expansions in fly and mouse models of Huntington disease. *Nat Genet* **36**: 585-595.

Rose AB, Broach JR. 1990. Propagation and expression of cloned genes in yeast: 2-microns circle-based vectors. *Methods Enzymol* **185**: 234-279.

Ross CA, Poirier MA. 2004. Protein aggregation and neurodegenerative disease. *Nat Med* **10 Suppl**: S10-17.

Ross CA, Tabrizi SJ. 2011. Huntington's disease: from molecular pathogenesis to clinical treatment. *Lancet Neurol* **10**: 83-98.

Ross CA, Wood JD, Schilling G, Peters MF, Nucifora FC, Jr., Cooper JK, Sharp AH, Margolis RL, Borchelt DR. 1999. Polyglutamine pathogenesis. *Philos Trans R Soc Lond B Biol Sci* **354**: 1005-1011.

Russell DW, Jensen R, Zoller MJ, Burke J, Errede B, Smith M, Herskowitz I. 1986. Structure of the Saccharomyces cerevisiae HO gene and analysis of its upstream regulatory region. *Mol Cell Biol* **6**: 4281-4294.

Sambrook J, Russell DW. 2001. *Molecular cloning : a laboratory manual*. Cold Spring Harbor Laboratory Press, Cold Spring Harbor, N.Y.

Scherzinger E, Lurz R, Turmaine M, Mangiarini L, Hollenbach B, Hasenbank R, Bates GP, Davies SW, Lehrach H, Wanker EE. 1997. Huntingtin-encoded polyglutamine expansions form amyloid-like protein aggregates in vitro and in vivo. *Cell* **90**: 549-558.

Scolnick E, Tompkins R, Caskey T, Nirenberg M. 1968. Release factors differing in specificity for terminator codons. *Proc Natl Acad Sci U S A* **61**: 768-774.

Serio TR, Cashikar AG, Moslehi JJ, Kowal AS, Lindquist SL. 1999. Yeast prion [*PSI*$^{+}$] and its determinant, Sup35p. *Methods Enzymol* **309**: 649-673.

Seufert W, Jentsch S. 1990. Ubiquitin-conjugating enzymes UBC4 and UBC5 mediate selective degradation of short-lived and abnormal proteins. *EMBO J* **9**: 543-550.

Shao J, Diamond MI. 2007. Polyglutamine diseases: emerging concepts in pathogenesis and therapy. *Hum Mol Genet* **16 Spec No. 2**: R115-123.

Sherman F. 2002. Getting started with yeast. *Methods Enzymol* **350**: 3-41.

Sherman F, Hicks J, Fink G. 1987. *Methods in Yeast Genetics: A Laboratory Course Manual*. Cold Spring Harbor Laboratory Press.

Sikorski RS, Hieter P. 1989. A system of shuttle vectors and yeast host strains designed for efficient manipulation of DNA in Saccharomyces cerevisiae. *Genetics* **122**: 19-27.

Stack EC, Kubilus JK, Smith K, Cormier K, Del Signore SJ, Guelin E, Ryu H, Hersch SM, Ferrante RJ. 2005. Chronology of behavioral symptoms and neuropathological sequela in R6/2 Huntington's disease transgenic mice. *J Comp Neurol* **490**: 354-370.

Stansfield I, Jones KM, Kushnirov VV, Dagkesamanskaya AR, Poznyakovski AI, Paushkin SV, Nierras CR, Cox BS, Ter-Avanesyan MD, Tuite MF. 1995. The products of the SUP45 (eRF1) and SUP35 genes interact to mediate translation termination in Saccharomyces cerevisiae. *EMBO J* **14**: 4365-4373.

Steffan JS, Kazantsev A, Spasic-Boskovic O, Greenwald M, Zhu YZ, Gohler H, Wanker EE, Bates GP, Housman DE, Thompson LM. 2000. The Huntington's disease protein interacts with p53 and CREB-binding protein and represses transcription. *Proc Natl Acad Sci U S A* **97**: 6763-6768.

Storici F, Resnick MA. 2006. The delitto perfetto approach to in vivo site-directed mutagenesis and chromosome rearrangements with synthetic oligonucleotides in yeast. *Methods Enzymol* **409**: 329-345.

Tabor CW, Tabor H. 1984. Polyamines. *Annu Rev Biochem* **53**: 749-790.

Taylor JP, Tanaka F, Robitschek J, Sandoval CM, Taye A, Markovic-Plese S, Fischbeck KH. 2003. Aggresomes protect cells by enhancing the degradation of toxic polyglutamine-containing protein. *Hum Mol Genet* **12**: 749-757.

Ter-Avanesyan MD, Kushnirov VV, Dagkesamanskaya AR, Didichenko SA, Chernoff YO, Inge-Vechtomov SG, Smirnov VN. 1993. Deletion analysis of the SUP35 gene of the yeast Saccharomyces cerevisiae reveals two non-overlapping functional regions in the encoded protein. *Mol Microbiol* **7**: 683-692.

The Huntington's Disease Collaborative Research Group. 1993. A novel gene containing a trinucleotide repeat that is expanded and unstable on Huntington's disease chromosomes. *Cell* **72**: 971-983.

Tuite MF, Cox BS. 2003. Propagation of yeast prions. *Nat Rev Mol Cell Biol* **4**: 878-890.

Urakov VN, Vishnevskaya AB, Alexandrov IM, Kushnirov VV, Smirnov VN, Ter-Avanesyan MD. 2010. Interdependence of amyloid formation in yeast: implications for polyglutamine disorders and biological functions. *Prion* **4**: 45-52.

Valouev IA, Kushnirov VV, Ter-Avanesyan MD. 2002. Yeast polypeptide chain release factors eRF1 and eRF3 are involved in cytoskeleton organization and cell cycle regulation. *Cell Motil Cytoskeleton* **52**: 161-173.

Vishveshwara N, Bradley ME, Liebman SW. 2009. Sequestration of essential proteins causes prion associated toxicity in yeast. *Mol Microbiol* **73**: 1101-1114.

Waelter S, Boeddrich A, Lurz R, Scherzinger E, Lueder G, Lehrach H, Wanker EE. 2001. Accumulation of mutant huntingtin fragments in aggresome-like inclusion bodies as a result of insufficient protein degradation. *Mol Biol Cell* **12**: 1393-1407.

Wang P, Kim Y, Pollack J, Narasimhan B, Tibshirani R. 2005. A method for calling gains and losses in array CGH data. *Biostatistics* **6**: 45-58.

Wang W, Czaplinski K, Rao Y, Peltz SW. 2001. The role of Upf proteins in modulating the translation read-through of nonsense-containing transcripts. *EMBO J* **20**: 880-890.

Wang Y, Meriin AB, Zaarur N, Romanova NV, Chernoff YO, Costello CE, Sherman MY. 2009. Abnormal proteins can form aggresome in yeast: aggresome-targeting signals and components of the machinery. *FASEB J* **23**: 451-463.

Wegrzyn RD, Bapat K, Newnam GP, Zink AD, Chernoff YO. 2001. Mechanism of prion loss after Hsp104 inactivation in yeast. *Mol Cell Biol* **21**: 4656-4669.

Wexler NS, Lorimer J, Porter J, Gomez F, Moskowitz C, Shackell E, Marder K, Penchaszadeh G, Roberts SA, Gayan J et al. 2004. Venezuelan kindreds reveal that genetic and environmental factors modulate Huntington's disease age of onset. *Proc Natl Acad Sci U S A* **101**: 3498-3503.

Wickner RB, Edskes HK, Shewmaker F, Nakayashiki T, Engel A, McCann L, Kryndushkin D. 2007. Yeast prions: evolution of the prion concept. *Prion* **1**: 94-100.

Yamanaka T, Tosaki A, Miyazaki H, Kurosawa M, Furukawa Y, Yamada M, Nukina N. 2010. Mutant huntingtin fragment selectively suppresses Brn-2 POU domain transcription factor to mediate hypothalamic cell dysfunction. *Hum Mol Genet* **19**: 2099-2112.

Yu B, Howell PL. 2000. Intragenic complementation and the structure and function of argininosuccinate lyase. *Cell Mol Life Sci* **57**: 1637-1651.

Zoghbi HY, Orr HT. 1999. Polyglutamine diseases: protein cleavage and aggregation. *Curr Opin Neurobiol* **9**: 566-570.

VITA

HE GONG

GONG was born in Tangshan, Hebei, China. She attended Beijing Normal Univeristy, Beijing, China in 2002 and received a B.S. in Biotechnology in July 2006. She came to Georgia Tech to pursue a doctoral degree in Molecular and Cell Biology in August 2006.